TAMPEREEN TEKNILLINEN YLIOPISTO
TAMPERE UNIVERSITY OF TECHNOLOGY

LAURA SALONEN

RHEOLOGICAL AND MECHANICAL PROPERTIES OF HYDROGELS

Master of Science Thesis

Examiners: Minna Kellomäki, Janne Koivisto
Examiners and topic approved in the Faculty of Engineering Sciences meeting 7. May 2014

ABSTRACT

TAMPERE UNIVERSITY OF TECHNOLOGY
Master's Degree Programme in Materials Science
SALONEN, LAURA: Rheological and mechanical properties of hydrogels
Master of Science Thesis, 85 pages
August 2014
Major: Biomaterial Engineering
Examiners: Professor Minna Kellomäki, Janne Koivisto
Keywords: Rheological properties, mechanical properties, hydrogels, gellan gum, hyaluronic acid, amplitude sweep, frequency sweep, storage modulus, loss modulus, complex shear modulus, Young's modulus

Aim of this thesis was to find out if the rheological oscillatory test is suitable to use for use as a measuring method to determine the stiffness of hydrogels. Due to the softness of hydrogels the measurement of the Young's modulus by compression test is limited, as the softer hydrogels do not maintain their shape. The compression test is suitable measuring method for hydrogels that have higher cross-linker concentrations. Materials that where used in this thesis were gellan gum and hyaluronic acid based hydrogels. In gellan gum hydrogels the cross-linker was spermine or spermidine and in hyaluronic acid hydrogels the cross-linker was polyvinyl alcohol. The total number of samples was 180.

The rheological properties were measured by a rheometer. The measuring program that was used was oscillatory test. The amplitude sweep was used to define the linear viscoelastic (LVE) range for hydrogels. From the LVE range, the storage modulus and the loss modulus were determined. The complex shear modulus was then calculated by using the storage and the loss modulus. Additionally, the frequency sweep from LVE range was measured. The stress-strain curves for hydrogels were determined by a compression test. The Young's modulus was calculated from the slope stress-strain curve.

As an observation the oscillatory test proved to be a more accurate measuring method than the compression test. The anisotropy of the sample structure caused variation of results and higher standard deviations. The compression test results were not affected by the anisotropy of the samples. The rheological measuring method turned out to be suitable for measuring the stiffness of the softer hydrogels. For the stronger hydrogels, on the other hand, the results had a high standard deviation. The reason for the high standard deviation is the anisotropy of the sample structure. The rheological moduli for gellan gum hydrogels were lower and the standard deviation higher than for the hyaluronic acid hydrogels. As a conclusion from both measuring methods, the stiffness of the hydrogels became higher when the cross-linker concentration increased. The rheological measurement method was found to be suitable for the softer hydrogels. However, for the hydrogels with the higher cross-linker concentration and the fast gelation time, the rheological measuring method needs further studies.

TIIVISTELMÄ

TAMPEREEN TEKNILLINEN YLIOPISTO
Materiaalitekniikan koulutusohjelma
SALONEN, LAURA: Hydrogeelien reologiset ja mekaaniset ominaisuudet
Diplomityö, 85 sivua
Elokuu 2014
Pääaine: Biomateriaalitekniikka
Tarkastajat: professori Minna Kellomäki, Janne Koivisto
Avainsanat: Reologiset ominaisuudet, mekaaniset ominaisuudet, hydrogeelit, gellan gum, hyaluronihappo, amplitudipyyhkäisy, taajuuspyyhkäisy, varastomoduuli, häviömoduuli, kompleksinen leikkausmoduuli, kimmomoduuli

Tämän diplomityön tarkoituksena oli selvittää reologian soveltuvuus hydrogeelien lujuusarvojen määrittämiseen puristustestin rinnalle. Ongelmana olivat pehmeät hydrogeelit, joissa ristisilloittajakonsentraatio oli matala ja hydrogeeli ei ylläpitänyt muotoaan. Pehmeitä hydrogeelejä ei pystytty puristamaan, joten niiden lujuuden määrittämiseksi tutkittiin reologisen oskilloivan mittaustavan soveltumista.

Tässä työssä käytettiin gellan gum -hydrogeelejä tai hyaluronihappohydrogeelejä. Ristisilloittajana gellan gum -hydrogeeleissä olivat spermiini tai spermidiini, kun taas hyaluronihappohydrogeeleissä ristisilloitajana oli polyvinyylialkoholi. Näytteiden lukumäärä oli 180.

Hydrogeelien reologisten moduulien määrittämiseen käytettiin reometriä ja mittausohjelmana oskilloivaa mittaustapaa. Oskilloivassa mittaustavassa suoritettiin näytteille amplitudipyyhkäisyt, joista määritettiin näytteen lineaarinen viskoelastinen alue (LVE). LVE-alueelta määritettiin näytteiden varasto- ja häviömoduulien arvot, joiden avulla saatiin laskettua kompleksinen leikkausmoduuli. Reometrillä suoritettiin myös taajuuspyyhkäisy LVE-alueelta, jolla haluttiin todentaa näytteiden geelimäinen käytös. Kimmomoduulin määritys suoritettiin puristuskoneella puristustestinä. Puristustestin avulla määritettiin materiaalille voima-venymä -käyrä, josta laskettiin hydrogeelille kimmomoduulin arvo.

Reologinen mittaustapa osoittautui erittäin spesifiseksi materiaalin rakenteen suhteen. Mikäli näyte oli anisotropinen, näkyi tuloksissa vaihteluja ja keskihajonta oli suuri. Puristustestimenetelmässä näytteen anisotropisuus ei aiheuttanut tuloksiin suurta vaihtelua. Reologinen mittaustapa soveltui hyvin lujuuden määrittämiseen pehmeille hydrogeeleille, mutta hydrogeeleille joissa ristisilloittajakonsentraatio oli suuri, keskihajonta oli suurta. Gellan gum -hydrogeelien reologiset moduulit olivat paljon pienempiä ja keskihajonnat suurempia kuin hyaluronihappohydrogeelien. Molemmat mittaustavat osoittivat, että hydrogeelit, joilla oli suurempi ristisilloittajakonsentraatio, olivat lujempia. Reologinen mittaustapa hydrogeelien lujuuden määrityksessä sopii erityisesti pehmeille hydrogeeleille. Ristisilloittajapitoisuuden noustessa myös näytteiden valmistus on haasteellista nopean geeliytymisen vuoksi.

PREFACE

This thesis project is part of the Human Spare Part project at the Institute of Biosciences and Medical Technology, BioMediTech. This thesis was performed at the Department of Electronics and Communications Engineering, Tampere University of Technology.

Supervisors of this thesis project were professor Minna Kellomäki and researcher Janne Koivisto. I want to thank Minna for the opportunity to take part in this research project and to make myself familiar with the research of biomaterials. I am very grateful to Janne for teaching of hydrogel testing and for the opportunity to learn about hydrogels.

For other researcher in hydrogels project, Jenny Parraga and Jennika Karvinen, I want to thank your advises with these hydrogels.

In Department of Materials Science, I want to thank Kari Kolppo and Ilari Jönkkäri for thoroughly teaching usage of rheometers and introducing the world of rheology.

I owe my deepest gratitude to my parents who have built great grounds to study and encouraged through the school years of my life. For my sister, Tiina and her family, I want to thank for the support during this thesis project.

Last but not least, there are no words to thank enough my dear boyfriend Jesse, for love and support during the last school years. I want to thank you for all encouragement and care. You have been invaluable support during this thesis project.

Tampere Finland, August 2014

Laura Salonen

TABLE OF CONTENTS

LIST OF SYMBOLS AND ABBREVIATIONS

E	Young's modulus, modulus of elasticity
G'	Storage modulus
G''	Loss modulus
G*	Complex shear modulus
η*	Complex viscosity
η'	Real part of complex viscosity
η''	Imaginary part of complex viscosity
sd	Standard deviation
tan δ	Loss factor
δ	Phase shift angle
σ(max)	Fracture strength
ε(max)	Fracture strain
AFM	Atomic force microscopy
CC MS	Coaxial cylinder measuring system
CP MS	Cone-and-plate measuring system
CSD	Controlled shear strain (deformation)
CSS	Controlled shear stress
DMA	Dynamic mechanical analysis
GG	Gellan gum
HA	Hyaluronic acid
HAGG	High-acyl gellan gum
IPNs	Interpenetrate networks
LAGG	Low-acyl gellan gum
LVE	Linear viscoelastic
MRE	Magnetic resonance elastography
MS	Measuring system
Poly(HEMA)	Poly (2-hydroxyethyl metacrylate)
PP MS	Parallel-plate measuring system
PVA	Polyvinyl alcohol
SPD	Spermidine
SPM	Spermine

1 INTRODUCTION

Hydrogels as biocompatible biomaterials have generated interest in the biomedical field. Due to the high amount of water in the structure, the hydrogels mimic the extracellular matrix of human body and they have proved to be suitable for implantable biomaterials. Hydrogels are developed for many different biomedical applications due to their superior chemical and physical properties. (Kishida & Ikada 2001)

There are several methods for measuring the mechanical properties of hydrogels, such as indentation testing, compression testing, tensile testing, dynamic mechanical analysis (DMA), rheology, atomic force microscopy (AFM) and magnetic resonance elastography (MRE). The limitation in mechanical measurements is the inherent weakness of the hydrogels. Due to the challenging nature of hydrogels, the rheological measuring method has made possible to measure weaker hydrogels. (ASTM F2900-11, Standard guide for characterization of hydrogels used in regenerative medicine 2011; Brandl et al. 2007) Hydrogels had been used in many biomedical applications such as drug delivery system, cell encapsulation, scaffolds for tissue engineering, tissue replacement, biosensors, wound dressing, intelligent cell culture substrates and contact lenses. (Patel & Mequanint 2011)

Aim of this thesis was to find out if the rheological oscillatory test is suitable to use as a measuring method to define stiffness of hydrogels. In the earlier studies, the stiffness of the hydrogels was determined by compression test. The problem has been the softer hydrogels with lower cross-linker concentration that do not maintain their shape and the compression test has not been possible to use for softer hydrogels. In the earlier studies, the stiffness of the softer hydrogels was impossible to measure.

Hydrogels that have been used in this thesis work were gellan gum and hyaluronic acid based hydrogels. The gellan gum hydrogels were cross-linked with spermine or spermidine and the hyaluronic acid hydrogels with polyvinyl alcohol. The compression test and the oscillatory test were used to measure the stiffness of these hydrogels. In rheological measurements, the amplitude and the frequency sweeps were used to determinate the viscoelastic (LVE) range of the hydrogels. The determination of the LVE range was done to define the rheological moduli of the hydrogels. The values of the rheological moduli represent the stiffness of the hydrogels.

To use the hydrogels as implantable biomaterials in soft tissue applications, the mechanical properties of the hydrogels are important to define. The mechanical properties of the hydrogels are measured to confirm adequate material properties. Due to the different required properties of the soft tissues, it is important to define the stiffness of the hydrogels with different cross-linker concentrations. Commonly, it is

desired that the mechanical properties of implantable material are similar to the target tissue.

The thesis starts with the theoretical background of the hydrogels and the rheological and the mechanical testing of hydrogels. In the following, the test methods and the results with discussion are described. Last section contains the conclusions and the future propositions.

2 THEORETICAL BACKGROUND

2.1 Hydrogels

2.1.1 Basics of hydrogels

Hydrogels are gel-like water-swollen polymeric biomaterials. The name hydrogel consists of the words *hydro* and *gel* that translates to aqueous (water-containing) gels. (Zavan et al. 2009) Hydrogels are materials that have a three-dimensional structure, which entrap inside a large amount of water. Hydrogels are polymeric and hydrophilic materials in which the amount of water is up to 90 %. (Barbucci 2009) Hydrogels consist of polymer networks that are insoluble in water. The polymeric network is hydrophilic and polymers are held together by covalent bonds. In structure there are weaker cohesive forces such as hydrogen and ionic bonds and intermolecular hydrophobic interactions. (Kishida & Ikada 2001)

The ability to entrap a large amount of water is based on the hydrophilic properties of polymer chains (Uchegbu & Schatzlein 2006). The human body consists of mainly water. Hydrogels are excellent structures to mimic the extracellular matrix of human body due to the large amount of water in their structure. Hydrogels have been used as scaffolds, for example, with cultured cells and proteins. They are promising biomaterials for the biomedical field due to them having good biocompatibility and the ability to mimic the tissue environment. (Barbucci 2009) The good biocompatibility results from high water content and soft-surface properties of hydrogels (Uchegbu & Schatzlein 2006).

Hydrogels have been developed in many different medical applications due to their superior chemical and physical properties. It has been found, when used hydrated hydrogels as implants, that their elastic nature minimized irritation to surrounding tissue. Also, the low interfacial tension between the hydrogel surface and the aqueous solutions minimize protein adsorption and cell adhesion. (Kishida & Ikada 2001) Depending on the usage of the hydrogel, the ability to protein adsorption and cell adhesion can be required.

There are plenty of different hydrogels with different chemical structure of the constituting polymers. Hydrogels can be tailored to respond to external stimulus, such as temperature, pH, electric field, light, solvent composition, ionic strength, salt type, light, pressure and specific biomolecules. Hydrogels that are environmental-sensitive are often called “smart hydrogels”. They respond (i.e., either swell, shrink, bend, or degrade) to changes in environmental conditions. One main property of “smart

hydrogels" is that they change their swelling ratio rather abruptly upon small changes in environmental factors. (Park & Park 1996)

Thermoplastic hydrogels are physical gels, they are based on linear copolymers of hydrophilic and hydrophobic monomers. Thermoplastic hydrogels are easy to process due to their hydrophobic interactions between hydrophobic chains of the copolymer. They also dissolve in organic solvent, but swell without dissolving in water. (Park & Park 1996)

Hydrogel foams are developed to overcome slow swelling of hydrogels. Usually the equilibrium swelling takes from hours to days depending on the size and the shape of hydrogels. Hydrogel foams have a porous structure that is made by synthesizing hydrogels in the presence of gas bubbles. The size of the pores in the hydrogels foams is larger than in hydrogel sponges or microporous hydrogels. Hydrogel foams have much faster kinetics and extent of swelling than other hydrogels since water is absorbed into hydrogel foams by capillary reaction through the pores. Hydrogel foams are useful in many biomedical applications in which is required the property of fast swelling with a very large swelling ratio. (Park & Park 1996)

Hydrogels are not perfect biomaterials therefore they still cause foreign body reactions. In addition, hydrogels have rather poor mechanical strength and durability for some biomedical applications. Enhancing these weaknesses gives more opportunities for the use of hydrogels in many applications to come. (Park & Park 1996)

2.1.2 Classification of hydrogels

Hydrogels can be classified in several ways. One way to classify hydrogels depends on preparation method, source, physical properties, ionic charge, biodegradability, crosslinking or function. When classified hydrogels by source there are two different hydrogels: natural hydrogels and synthetic hydrogels. (Kishida & Ikada 2001) The composition of hydrogels could also be combination of natural and synthetic monomers (Hoffman 2002). Natural hydrogels include such as agarose, alginate, chitosan, collagen, fibrin, gelatin and hyaluronic acid. (Barbucci 2009) Synthetic hydrogels include such as poly(acrylic acid), poly(hydroxyethyl methacrylate), poly(N-isopropylacrylamide), poly(ethylene glycol) and copolymers among others. (Gila et al. 2012) The Figure 2.1 shows examples of monomers that are used in synthetic hydrogels.

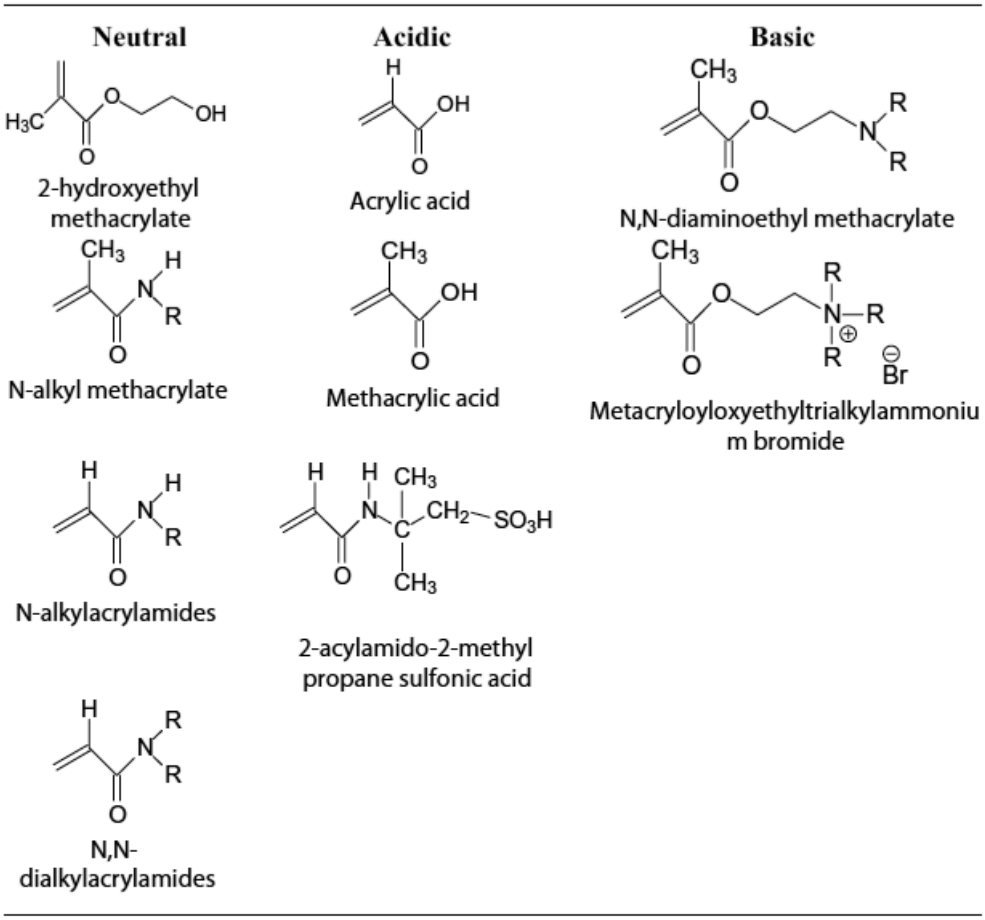

Figure 2.1 *Examples of neutral, acidic and basic monomers that have been used in synthetic hydrogels* (Gila et al. 2012).

Hydrogels are classified in four groups based on the preparation method: homopolymer hydrogels, copolymer hydrogels, multi-polymer hydrogels and interpenetrating polymeric hydrogels. (Kishida & Ikada 2001) In multi-polymer hydrogels more than three types of monomers are present. Interpenetrating polymeric hydrogels are prepared by swelling a network of polymer 1 in monomer 2 to make an intermeshing network of those polymers. (Barbucci 2009) Based on electric charge, hydrogels are classified as neutral, cationic, anionic or ampholytic hydrogels. Based on physical structure hydrogels are classified as amorphous, semicrystaline and hydrogen bonded hydrogels. One way to classify hydrogels is based on crosslinking method. In chemical crosslinking the functional groups on polymer chain are bound with crosslinking agent or radiation to form insoluble gels. (Kishida & Ikada 2001) In chemical cross-linking the polymer chains of a hydrogel are covalently linked to each other and they are known as chemical gels. Because of the covalent bonds, chemical hydrogels cannot be reshaped and they are called thermoset hydrogels. (Uchegbu & Schatzlein 2006) In physical crosslinking method the cross-links are formed by physical interactions such as van der Waals force, by hydrophobic interactions or by hydrogen bonds (Kishida & Ikada 2001). In physical crosslinking cross-links are noncovalent and reversible. Hydrogels that undergoes physical crosslinking method are physical

hydrogels. Physical hydrogels can be processes by solvent casting or heating and they are called thermoplastic hydrogels. (Uchegbu & Schatzlein 2006) Classification of hydrogels could also be based on function of hydrogels. There are several functional hydrogels such as biodegradable, stimuli responsible and superabsorbent hydrogels. (Kishida & Ikada 2001) In the Table 2.1 the classification of hydrogels is presented in one way.

Table 2.1. *Classification of hydrogels.* (Kishida & Ikada 2001).

Classification	Contents
Source	Natural
	Synthetic
Component	Homopolymer
	Copolymer
	Multipolymer
Preparation method	Simultaneous polymerization
	Crosslink of polymer
Electric charge	Nonion
	Anion
	Cation
	Zwitter ion
Physical structure	Amorphous
	Semicrystaline
	Hydrogen bonded
Crosslink	Covalent bond
	Intermolecular force
Functions	Biodegradable
	Stimuli responsive
	Superabsorbent
	Etc.

Furthermore, there are plenty of different ways to classify hydrogels. Various criteria to classify hydrogels could also base on, for example, the biodegradability and porosity of hydrogels. These groups consist of biodegradable, nondegradable, nonporous, microporous, macroporous and superporous hydrogels. (Uchegbu & Schatzlein 2006)

2.1.3 Preparation and chemical structure of hydrogels

There are various methods to prepare hydrogels. The initial formation of the cross-linked structure of hydrogels can be prepared in water or in biological fluids containing water. Typical methods to prepare hydrogels are irradiation, chemical reactions and physical associations. Irradiation methods include electron beams, gamma rays, x-rays or ultraviolet light. The radiation method excites polymer chains to produce a crosslinking point. Chemical reactions require a di- or trifunctional crosslinking agent and polymers with reactive functional groups. The functional group could be in the side chain or in the ends of the chain. Also simultaneous copolymerization–crosslinking reaction between one or more monomers using a polymerizable crosslinking agent is possible in chemical crosslinking. A physical reaction introduces physical crosslinks between polymer chains through the intermolecular force. (Kishida & Ikada 2001) Figure 2.2 shows representative methods of hydrogel formation. (A) shows chemical reactions in which the chemical hydrogels are prepared from monomers, oligomers or polymers using crosslinking agents. The chemical reaction proceeds via radical polymerization or polycondensation reactions. (B) shows physical reactions in which the physical hydrogels are prepared by ionic interactions, hydrophobic interactions or hydrogen bonding. (Park et al. 2012)

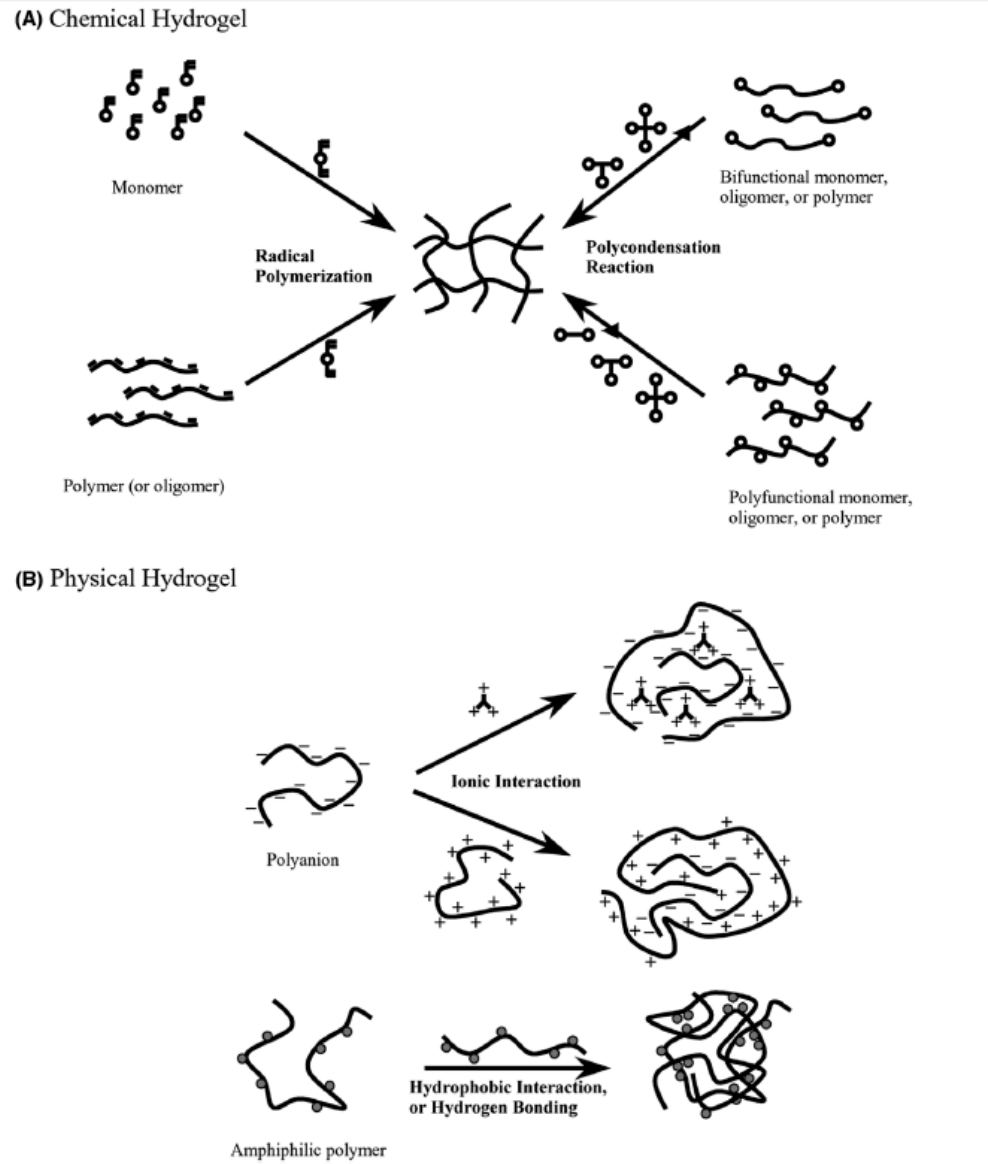

Figure 2.2. *Representative methods of hydrogel formations to produce chemical hydrogels (A) and physical hydrogels (B)* (Park et al. 2012).

There are many different molecular structures in physical and chemical hydrogels, such as linear polymers, block copolymers, graft copolymers, interpenetrate networks (IPNs) and polyblends. There are also many different physical forms in hydrogels, such as solid molded forms (e.g. soft contact lenses), pressed powder matrices (e.g. pills or capsules for oral ingestion), microparticles (e.g. as bioadhesive carriers or wound treatments), coatings (e.g. on implants or catheters, on pills or capsules or coatings on the inside capillary wall in capillary electrophoresis), membranes or sheets (e.g. as a reservoir in a transdermal drug delivery patch or for 2D electrophoresis gels), encapsulated solids (e.g. in osmotic pumps), and liquids (e.g. that form gels on heating or cooling). (Hoffman 2002)

Hydrogels can be created from three basic types of monomers and polymers: neutral, acidic or anionic and basic or cationic. Most of the monomers of hydrogels are

hydrophilic. Water-soluble groups of hydrophilic monomers contribute to swelling. To enhance mechanical strength of hydrogels, hydrophobic groups in monomers and polymers are obligatory. Hydrophilic groups, such as hydroxyl, amide and ether group can be applied to incorporate water into hydrogels. To minimize calcification when the hydrogel is implanted, monomers with acidic groups are applied. Cationic hydrogels have positive charge that has a favourable effect on the permeability of anions such as phosphate. (Kishida & Ikada 2001)

There are three parameters that define hydrogel structure: the polymer volume fraction in swollen state $\upsilon_{2,s}$, the average of molecular weight between crosslinks M_c and the correlation length ξ, that is also known as the network mesh (or pore) size. (Barbucci 2009)

The polymer volume fraction in the swollen state $\upsilon_{2,s}$ is defined as follows:

$$\upsilon_{2,s} = \frac{V_p}{V_{gel}} = Q^{-1} \qquad \textit{(1)}$$

The definition of the polymer volume fraction $\upsilon_{2,s}$ consists of ratio of the polymer volume V_p and the volume of swollen gel V_{gel}. The polymer volume fraction is a reciprocal of the volume swelling ratio Q and it can be determined by equilibrium swelling experiments. (Barbucci 2009)

The average of molecular weight of crosslinks can be defined as follows:

$$M_c = \frac{M_0}{2X} \qquad \textit{(2)}$$

where M_0 is the molecular weight of the repeating unit of the polymer and X is the degree of crosslinking. (Barbucci 2009)

The correlation length or the network mesh size ζ indicates the distance between consecutive junctions, crosslinks or tie points. All of these three parameters can be measured through a range of experimental techniques or calculated by the application of the network deformation theory. (Barbucci 2009)

There are three different ideal network structures of hydrogels: the first network with tetra-functional crosslinks in which M_c is the average of the weight between crosslinks, multifunctional junctions or molecular entanglements that are permanent or semi-permanent. Defects in the structure of hydrogels are always possible. Examples of such defects are unreacted functionality and chain loops. Neither of these two configurations improves the mechanical strength or the physical properties of network. (Barbucci 2009) Figure 2.3 shows schematic pictures of network structures where structures a-c are ideal network structures and d-e are network structures with defects.

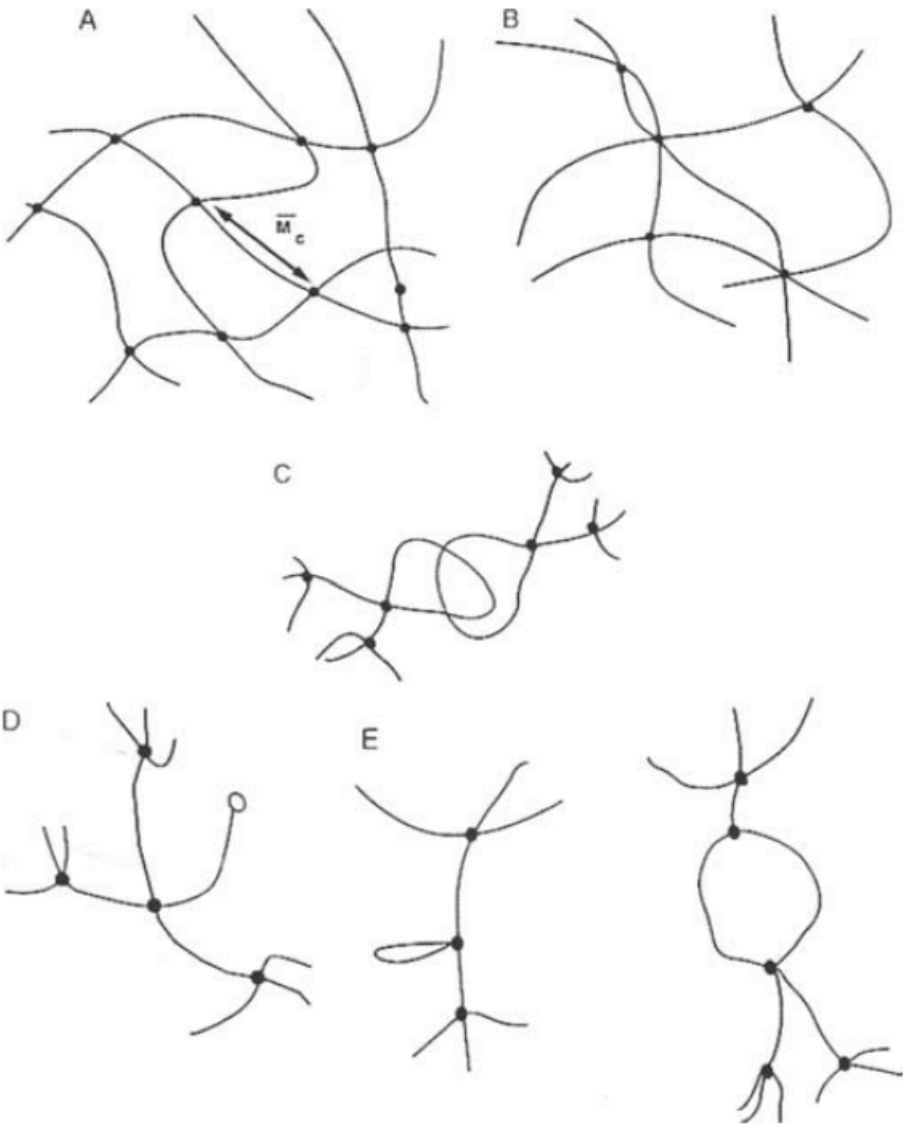

Figure 2.3. *Network structure. A is an ideal networks structure with tetra-functional crosslinks, B multifunctional junctions, C molecular entanglement, D unreacted functionality and E chain loops* (Barbucci 2009).

2.1.4 General properties of hydrogels

The most important property of hydrogels is swelling. Measuring hydrogels' capacity to absorb water or aqueous solution determines the swelling property. The most commonly used swelling parameter of hydrogels is the swelling ratio (R_s). The swelling ratio is defined as follows:

$$R_s = \frac{(W_s - W_d)}{W_d} \qquad \textbf{(3)}$$

where W_s is weight of swollen hydrogels and W_d is weight of dried hydrogels. (Uchegbu & Schatzlein 2006)

There are plenty of factors that determine the swelling property of hydrogels, such as the type and composition of monomers, cross-linking density and environmental factors, for example temperature, pH and ionic strength. The crosslink of the hydrogels' network induce the counterbalance of the swelling force and the retractive force. Swelling of the hydrogels reaches its equilibrium state when the swelling force and retractive force are equal. By measuring equilibrium swelling or elastic modulus, the degree of cross-linking can be measured. (Uchegbu & Schatzlein 2006)

The cross-linking density of a hydrogels determines important properties such as mechanical strength and permeability. Hydrogels are mechanically very weak due to their high water content. By modifying the structure of hydrogels, the low mechanical strength can be improved. Such modifying methods are increasing cross-linking density, making a interpenetrate network (IPN) structure or copolymerization of hydrophobic comonomers. These methods usually decrease swelling property. (Uchegbu & Schatzlein 2006)

Highly hydrophilic polymers that contain few cross-links, adsorb large amounts of water with a high degree of swelling whereas less hydrophilic monomers, incorporation of hydrophobic comonomers or a high degree of cross-linking, reduce water adsorption. That water adsorption of less hydrophilic polymers usually leads to a more rigid and firmer gel. Hydrogels have good biocompatibility due to the high water content within either a bioinert or a biodegradable polymer network. (Davis & Higson 2012)

There are three degradation mechanisms for hydrogels: hydrolysis, enzymatic cleavage and dissolution. A common degradation mechanism of synthetic hydrogels is hydrolysis of ester linkages. (Barbucci 2009) Degradation of physical cross-links occurs via dissolution. The degradation can occur in covalently cross-linked systems through the cleavage of hydrolytically labile bonds such as anhydride or ester groups or enzymatically cleavable peptide or protein linkages. These labile bonds can be present in the cross-link segments (synthetic polymer networks) or along the backbone chains (naturally derived polymer networks). (Drury & Mooney 2003) Hydrolytically labile gels, such as PEG-PLA copolymers, degrade via hydrolysis. Hydrogels that degrade enzymatically include, for example, collagen, HA and chitosan. (Barbucci 2009) The degradation of cross-linked networks occurs by surface degradation or bulk degradation. The surface degradation is limited to the surface of the material and therefor the surface-degrading networks maintain their cross-linking density and structural integrity throughout the degradation process. When the rate of bond hydrolysis is much faster than the rate of water transport into a polymeric device, surface degradation often occurs. Surface degrading networks are advantageous for drug-delivery applications. In bulk erosion, penetration of water into the bulk polymer is much faster than degradation reaction. Bulk degradation does not maintain the cross-linking density and the structural integrity throughout the degradation process and that reduce mechanical properties. All

hydrolytically degradable hydrogels will exhibit bulk-degrading characteristics. (Drury & Mooney 2003)

2.1.5 Hydrogels in biomedical applications

Hydrogels are ideal biomaterials in many biomedical applications such as drug delivery system, cell encapsulation, contact lenses, scaffolds for tissue engineering, biosensors, intelligent cell culture substrates, wound dressing and soft tissue replacement. (Patel & Mequanint 2011) According to (Patel & Mequanint 2011) certain important properties of hydrogels for their biomedical applications are superior biocompatibility, good oxygen permeability, low protein adsorption and cell adhesion, soft and tissue-like physical properties, minimal frictional irritation within the surrounding tissues upon transplantation, micro-porous structure for additional transport channels, easy of surface modification with specific biomolecules, can be injected *in vivo* as a solution that gels at body temperature and aqueous surface environment to protect cells and therapeutic drugs (peptides, proteins, oligonucleotides, DNA). (Patel & Mequanint 2011)

Hydrogels have two distinct advantages to control drug release in drug delivery applications. The first advantage is that the diffusion of drugs through the hydrogel happens easily. The drug release rate can be controlled, for example, by changing the crosslinking density, preparing the hydrogel with monomers of controlled hydrophilicity and/or controlling the ratio of hydrophilic to hydrophobic monomers. The second advantage is that hydrogels may interact less strongly with drugs when compared with hydrophobic materials. The most of active molecules of drugs can be released through hydrogel carriers, especially proteins and peptides. (Patel & Mequanint 2011)

Hydrogels are suitable material for cell encapsulation systems. Hydrogels are biocompatible, they have a microporous structure and minimal surface irritation within the surrounding tissue. Hydrogels can be designed with a porosity that resists any entrance of immune cells and allows stimulus, oxygen, nutrients and waste transfer through the pores. Polyethylene oxide based hydrogels and modified alginates have been studied as cell encapsulation systems. Cell encapsulation systems provide a promising therapeutic system for diabetes, hemophilia, cancer and renal failure. (Patel & Mequanint 2011)

The first hydrogel that has been used as contact lenses was poly(HEMA) in 1960. When the refractive power of the cornea is compromised, synthetic hydrogels have been found to be suitable for contact lens applications. The transparent structure of protein fibers of the cornea contains about 80 % water and 20 % formed materials. The structure of the cornea makes it a natural hydrogel. Biocompatibility, softness, interconnected microstructure of hydrogels help oxygen diffusivity to the epithelial layer of the cornea. Certain hydrogels required to fit for this applications. Such hydrogels possess high refractive index, modulus and transparency. Since no single hydrophilic polymer structure provides all required properties, copolymers are utilized

to design contact lenses. These copolymers are developed from a group of hydrophilic and hydrophobic monomers. (Patel & Mequanint 2011)

Scaffolds are 3D structural templates that support cell adhesion, differentiation, migration and proliferation (Patel & Mequanint 2011). The scaffold should provide physical and biological properties such as sufficient mechanical strength, cell signalling, stimulating matrix production by cells and preventing cells from floating out of the defect. (Ottenbrite et al. 2010) The scaffold material should be biocompatible and reproducible without any batch-property variation with high porosity and well-organized interconnectivity. Hydrogels play an important role as useful scaffolding biomaterials because they most closely resemble natural tissue. Hydrogels are porous for nutrients and waste diffusion and as already mentioned they are biocompatible. (Patel & Mequanint 2011) On demand biofunction can be obtained by the incorporation of growth factors into hydrogels. Growth factors enhance cellular proliferation in the tissue-engineered matrices. Hydrogels can be used either preformed and inserted, or injected. The preformed hydrogels are processed *in vitro* prior to cell seeding and the implantation occurs *in vivo*. The injectable hydrogels are implanted into the body as a liquid that gels *in situ*. Cells and growth factors can be incorporated and suspended in the gels precursors prior to gelation, enabling homogenous cell seeding and easy implantation. (Ottenbrite et al. 2010) Figure 2.4 shows tissue-engineering methods using preformed and injectable hydrogels in combination with cells.

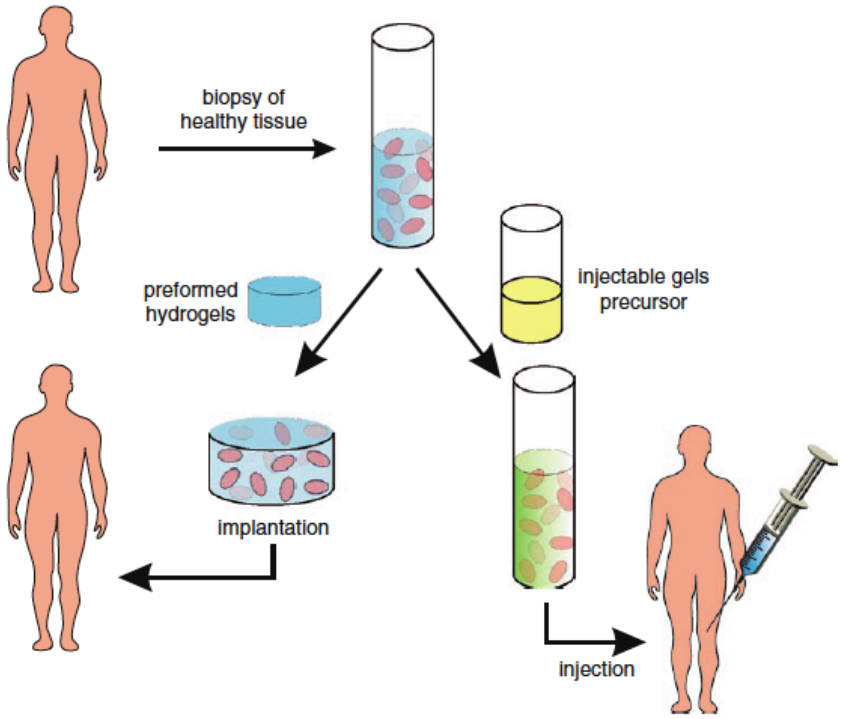

Figure 2.4. *Tissue-engineering methods using preformed and injectable hydrogels in combination with cells.* (Ottenbrite et al. 2010)

Both synthetic and natural hydrogels have been used as scaffolds for tissue engineering in order to repair tendon, ligament, cartilage, skin, blood vessels and heart valves. Synthetic hydrogels that have been used as scaffolds are polyurethanes (PU), poly(ethylene oxide) (PEO), poly(N-isopropylacrylamide) (PNIPAAm), poly(vinyl alcohol) (PVA), poly(acrylic acid) (PAA) and poly(propylene furmarate-*co*-ethylene glycol) (P(PF-*co*-EG)). Naturally derived hydrogels, that have been used as scaffolds are agarose, alginate, chitosan, collagen, fibrin, gelatin and hyaluronic acid (HA). (Patel & Mequanint 2011)

Hydrogels can be used as wound dressing materials. They are flexible, durable and non-antigenic. (Park & Park 1996) Due to their high water content, hydrogels have been investigated for use as burn and other wound dressing (Davis & Higson 2012). In addition, hydrogels are permeable to water vapour and metabolites while they securely cover the wound to prevent bacterial infection. Additionally, hydrogels are used as coating material such as urinary catheter surface to improve its biocompatibility. The hydrogel layer not only provides a smooth slippery surface, but it also prevents bacterial colonization on the surface. (Park & Park 1996)

Another biomedical application where hydrogels are useful materials is implantable membranes. The function of implantable membranes is to prevent postsurgical adhesion formation. These adhesions are scars that form abnormal connections between tissue surfaces. The formation of postsurgical adhesion is a consequence of surgery when tissue repairs itself following trauma such as incision, suturing and cauterization. The formation of postsurgical adhesion can lead to complications such as infertility. Implantable membranes are placed between tissue surfaces. Implantable membranes must be sterile, noninflammatory, nontoxic and bioresorbable. There are few commercially available products that are marketed in gel form such as Oxiplex-SP®, Spraygel® and Resolve®. These products can be applied directly to the site and rapidly form a hydrogel to prevent adhesions. They are absorbed to the body after approximately one week. (Davis & Higson 2012)

Hydrogels have been used in biosensors as reactive matrix membranes. Hydrogels have many advantageous properties such as rapid and selective diffusion of substance and they can be made tough and flexible with desirable refractive indices. Poly(HEMA) is one example of a hydrogel that has been used in biosensors as a salt bridge which separate metallic electrodes from the biological system. The aim of the bridge is to prevent contamination by electrolysis products. Poly(HEMA) bridges are easy to make and sterilize, inexpensive, very durable, and nontoxic to cell systems. They are an alternative to the widely used agar salt bridge. (Park & Park 1996)

Hydrogels can be also used in regenerative medicine with the addition of drugs and biologics in their structure. Examples of these kinds of applications are drug delivery devices, cell encapsulations, tissue scaffolds or barriers. (ASTM F2900-11, Standard guide for characterization of hydrogels used in regenerative medicine 2011)

2.2 Hydrogel materials

2.2.1 Gellan gum hydrogels

Gellan gum (GG) is a polysaccharide, which is produced by a pure culture fermentation of carbohydrates by *Shingomonas elodea*. (Silva et al. 2013) GG can be dissolved in water, and when heated and mixed with mono or divalent cations, it forms a gel upon lowering the temperature under mild conditions. (Oliveira et al. 2010) GG is a biopolymer with high molecular mass and in its native form, usually referred to as high-acyl gellan gum (HAGG), the tetrasaccharide repeat unit consists of residues of β-D-glucose, β-D-glucuronate and α-L-glucose with two acyl substituents on one of the glucose residues. (Bajaj et al. 2007; Silva et al. 2013) The other form of GG is the low-acyl gellan gum (LAGG), which is produced by removing these substituents from the native HAGG form by strong alkali treatment. (Silva et al. 2013) Figure 2.5 illustrates these two forms of GG, the upper form is the LAGG and the lower form is the HAGG.

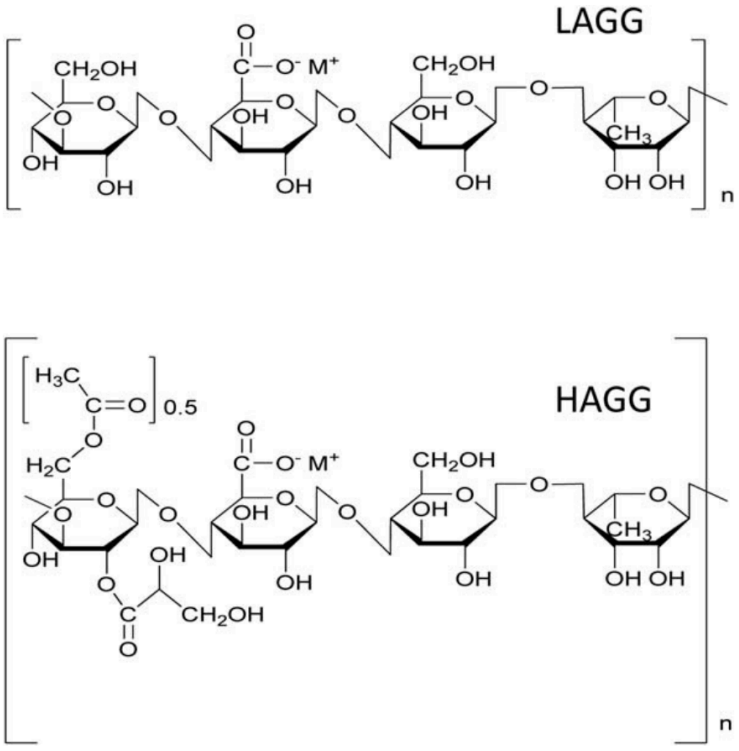

Figure 2.5. *Two forms of gellan gum; the low-acyl GG (LAGG) and the high-acyl GG (HAGG)* (Silva et al. 2013).

GG molecules form a threefold double-helical structure under a suitable aqueous environment. A so-called true gel structure forms by the aggregation of these helical segments and the aggregation is enhanced by the presence of monovalent (Na^{+}) and/or divalent (Ca^{2+}) cations. These cations increase the mechanical properties of the gels. However, reaching optimum gel strength requires an order of magnitude larger concentration of monovalent than divalent ions. There is a difference between the

LAGG and HAGG forms in the aggregation; in HAGG form, the presence of the acyl substituents does not change the overall helical structure, but change the binding (cross-linking) sites for the cations. This change is responsible for the loss of so-called "cation-mediated aggregation" between the HAGG helices. HAGG gels form soft (elastic) and non-brittle gels, whereas LAGG gels are hard (nonelastic) and brittle gels. The mixtures of LAGG and HAGG forms can be used to tune gel characteristics depending on the ratio of the mixture. (Silva et al. 2013; Oliveira et al. 2010)

The cross-linking method of GG hydrogels is ionic cross-linking and due to that they are classified as physical hydrogels. The ionic cross-linking of GG hydrogels requires multivalent counter ions, anionic molecules (trisodium trimetapolyphosphate) or polymers (polyvinyl alcohol, polyacrylic acid, polyacrylamide). (Rana et al. 2011) The gelation mechanism of GG hydrogels involves the formation of double helical junction zones followed by aggregation of the double helical segments to form a three-dimensional network by cations and hydrogen bonding with water. (Bajaj et al. 2007) The formation of the gel structure occurs upon heating and cooling of gellan gum solutions in the presence of cations. The formation depends on cations used in cross-linking. Divalent cations, such as Ca^{2+} and Mg^{2+}, form direct bridges by site binding between pairs of double helicons and monovalent ions, such as Na^{+} and K^{+}, suppress repulsion by binding to the surface of the helices balancing the negative charge of the carboxyl groups. (Smith et al. 2007)

Examples of used cross-linkers in GG hydrogels are biological amines such as putrescine, spermine and spermidine. (López-Cebral et al. 2013) In this thesis project the cross-linking agents for GG based hydrogels are spermine (SPM) and spermidine (SPD). These two are the most prevalent polyamines in mammalian cells, where they fulfil different fundamental functions. SPD has been described to have anti-inflammatory effects, to provide DNA protection against oxidative stress, to play a positive role in several regenerative processes and age-related diseases. SPD has been proven to increase the life span of various model organism and human cells. (López-Cebral et al. 2013) SPM forms from spermidine and it regulates gene expression, stabilizes chromatin, prevents endonuclease-mediated DNA fragmentation and inhibits DNA damage. (Ha et al. 1998) The rationale behind the use of SPM and SPD as a cross-linker is the fact that these polyamines are fully protonated at physiological pH and they are very prone to interact with negatively charged compounds under these conditions. The cross-linking method between GG and SPM or SPD is spontaneous and it occurs by ionic cross-linking method. (López-Cebral et al. 2013)

The GG is US Food and Drug Administration (USFDA) and European Union food additive (E418), which has been used as a multifunctional gelling, stabilizing and suspending agent. (Silva et al. 2013) Table 2.2 illustrates the food application in which the GG is used and the conventional agents that are used instead of GG.

Table 2.2. *Food applications of gellan gum* (Bajaj et al. 2007).

Food area	Example of products	Conventional agents used
Water-based gels	Dessert gels, aspic	Gelatin, alginate, carrageenan
Confectionery	Pectin jellies, fillings, marshmallow	Pectin, gelatin, starches, agar, xanthan, locust been gum
Jams and marmalades	Diet jams, imitation jams, bakery fillings	Pectin, carrageenan, algin
Pie fillings and puddings	Desserts, pie fillings, canned/precooked puddings	Alginate, carrageenan, starches
Fabricated foods	Restructured meat, fruits and vegetables	Alginate, carrageenan, locust been gum
Pet foods	Canned/gelled pet foods	Alginate, carrageenan, locust been gum
Dairy products	Yogurt, milk shakes, gelled milk, ice cream	Alginate, carrageenan, gelatin

GG advantageous use in the context of biomedical applications includes its lack of toxicity, the ability to use as an injectable system in a minimally invasive manner and processing under mild conditions. (Oliveira et al. 2010) GG hydrogels are biocompatible, biodegradable and various cell types can be immobilized into or onto GG based hydrogels maintaining high viability and appropriate functionalities. GG hydrogels have high potential for tissue engineering purposes because of their ability to support cell encapsulation, adequate mechanical properties and noncytotoxicity. (López-Cebral et al. 2013)

The capability to form hydrogels under mild conditions has created significant interest in the use GG as materials for tissue engineering and the pharmaceutical industry. GG hydrogels have been used in controlled drug delivery release and adsorption applications, as a microbial media, in different tissue engineering applications, such as cartilage, and for example in personal care products. (Bajaj et al. 2007; Silva et al. 2013) In biomedical purposes and in the processing of conducting fillers, the GG's unique suspending (dispersing), gelation and rheological properties have been utilized. Such examples are a versatile encapsulating agent and active ingredient in numerous controlled drug delivery systems in nasal, gastric, ocular and colonic drug delivery applications, for wound healing applications and as implants for insulin delivery. (Ferris et al. 2013)

2.2.2 Hyaluronic acid hydrogels

Hyaluronic acid (HA) is a member of the glycosaminoglycan family. HA is a linear, high molecular weight polysaccharide (Figure 2.6.) with repeating disaccharide units composed of (β-1,4)-linked D-glucuronic acid and (β-1,3)-linked N-acetyl-D-glucosamine. (Nair & Laurencin 2007; Slaughter et al. 2009) HA is present in all mammals. In the body, HA occurs in the salt form as hyaluronate and it is found in high concentrations in several soft connective tissues, such as skin, umbilical cord, synovial fluid and vitreous humor. In commercial products, HA is extracted from rooster comb and human umbilical cord or it is manufactured in large quantities by bacterial fermentation. In the body, HA is degraded by hyaluronidase (hyase) into smaller oligosaccharides, while N-acetyl-hexoaminidase and D-glucuronidase further degrade

the oligosaccharide fragments by removing nonreducing terminal sugars. In addition to enzymatic degradation, HA can also be degraded by reactive oxygen intermediates. (Slaughter et al. 2009)

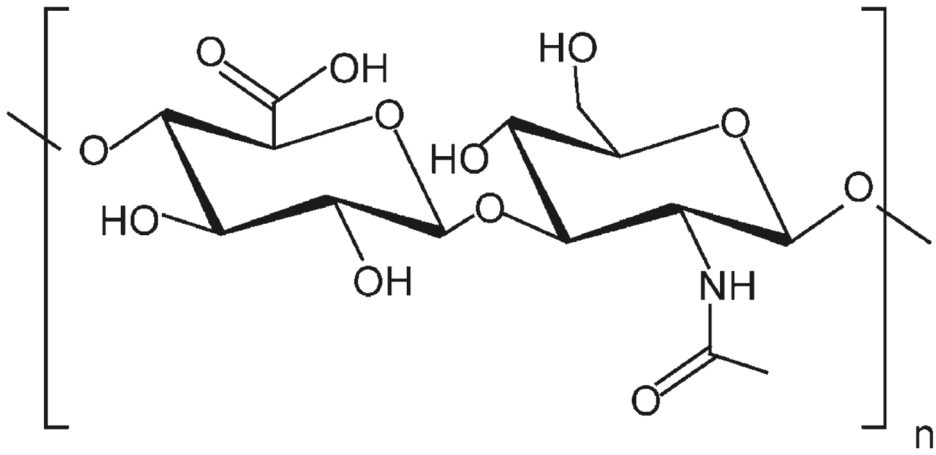

Figure 2.6. *The structure of hyaluronic acid. Repeat units, D-glucuronic acid and D-N-acetylglucosamine, are linked together via alternating β-1,4 and β-1,3 glycosidic bonds* (Slaughter et al. 2009).

HA is water-soluble and it forms highly viscous solutions with unique viscoelastic properties. Due to its high viscoelasticity and space filling properties, HA is particularly good for tissue engineering applications. This rheological feature is directly exploited in the application of hyaluronic acid in the treatment of osteoarthritis and for ophthalmic surgery. HA has been successfully used in cosmetic applications such as soft tissue augmentation due to its ability to form hydrated, expanded matrices. (Slaughter et al. 2009) Due to the high functionality and charge density of HA, it can be cross-linked by a variety of physical and chemical methods. Cross-linked HA hydrogels have been extensively investigated for wound dressing applications. (Nair & Laurencin 2007) Due to the hydrophilic nature of HA, it is well suitable for applications that require minimal cellular adhesion such as post-surgical adhesion barriers. HA can be modified with peptides to create a biomaterial that supports cell attachment, spreading and proliferation. (Slaughter et al. 2009)

In HA hydrogels, the cross-linking method is chemical cross-ling of pendant reactive groups by addition or condensation chemistry by radical polymerization. HA hydrogels are classified to chemical hydrogels. (Burdick & Prestwich 2011) Examples of used cross-linking agents in HA hydrogels are poly(ethylene glycol) diacrylate (PEGDA), bisepoxide, divinyl sulfone derivatives, glutaraldehyde, 1-ethyl-3-(3-dimethylamonipropyl) carbodiimide hydrochloride, biscarbodiimide and multifunctional hydrazides. (Burdick & Prestwich 2011; Xu et al. 2012)

In this thesis project, hyaluronic acid based hydrogels are cross-linked with poly(vinyl alcohol) (PVA). The cross-linking method in studied HA hydrogels is a covalent cross-linking. The cross-linking occurs by “click” chemistry. “Click”

chemistry is a chemical synthesis in which small units are jointed together in quick reaction. (Ossipov & Hilborn 2006) The HA and the PVA have been modified to allow the cross-linking. (Kim et al. 2003) PVA is a hydrophilic polymer, which is nontoxic and nonimmunogenic material. The hydrophilic nature of PVA results from its hydroxyl side groups. (Kim et al. 2003) Figure 2.7 illustrates the structure of PVA.

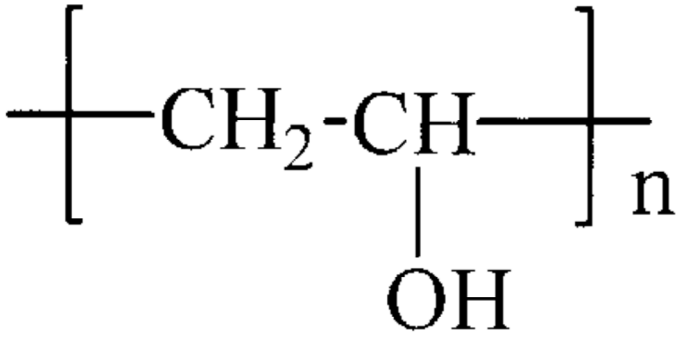

Figure 2.7*. A structure of the PVA* (Kim et al. 2003).

2.3 Principals of rheology

2.3.1 Rheological behaviour of materials

Rheology is literally "flow science". The word "rheology" originates from the Greek word "rheos" which means "the river", "flowing" and "streaming". Rheological experiments do not only mean study the flow behaviour of liquids but also the deformation behaviour of solids. The connection between these two is that large deformations caused by shear forces and those shear forces cause many materials to flow. (Mezger 2002)

There are several fields where rheology plays an important role, such as quality control, production and application, chemical and mechanical engineering, materials science and industrial research and development. The aim of rheology is to examine the rheological properties of several materials such as polymers, adhesives, paints, paper coatings, foodstuff, cosmetics, pharmaceutics and medicaments, surface technology, ceramic, glass and metal casting. Rheological properties have a huge effect on the processability and the final properties of a product. Depending on the final purpose of the product, it is important to study the flow and the deformation behaviour of materials and how they react in target purpose and in target environments. (Mezger 2002; Hutton et al. 1989)

All forms of shear behaviour can be viewed as lying in between two extremes such as the flow of ideal viscous liquids and the deformation of ideal elastic solids. The behaviour of real materials is a combination of both the viscous and the elastic behaviour, it is called viscoelastic behaviour. Wallpaper paste is an example of a

viscoelastic liquid and a gum eraser is an example of a viscoelastic solid. (Mezger 2002; Hutton et al. 1989)

For ideal elastic material the deformation occurs immediately after the stress is applied (the strain is independent of time) and the deformation recovers completely after the external stress is released. Elastic deformation is instantaneous. This behaviour is demonstrated in Figure 2.8 (b) as strain versus time for the instantaneous load-time curve, shown in Figure 2.8 (a). For ideal viscous behaviour the deformation or strain is not instantaneous; in response to an applied stress, deformation is delayed or dependent on time. The deformation of viscous material is irreversible. This phenomenon is presented in Figure 2.8 (d). As mentioned above, viscoelastic behaviour is a combination of elastic and viscous behaviour. In viscoelastic materials part of the deformation occurs immediately after the external stress is applied and part of the deformation is delayed. In Figure 2.8 (c) demonstrates viscoelastic behaviour where an instantaneous elastic strain is followed by a viscous, time-dependent strain. (Callister & Rethwisch 2007)

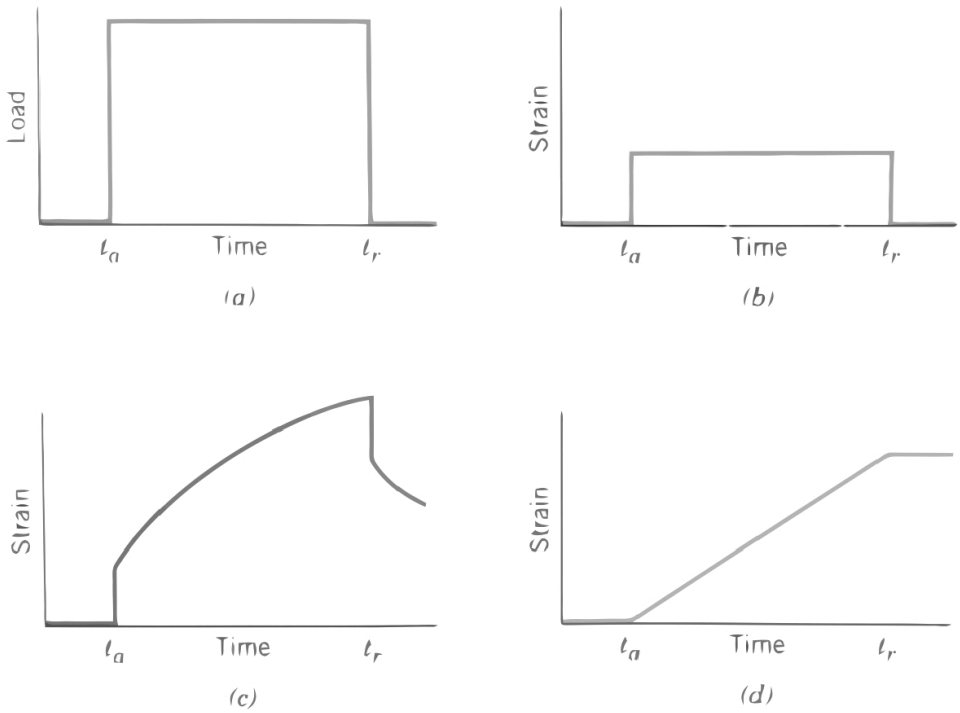

Figure 2.8. *A demonstration of elastic (b), viscoelastic (c) and viscous (d) behaviour of material under instantaneous load-time (a)* (Callister & Rethwisch 2007).

Ideal elastic solid or Hookean deformation behaviour obeys the equation

$$\tau = G \times \gamma \qquad \textbf{(4)}$$

where τ is the shear stress, G is the shear modulus and γ is the corresponding deformation. This law is named as the Hooke's law. The shear force acting on a solid is proportional to the resulting deformation. If the τ/γ function is shown in a diagram, ideal elastic behaviour is performed as a straight line coming from the point of origin with a constant slope. The slope corresponds to the value of G. (Callister & Rethwisch 2007; Mezger 2002) For tensile and compression tests, Hooke's law applies similarly in following form

$$\sigma = E \times \varepsilon \qquad \textbf{(5)}$$

where σ is the stress, ε is the strain and E is the modulus of elasticity or Young's modulus. (Callister & Rethwisch 2007) Elastic behaviour can be illustrated by the use of a spring; Figure 2.9 demonstrates the Hooke's spring model. Under a constant shear force, the spring displays immediately corresponding deformation that remains at a constant value as long as the external force is applied. When forces of various strengths are applied to the spring, it can be noticed that in all cases the force and the defection are proportional. The proportionality factor corresponds to the rigidity of the spring. After removing the shear force, the spring returns to the initial state immediately and completely. No permanent deformation remains. (Mezger 2002)

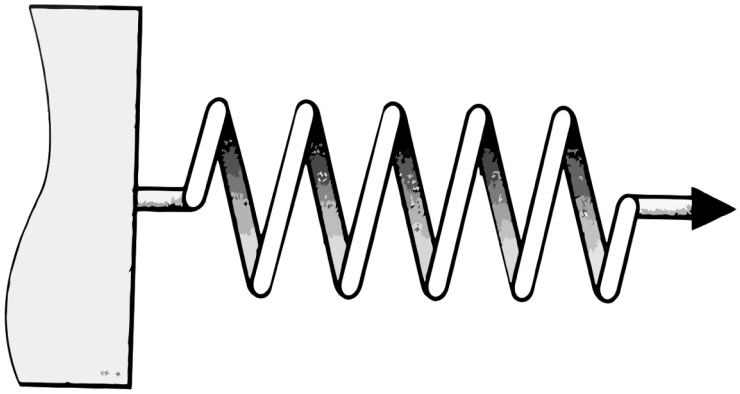

Figure 2.9. *Hooke's spring model* (Mezger 2002).

Ideal viscous liquid or Newtonian flow behaviour is described formally using Newton's law

$$\tau = \eta \times \dot{\gamma} \qquad \textbf{(6)}$$

where τ is the shear stress, $\dot{\gamma}$ is the shear rate and η is the shear viscosity. The shear force acting on a liquid is independent of the degree or duration of the shear load. Examples of ideal viscous materials are low molecular liquids such as water, solvents,

mineral oils and blood plasma. The behaviour of ideal viscous liquids is demonstrated by use of a dashpot. Figure 2.10 illustrates this behaviour. Under a constant shear force the piston moves continually as long as this force is applied. This occurs with a constant deformation velocity. After removing the shear force, the ideal viscous fluid completely remains in the deformed state. (Mezger 2002)

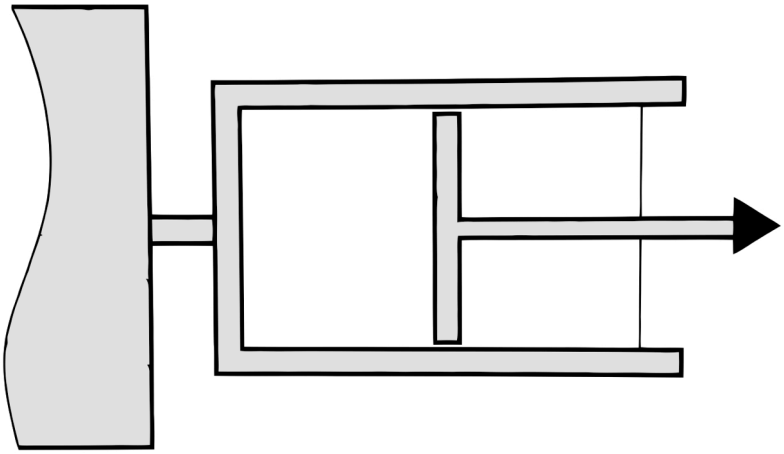

Figure 2.10. *Newton's dashpot model* (Mezger 2002).

Newtonian liquids are liquids of which viscosity stay constant during the shear rate change. Where as, liquids whose viscosity change during the shear rate change are called non-Newtonian liquids. (Hutton et al. 1989) Most of the non-Newtonian liquids obey shear-thinning behaviour when the shear viscosity is dependent on the degree of shear load. The flow curve shows a decreasing curve slope (Figure 2.11 left) and the shear viscosity decreases with increasing load (Figure 2.11 right). (Mezger 2002)

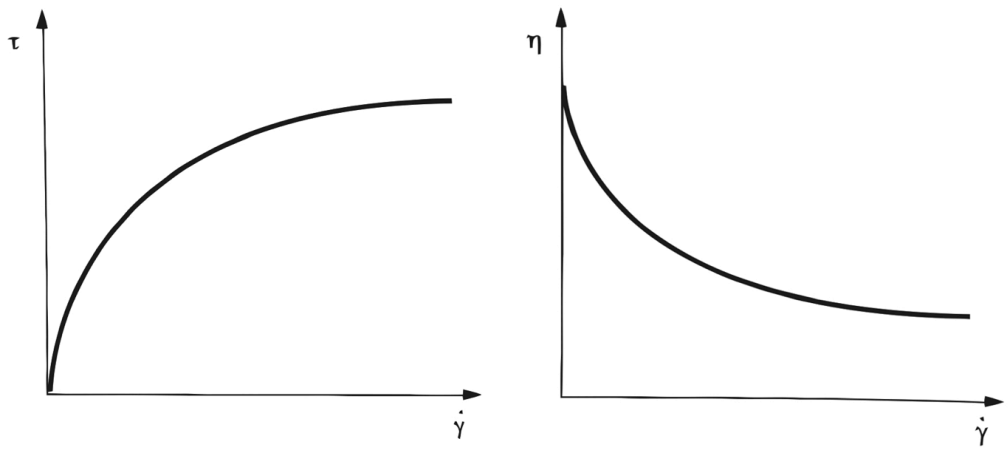

Figure 2.11. *Flow curve (left) and viscosity curve of a shear-thinning material (right)* (Mezger 2002).

Some non-Newtonian liquids obey shear-thickening behaviour when the shear viscosity is dependent on the degree of shear load. The flow curve shows an increasing curve slope (Figure 2.12 left) and the shear viscosity increases with increasing load (Figure 2.12 right). (Mezger 2002)

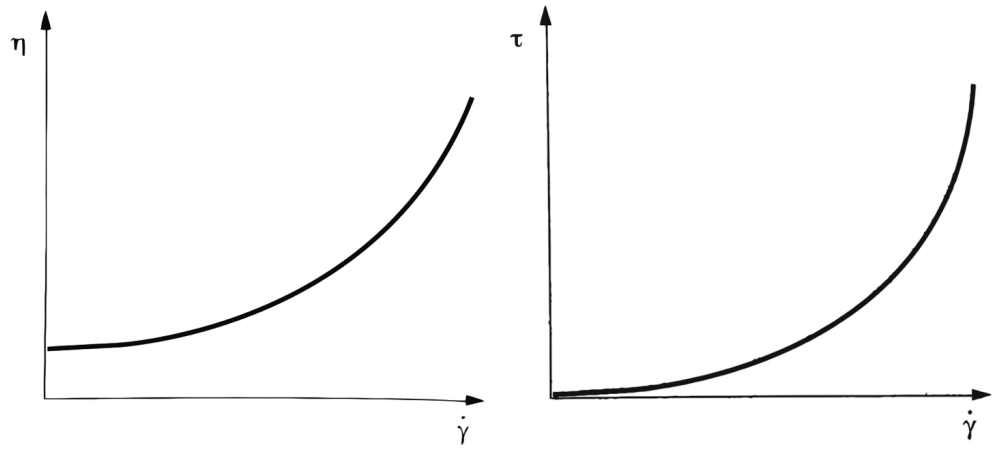

Figure 2.12. *A flow curve (left) and viscosity curve (right) of a shear-thickening material* (Mezger 2002).

A viscoelastic material shows viscous and elastic behaviour. The elastic portion behaves according to Hooke's law and the viscous according to Newton's law. Viscoelastic liquid behaviour differs from viscoelastic solid behaviour. The behaviour of viscoelastic liquid can be demonstrated using the combination of a spring and a dashpot in serial connection. The spring behaves like the Hooke's spring model and the dashpot like the Newton's dashpot model. Both components can be deflected independently of each other. This viscoelastic model is called the Maxwell model (Figure 2.13). (Mezger 2002)

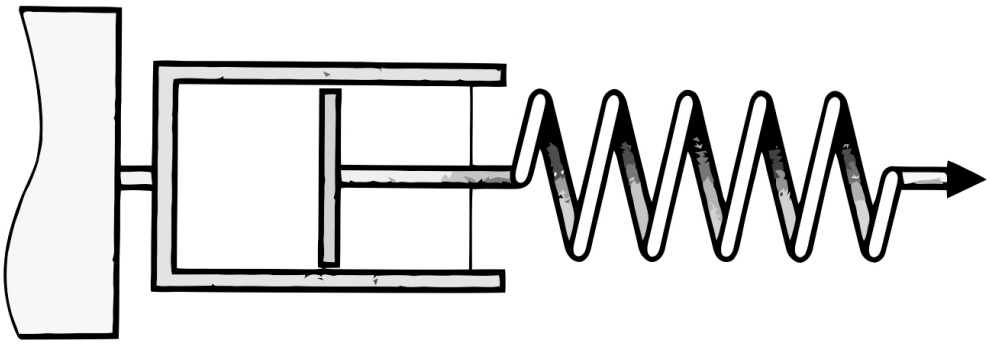

Figure 2.13. *Maxwell model.* (Mezger 2002)

Figure 2.14 demonstrates the deformation behaviour of a viscoelastic liquid according to the Maxwell model. Both components are undeformed in phase 1. Under

the load the spring displays immediate deformation (phase 2a) and this deflection is proportional to the constant load force. Then, under the still acting constant force, the dashpot piston moves continuously (phase 2b) and both components show a certain extent of deformation that corresponds to the degree of the force applied. When the load is removed, the spring retires elastically when it moves back immediately and completely and the dashpot remains deflected (phase 3). In the Maxwell model, after the load cycle the sample remains partly deformed. The reformation represents the elastic portion and the extent of permanently remaining deformation corresponds to the viscous portion. The deformation is irreversible because the reformation of the sample is not complete. (Mezger 2002)

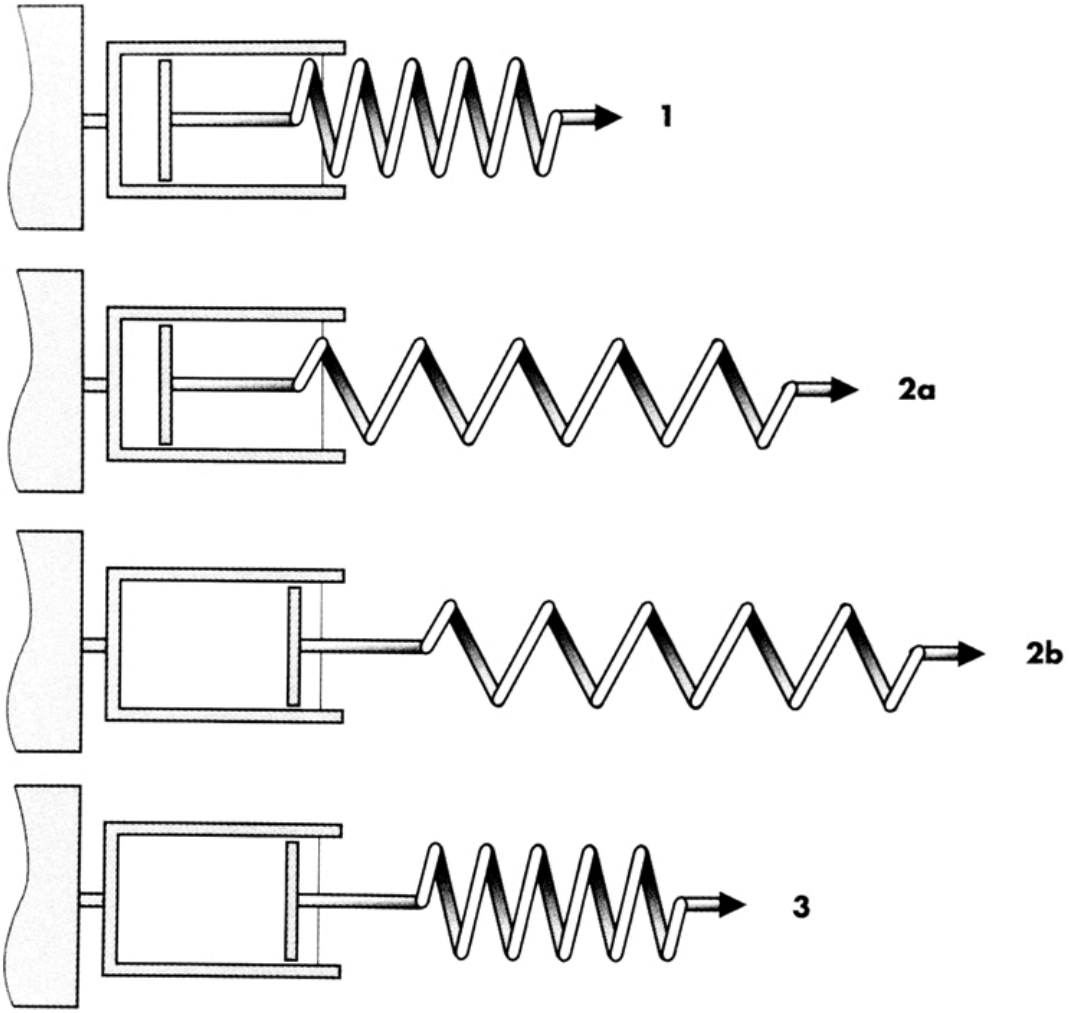

Figure 2.14. *Maxwell model under load (Mezger 2002).*

The behaviour of viscoelastic solids can be illustrated using a combination of a spring and a dashpot in parallel connection. The spring and the dashpot are connected via a rigid frame. This model is called Kelvin/Voigt model (Figure 2.15.)

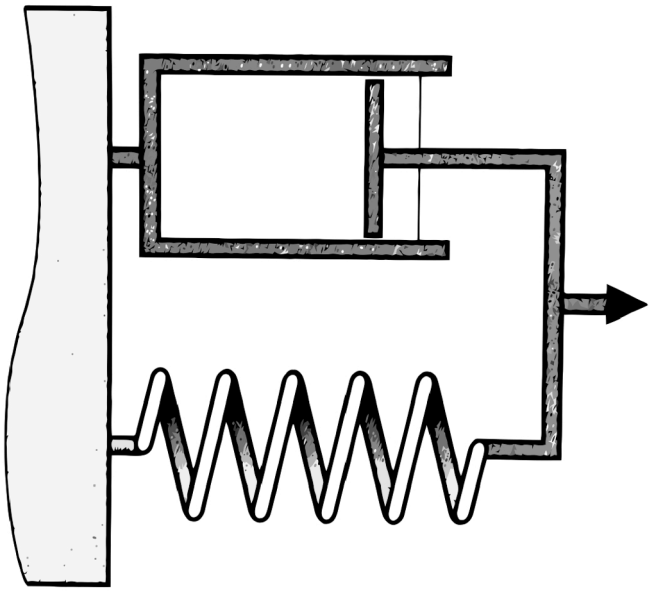

Figure 2.15*. Kelvin/Voigt model (Mezger 2002).*

Figure 2.16 illustrates the deformation behaviour of a viscoelastic solid. The phase 1 demonstrate situation before the load phase, in this phase 1 both components are undeformed. Under the load the two components can only be deformed together because they are connected together via a rigid frame. The deformation increases as long as the constant load force is applied and the spring cannot be deformed spontaneously because its movement is slowed down by the presence of the dashpot (phase 2). When the load is removed the spring immediately tries to re-form elastically and this causes both components to reach their initial positions after the certain period of time. This process is delayed due to the dashpot. When the load is removed the model no longer displays any deformation. After load cycle, the sample of the Kelvin/Voigt model shows delayed but complete re-formation. The deformation process is reversible and the material behaves essentially as a solid and is referred to as a viscoelastic or Kelvin/Voigt solid. (Mezger 2002)

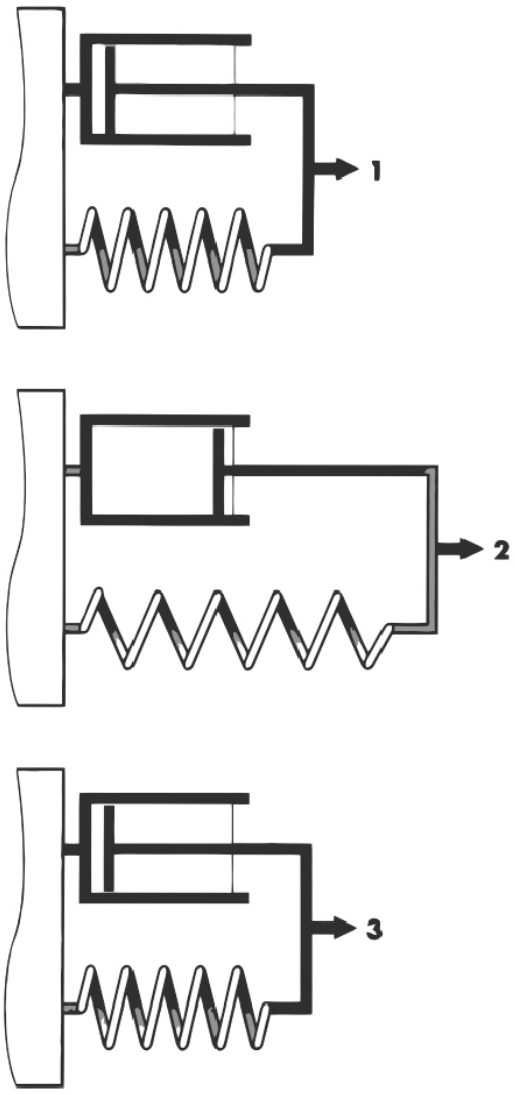

Figure 2.16. *Kelvin/Voigt model under load (Mezger 2002).*

2.3.2 Rheometry

Rheometry is the measuring technology used to determine rheological properties. Rheometer is an instrument used to measure and analyse rheological properties of materials and their behaviour under determined parameters, such as deformation and shear stress. Both liquids and solids can be examined using rotational and oscillatory rheometers. Usually, in study of the flow behaviour of ideal viscous liquids that obeys the Newton's law, the flow or the viscosity curves are determined. Using rheometer for determining the flow behaviour of viscoelastic liquid, the deformation behaviour of viscoelastic solids or ideal elastic solids that obeys Hooke's law, the creep tests, relaxation tests and oscillatory tests are used. (Hutton et al. 1989; Mezger 2002)

To measuring the flow behaviour a flow curve is present with the shear stress as a function of the shear rate $\dot{\gamma}$ and a viscosity curve is present with the shear viscosity η as a function of shear rate $\dot{\gamma}$. Creep tests are used to examine chemically unlinked and

unfilled polymers in the form of melts and solutions. The behavior of chemically cross-linked polymers, gels and dispersions with physical network of forces can be determined. In creep test the creep curve is presented with the deformation as a function of the time. Figure 2.17 shows the creep curve where the time interval between t_0 and t_2 is called the creep curve (or deformation curve) and the second part between t_2 and t_4 is referred to as the creep recovery curve (or reformation curve). The reformation γ_e represents the elastic portion of the viscoelastic behaviour and the deformation γ_v represents the viscous portion. In some cases there is no deformation and the creep recovery curve goes down because the complete reformation. Commonly, viscoelastic liquids show the incomplete reformation and viscoelastic solids show the complete reformation. (Mezger 2002)

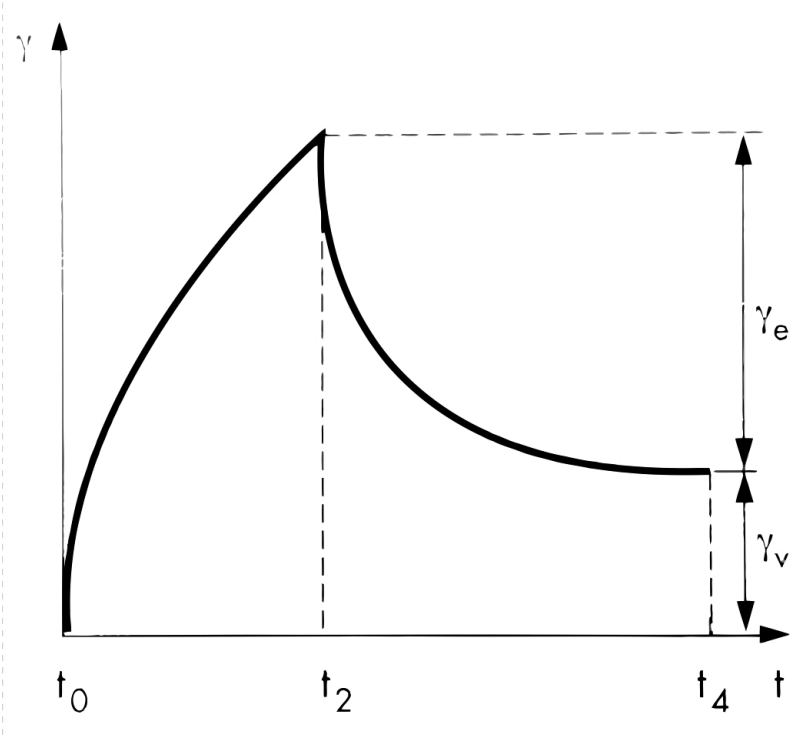

Figure 2.17*. Creep and creep recovery curve with the reformation γ_e and the deformation γ_v (Mezger 2002).*

As the creep test, the relaxation test is also used to examine chemically unlinked and unfilled polymers in the form of melts and solutions. The relaxation test is also suitable for determining the behaviour of chemically cross-linked polymers, gels, and dispersions with a physical network of forces. The relaxation test is also called a step strain or step deformation test or the relaxation test. The viscoelastic behaviour is investigated by performing a strain step in the relaxation test. Figure 2.18 shows the strain step relaxation curve. Low pre-strain γ_1 is set in the time interval between t_1 and t_2 to level out those shear loads that have already acted on the sample during the test preparation. The strain step from γ_1 to constant γ_0 is performed quickly and the strain γ_0

is kept constant in the time interval between t_2 and t_3. (Mezger 2002; Dealy & Larson 2006)

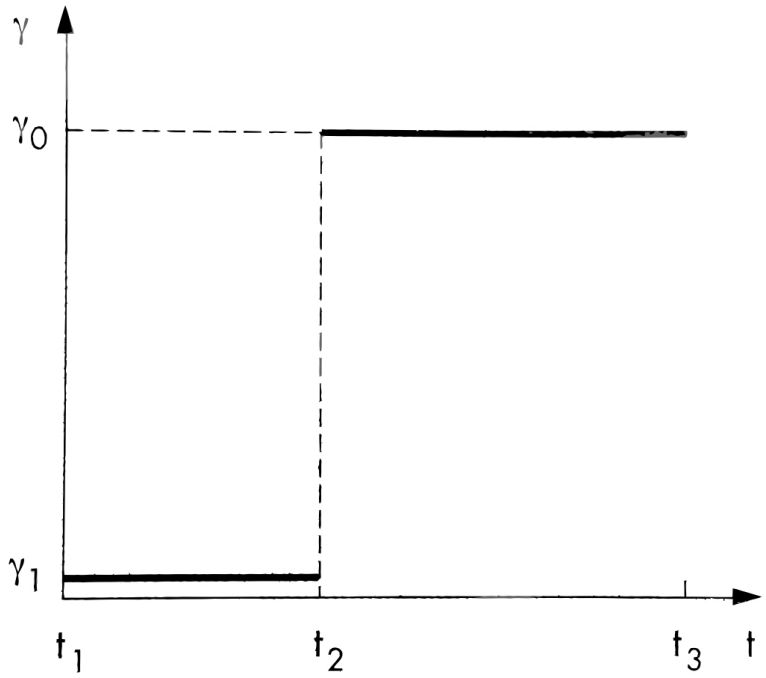

Figure 2.18. *Relaxation test with strain step. (Mezger 2002)*

The relaxation test is represented by a shear stress relaxation curve as in Figure 2.19, which is the stress relaxation curve of viscoelastic material. In Figure 2.19 the viscoelastic liquid (1) shows delayed, complete relaxation and the viscoelastic solid (2) displays delayed, incomplete relaxation. The equilibrium stress τ_e is a final value in which the molecules are chemically or physically connected and cannot move freely. Gels and chemically cross-linked materials display this behaviour. For viscoelastic solid (2) the shear stress only relaxes to a certain extent. The relaxation test may also be represented by a relaxation modulus curve where the relaxation modulus G is a function of time t. The relaxation modulus can be calculated from the strain γ_0 and the stress relaxation function $\tau(t)$. (Mezger 2002; Dealy & Larson 2006)

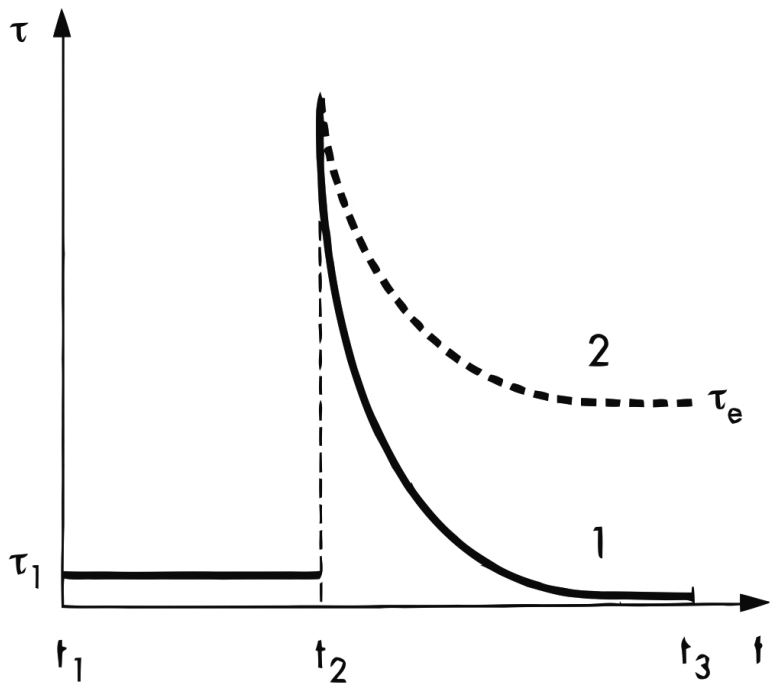

Figure 2.19. *Stress relaxation curves of viscoelastic material (Mezger 2002).*

Oscillatory tests are used to examine all types of viscoelastic materials from low viscosity liquids, gels, polymer melts to elastomers and rigid solids. The flow and the deformation behaviour of a material are measured by an oscillation test. The two-plate-model (Figure 2.20) is used to explain the oscillation test. An eccentrically placed wheel produces the oscillations of the upper plate. (Hutton et al. 1989; Mezger 2002)

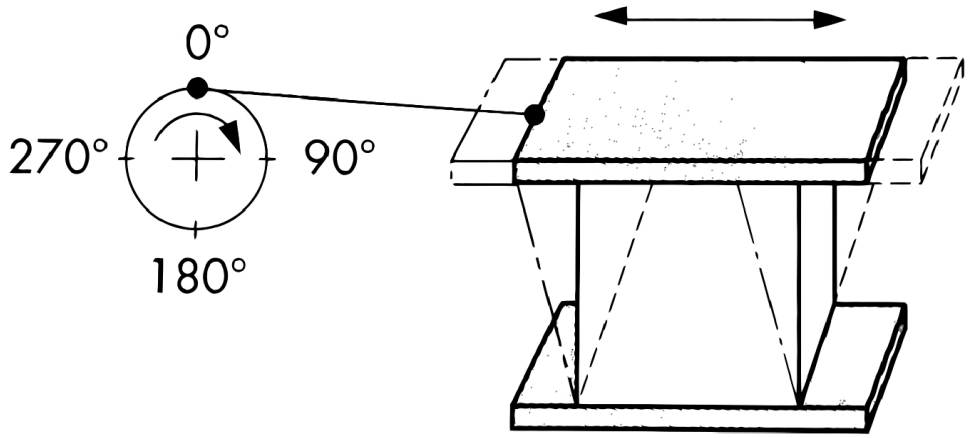

Figure 2.20. *Oscillatory test demonstrated with two plate model (Mezger 2002).*

The upper plate with the shear area A is moved back and forth by the shear force ± F (Figure 2.21). The lower plate stays still. This oscillation causes shearing of a sample that is placed between the two plates. When measuring s sample by oscillatory test, it is important that the sample adheres to both plates and does not slide or slip

along them and the volume of the sample fills homogeneously the whole shear gap (in Figure 2.21 the distance h). Figure 2.21 illustrates shear forces ± F, deflection ± s and deflection angle ± φ of the sample in the shear gap h during an oscillatory test. (Mezger 2002)

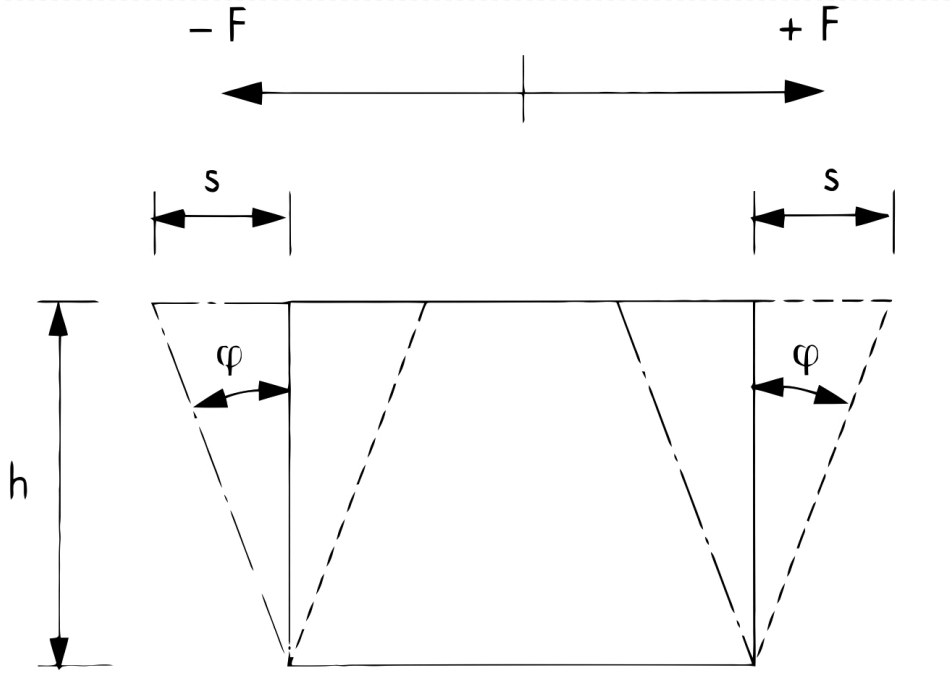

Figure 2.21. *A schematic figure in oscillatory test with shear force ±F, deflection ±s and deflection angle ±φ of the sample in the shear gap. (Mezger 2002)*

Using oscillatory test to determine materials rheological properties amplitude and frequency sweeps, time-dependent behaviour at constant mechanical and isothermal conditions and temperature-dependent behaviour at constant mechanical conditions can be measured. The amplitude sweep is an oscillatory test with variable amplitude and constant frequency values and the frequency sweep is an oscillatory test with variable frequency and constant amplitude values. (Mezger 2002) The oscillatory amplitude and frequency sweeps are presented more closely in Chapter 2.3.3. In time-dependent behaviour at constant dynamic mechanical and isothermal conditions, the amplitude and the frequency are set at a constant value in each individual test interval. The measuring temperature is kept constant (isothermal conditions). The constant dynamic mechanical shear conditions are given. In temperature-dependent behaviour at constant mechanical conditions the amplitude and the frequency are kept constant in each test interval. The temperature is often set as a temperature/time profile T(t) using linear heating or cooling rate in the form of ramps upwards or downwards. This procedure is sometimes called (dynamic) temperature sweep. Alternatively, the temperature is set by using incremental steps in the form of several test intervals, each with a constant temperature for a certain time period. This procedure is called step-and-hold function. Often, these kinds of

temperature-dependent behaviour at constant mechanical conditions are referred to as dynamic mechanical thermoanalysis (DMTA) or dynamic thermomechanical analysis (DTMA). (Dealy & Larson 2006; Mezger 2002)

2.4 Measuring rheological and mechanical properties of hydrogels

2.4.1 Principals of oscillatory testing

The amplitude sweep of oscillatory test is used to determine the linear viscoelastic (LVE) range for hydrogels and to determine moduli of hydrogels. The frequency sweep of oscillatory test is used to examine the behaviour of the storage and loss moduli in the LVE range (using constant deformation). The complex shear modulus is calculated from storage and loss moduli of LVE range. (Mezger 2002)

There are a great numbers of different parameters that are given as results of oscillatory tests. These include a storage modulus G', a loss modulus G'', a complex shear modulus G*, a complex viscosity η*, a real part of complex viscosity η' (represents the viscous behaviour), an imaginary part of complex viscosity η'' (represents the elastic behaviour), a phase shift angle δ and a loss factor tan δ. Moduli, the phase shift angle and the loss factor are the most interesting parameters that are measured to determine rheological properties of hydrogels. There are two ways to determine the presets in oscillatory tests; with controlled shear strain (or controlled shear deformation, CSD) or with controlled shear stress (CSS). In oscillatory tests, the rheometry measures two independent variables. Using the controlled shear strain, the strain (deformation) γ(t) [%] is set as a rheological test presetting parameter and the measuring system of rheometry change the strain as a deflection angle φ(t) [mrad]. Parameters that rheometry measures during the oscillatory test with controlled shear strain are torque M(t) [mNm] and phase shift angle δ [°]. From the torque the shear stress τ(t) [Pa] is calculated. The calculation formulas depend on measuring plates that are used in the rheometer. Using the controlled shear stress, the shear stress τ(t) [Pa] is set as a rheological test presetting parameter. The measuring system of rheometer changes the shear stress to a torque M(t) and measures the deflection angle φ(t) and the phase shift angle δ. The deformation γ(t) [1] is calculated from the deflection angle φ(t). From the raw data of CSD or CSS, the moduli are calculated. (Mezger 2002)

The measured data is always represented on a double logarithmic scale in oscillatory tests. Reason for the logarithmic scale is that the parameter function, which is most interesting for the analysis, shows very low values and the numeral values of the measuring curves usually stretch over several decades. For example the storage modulus lg G' is represented as a function of the strain lg γ as log/log diagram. One exception is time and temperature axes that are generally plotted on a linear scale. For example the storage modulus as a function of time t (lg G'(t)) or temperature T (lg G'(T)) as semi-

logarithmic (log/lin) diagrams. Generally, the storage and the loss moduli are represented together in the same diagram. (Mezger 2002; Dealy & Larson 2006)

When measuring viscoelastic behaviour of a material by an oscillatory test the sample is subjected to a homogeneous deformation at a sinusoidal varying shear strain or shear stress. (Dealy & Larson 2006) The sinusoidal strain can be represented as a sine function is $\gamma(t) = \gamma_A \times \sin\omega t$ with the strain amplitude γ_A [%] and the angular frequency ω [1/s]. The preset sine curve with controlled shear strain γ is represented in Figure 2.22 (left) If the strain amplitude is sufficiently small that the response is linear, the resulting stress is also sinusoidal. The resulting stress can be written in terms of the stress amplitude τ_A [Pa] and the phase shift angle δ. The resulting stress sine function is $\tau(t) = \tau_A \times \sin(\omega t + \delta)$. Figure 2.22 (right) represents the resulting sine curve of controlled shear stress with the phase shift angle δ. Sometimes the phase shift angle between the preset and the resulting curve is called a loss angle. The phase shift angle is always given in degrees [°], not in rad and this phase shift angle is always between 0° and 90°. With controlled shear stress the preset sine function is $\tau(t) = \tau_A \times \sin\omega t$ with the shear stress amplitude τ_A [Pa] and the resulting strain curve as a phase shifted sine function is $\gamma(t) = \gamma_A \times \sin(\omega t + \delta)$. (Mezger 2002)

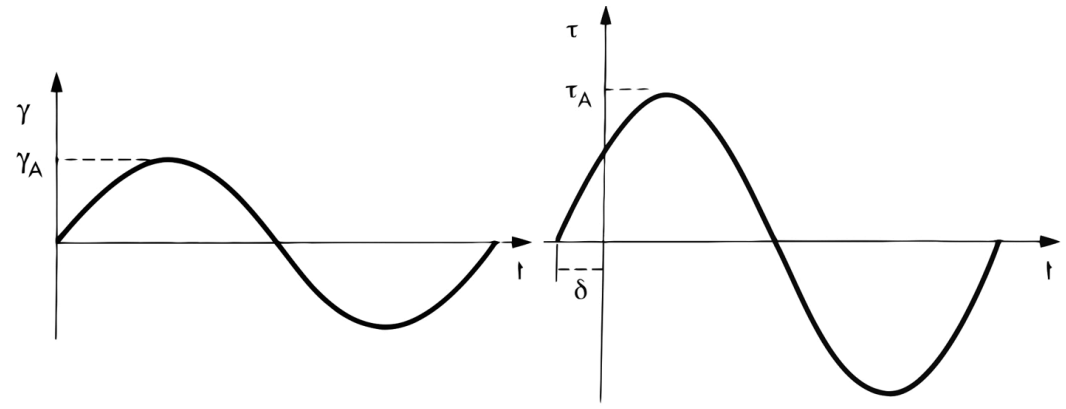

Figure 2.22. *Preset (left) and resulting (right) sine curves with controlled shear strain. In resulting curve shows the phase shift angle δ (Mezger 2002).*

When measuring rheological parameters using an oscillatory test, the complex shear modulus, the storage modulus and the loss modulus are calculated. The complex shear modulus G* [Pa] is calculated as follows

$$G^* = \frac{\tau(t)}{\gamma(t)} \qquad (7)$$

where the function of the sinusoidal $\tau(t)$ is in [Pa] and the sinusoidal $\gamma(t)$ is with unit [1] or in [%]. The complex shear modulus represents the rigidity of the sample, i.e. resistance to deformation. (Mezger 2002; Dealy & Larson 2006) The complex shear modulus is always marked with a star to differentiate it from normal shear modulus G

that is not measured in an oscillatory test. Parameters that result from a harmonic-periodic, sinusoidal shear load should always be marked in the complex form, using a star. It is important to differentiate G* from a complex modulus E* which is measured in tension, compression or bending. (Mezger 2002)

The storage modulus G' represents the elastic behaviour (also called elastic modulus) of a sample and it is calculated from cosine function

$$G' = \left(\frac{\tau_A}{\gamma_A}\right) \times cos\delta \qquad \textbf{(8)}$$

where τ_A is the stress amplitude, γ_A is the strain amplitude and δ is the phase shift angle. The G' is a measure of the deformation energy stored in the sample during the shear process. This energy is completely available after the load is removed and this energy acts as the driving force for the reformation that partially or totally compensates the previous deformation. If the sample remains in an unchanged form after the load is removed, it displays reversible deformation behaviour and is called an energy storing material. (Dealy & Larson 2006; Mezger 2002)

The loss modulus G'' represents the viscous behaviour (also called viscous modulus) of a sample and it is calculated from sine function

$$G'' = \left(\frac{\tau_A}{\gamma_A}\right) \times sin\,\delta \qquad \textbf{(9)}$$

G'' is a measure of the deformation energy used up in the sample during the shear process and lost after the load is removed. This energy is either used up during the process of changing the structure of the sample or wasted into the surrounding environment in the form of heat. If the sample is found to be in a changed form after the load cycle, it displays irreversible deformation behaviour and is called an energy losing material. (Dealy & Larson 2006; Mezger 2002)

The loss factor, also called the damping factor, tan δ is calculated as the quotient of the lost and storage deformation energy. The loss factor is a ratio of the viscous and the elastic portion and it is calculated from formula

$$tan\,\delta = \frac{G''}{G'} \qquad \textbf{(10)}$$

The tan δ gets values $0 \leq \tan\delta \leq \infty$ because $0° \leq \delta \leq 90°$. Ideal elastic deformation behaviour is expressed as tan δ = 0 or δ = 0° because G' completely dominates G''. Whereas, ideal viscous flow behaviour is expressed as tan δ = ∞ or δ = 90° because G'' completely dominates G'. When G' = G'', viscous and elastic behaviour are balanced and tan δ = 1 or δ = 45°. For example when examining hardening or gel formation process (sol/gel transition point) reaching tan δ = 1 is an important analysis criterion. In

liquid state tan δ > 1 because G'' > G' and in the gel state tan δ < 1 because G' > G''. (Mezger 2002)

The complex shear modulus G* can be illustrated in a vector diagram where G'' is represented in a function of G'. The vector diagram represents the viscoelastic behaviour of material including the viscous and elastic portion. The vector diagram is demonstrated in Figure 2.19 where G' is plotted on the x-axis and the G'' on the y-axis. The length of the vectors illustrates the value of the corresponding parameter. G* represents the complete viscoelastic behaviour which consists of the both the elastic and the viscous components and therefor, G* is the vector sum. The total amount of G* can be calculated from Pythagoras' theorem

$$|G^*| = \sqrt{(G')^2 + (G'')^2} \qquad \textit{(11)}$$

As seen in Figure 2.23, the loss factor is calculated from the formula (10) due to the trigonometric relation in a rectangular triangle. (Mezger 2002)

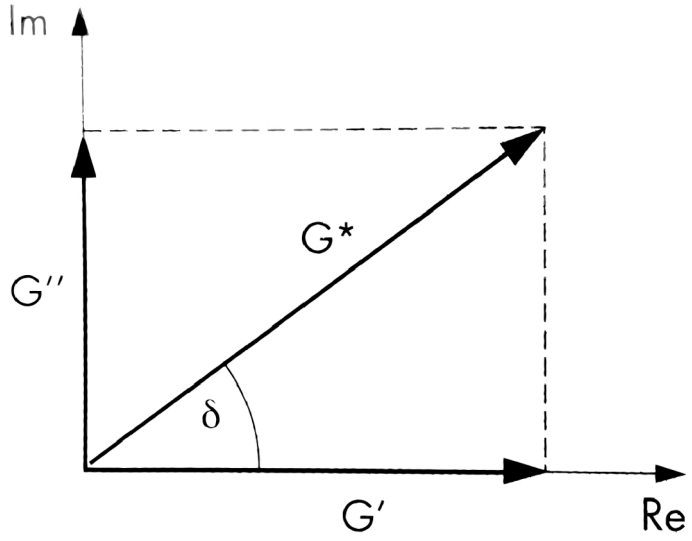

Figure 2.23. *Vector diagram with G', G'' and the resulting vector G* (Mezger 2002).*

In rheometry it is possible to use various measuring systems (MS), such as a coaxial cylinder measuring system (CC MS), a cone-and-plate measuring system (CP MS), a parallel-plate measuring system (PP MS) or relative measuring systems, for example different spindles. (Mezger 2002) In this thesis work PP MS is used as a measuring system.

The PP MS consists of two plates. Figure 2.24 demonstrates the PP MS where R is the plate radius and H is the distance between two parallel plates, the gap. According to (DIN 53018-1:1976-03, Viscometry; measurement of the dynamic viscosity of newtonian fluids with rotational viscometers; principles 1976) the gap must obey H <<

R. For materials with high cohesive forces and large gap it should be taken into account that the sample flows inhomogeneously across the entire shear gap. When the gap is large, there is an increasing risk that the degree of inhomogeneous shear behaviour in the gap will increase and causes errors in the results. When H > 1 mm, this kind of inhomogeneous shear behaviour should be taken account. (Mezger 2002)

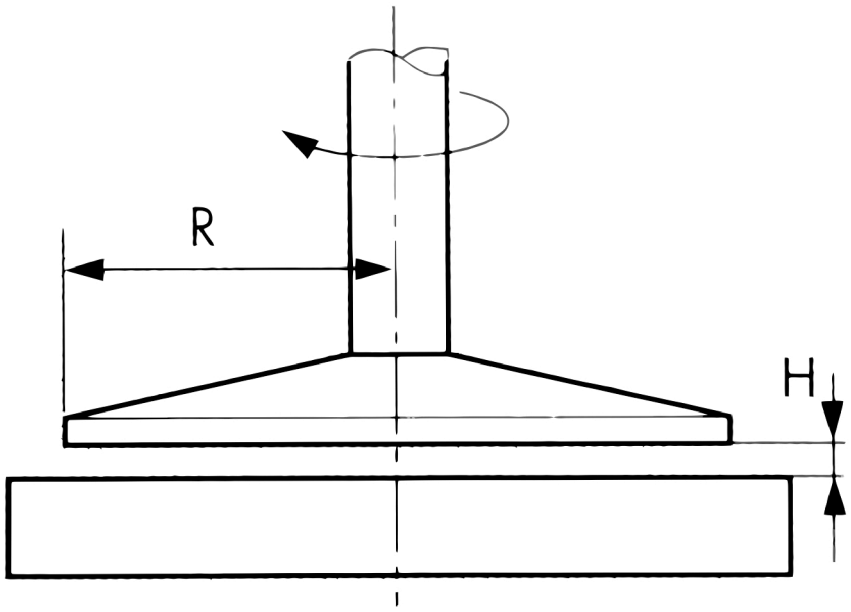

Figure 2.24. *The parallel-plate measuring system, PP MS (Mezger 2002).*

Amplitude sweeps are mostly carried out for the purpose of determining the limit of the LVE range. The amplitude sweep does not examine the sample in a state of rest because the sample is often tested at a frequency of 1 Hz. (Dealy & Wissbrun 1990) This shear load does not represent the condition at rest. In the amplitude sweep test, controlled shear deformation (CSD) $\gamma(t) = \gamma_A \times \sin\omega t$ with constant angular frequency ω and the variable strain amplitude γ_A (Figure 2.25) or controlled shear stress (CSS) $\tau(t) = \tau_A \times \sin\omega t$ with constant angular frequency ω and variable stress amplitude τ_A can be used. The angular frequency can be transformed to frequency by using formula $\omega = 2\pi f$. The unit for angular frequency is [1/s] or [rad/s] and the unit for frequency is [Hz] (Hertz), the angular frequency ω = 10 1/s corresponds to a frequency f = approx. 1.6 Hz. (Mezger 2002)

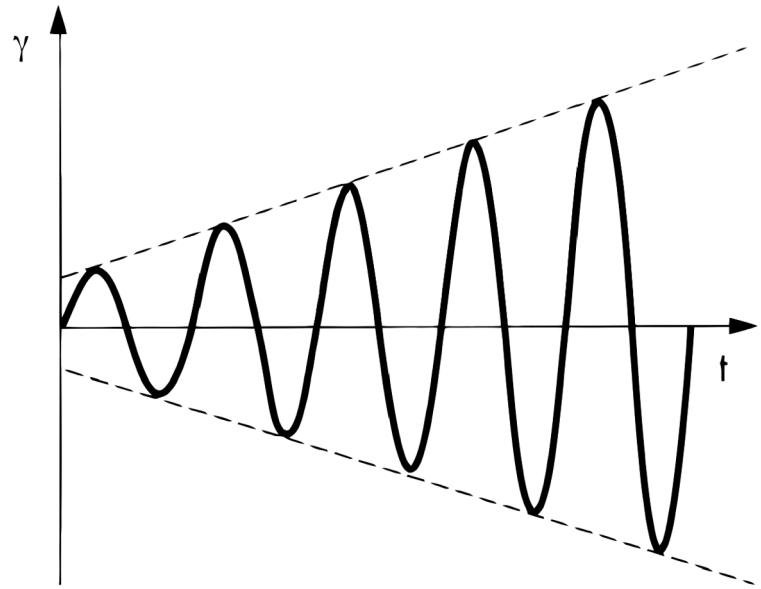

Figure 2.25. *Amplitude sweep with controlled shear strain (Mezger 2002).*

In the measurement results, the lg G' and lg G'' are presents as a functions of lg γ as seen in Figure 2.25. Sometimes the loss factor tan δ is also displayed on the y-axis. In Figure 2.26 the LVE deformation range with the limiting value γ_L is demonstrated. In the LVE range, both of the functions G'(γ) and G''(γ) have a constant plateau value and the resulting curves are linear straight lines in the diagram. The LVE range ends at the limiting value γ_L. At amplitudes lower than γ_L, the G' and G'' curves show a constantly high plateau value where the structure of the sample is stable under this low deformation condition. Whereas, at amplitudes higher than γ_L, the LVE range ends and the structure of the sample has already been irreversibly changed or even totally destroyed. (Mezger 2002)

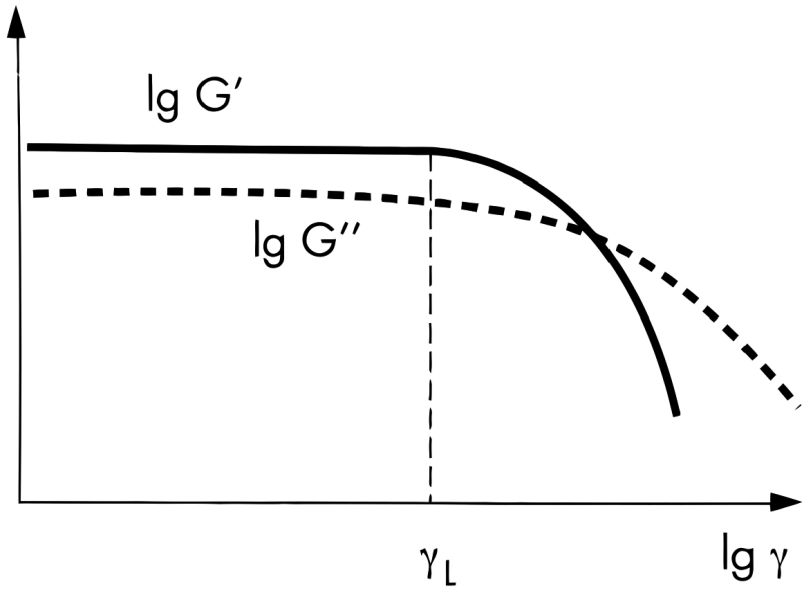

Figure 2.26. *Moduli of the G', the G'' and LVE range in a function of γ with limiting value γ_L (Mezger 2002).*

There are several options to determine the limit of the LVE range such as visual or manual analysis or automatic analysis using a software analysis program. In visual analysis, the user observes the curve and decides at which limiting value γ_L it falls obviously. To make the visual analysis easier, the straight line along the level of the plateau value can be drawn. This line is called analysis tangent. One option, which has been used also in this thesis work, is manual analysis from the measuring data table. The γ_L is taken at the point at which deviation tolerance that determines the change of the G'(γ) value, for example as 1 %, 5 % or 10 %. (Mezger 2002)

In the characterisation of a sample in the LVE range, it is important to determine the behaviour of both G' and G''. For gels, the elastic behaviour dominates over the viscous behaviour and G' > G''. The structure shows certain rigidity and the sample has gel structure. If G'' > G', the viscous behaviour dominates over the elastic behaviour. The sample shows the character of a liquid and it does not remain in stable form. (Mezger 2002)

The yield point τ_y is possible to determine from the amplitude sweep. The τ_y is the τ value at which the measuring curve deviates obviously from the plateau value or from the drawn analysis tangent. This τ_y value can be read off the measuring data table and using the tolerated deviation. The τ_y is also possible to determine using a software analysis program. (Dealy & Larson 2006) The τ_y defines a certain amount of force that must be applied before the material starts to flow. Below the τ_y the material shows elastic behaviour and it behaves like rigid solid. Under load it displays only a very small degree of deformation that does not remain after removing the load. Below the τ_y the

external forces F_{ext} are smaller than the internal forces F_{int} ($F_{ext} < F_{int}$) and above the $F_{ext} > F_{int}$. The yield point is also called as yield stress or yield value. (Mezger 2002)

Outside the LVE range for cross-linked materials, such as hydrogels, the curves of G' and G'' do not fall constantly with increasing deformation. The G'' curve shows increasing values at the same time the G' curve decreases. The range of irreversible deformation occurs outside the LVE range and before the crossover point where G' = G''. In this crossover point the structure of material is completely destroyed. (Mezger 2002)

Before the frequency sweep, the LVE range must be determined by amplitude sweep. After amplitude sweep the test conditions for the frequency sweep can be selected to ensure that the test is measured in the LVE range. The constant strain value is selected from LVE range and the range of oscillations per unit is chosen. There are two options to define the oscillations per time unit, as frequency f with the unit [Hz] or as angular frequency ω with the unit [1/s]. In the frequency sweep, controlled shear strain (deformation) $\gamma(t) = \gamma_A \times \sin\omega t$ with the constant γ_A and the variable angular frequency $\omega = \omega(t)$ or controlled shear stress $\tau(t) = \tau_A \times \sin\omega t$ with the constant τ_A and the variable $\omega = \omega(t)$ can be used. Figure 2.27 illustrates the frequency sweep with controlled shear strain and the variable frequency. Measuring results are presented in a diagram where the lg G' and the lg G'' are in a function of lg f. (Mezger 2002)

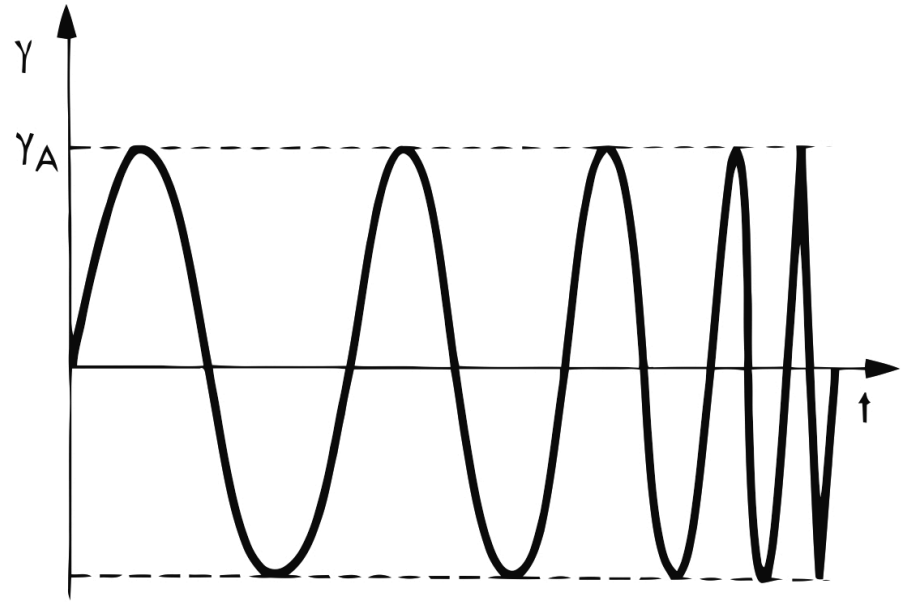

Figure 2.27*. Frequency sweep with controlled shear strain (Mezger 2002).*

In cross-linked materials, the networks between polymer chains prevent the chains to move along each other without cutting the bonds. The degree of deformation depends on the length of these linkages. For cross-linked materials with dense meshed networks, such as hydrogels, the LVE range is achieved when using only a considerable low maximum deformation. In a higher maximum deformation the LVE range for hydrogels is exceeded. Typical behaviour for cross-linked materials in frequency sweep

at low frequencies is that the G'(ω) and the G''(ω) curves are almost parallel straight lines in a constant limiting values (which are not zero). (Mezger 2002) This typical behaviour of cross-linker materials in frequency sweep is illustrated in Figure 2.28.

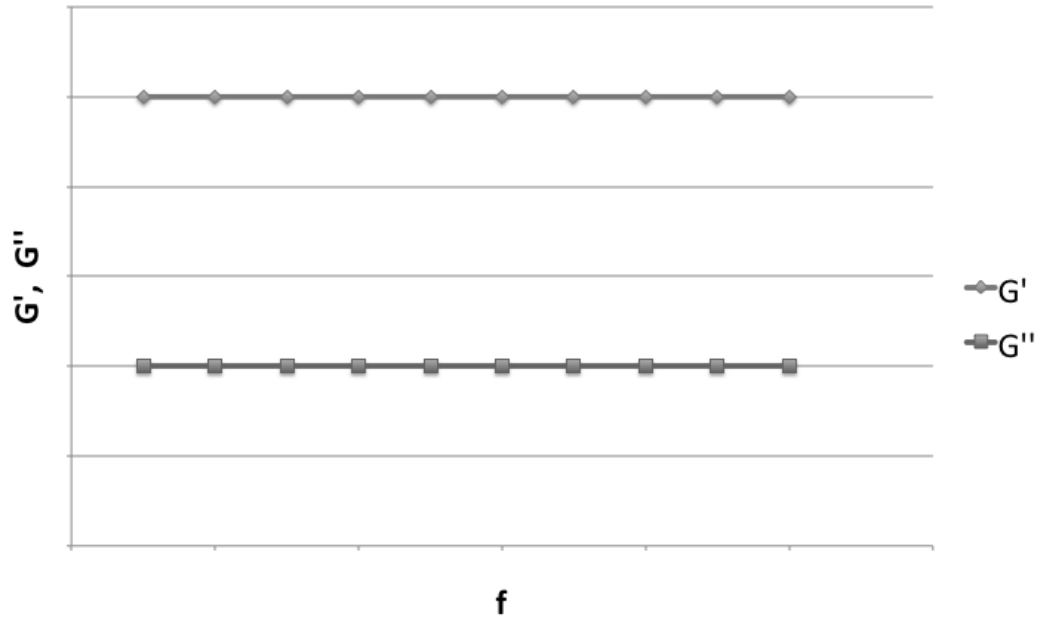

Figure 2.28*. Typical behaviour of cross-linked material in frequency sweep.*

Often for the densely cross-linked polymers, the G' is high in relation to the G'' and the relation could be G': G'' = 100:1 to 1000:1. Due to intermolecular interaction forces, hydrogels build up an internal network of forces. Under load within the LVE range, the hydrogel sample with stable structure typically displays G' > G'' and the elastic behaviour dominates over the viscous behaviour. (Mezger 2002)

Factors that should be considered for obtaining reliable data by rheometer are sample preparation, trimming of the sample, thermo-oxidative degradation, maximum amplitude for linear behaviour and repeat measurements to determine precision. One important factor for obtaining reliable data is the sample preparation. The preparation should be carried out in an order that no residual stresses are formed. This residual stress deforms the measuring data. Great care must be taken to make sure that the trimming of the samples after insertion in the rheometer and the procedure for loading are always the same. The sample must be trimmed very carefully to avoid destroying the sample. The measuring temperature should be under control because rheological properties depend strongly on temperature. Using a common type of temperature control chamber for rheometers in which a continuous flow of heated nitrogen flows through the chamber prevents thermo-oxidative degradation. To avoid thermo-oxidative degradation it is important to make sure that the sample is stabilized. The sample must be stable before measuring, the temperature must be established and residual stresses must be relaxed. To find the LVE range it must be pay attention to values of strains. A

good advice is to start from the lower strains towards the higher instead of destroying the sample at the beginning of the measurement by using the too high deformations. (Dealy & Larson 2006)

2.4.2 Principals of mechanical testing

The mechanical behaviour of hydrogels depends mainly on the network structure of the hydrogel. When the crosslinking density is increased, the mechanical properties are increased at the expense of swelling. Crosslinking of hydrogels can be produced by bulk or surface crosslinking. Bulk crosslinking leads to homogenous crosslinking and surface method to heterogeneous crosslinking. Bulk crosslinking occurs when the cross-linker is miscible in the monomer. Surface crosslinking is incorporated during the hydrogels synthesis using water-insoluble cross-linker or after the hydrogels is formed. In the swollen state, hydrogels with a high crosslinking density that are produced by bulk crosslinking are brittle whereas hydrogels that are produced by surface crosslinking are tough. (Ottenbrite et al. 2010)

Deswelling of hydrogels is related to mechanical properties of hydrogels. In weak hydrogels the absorpted water in a structure evaporates to a greater extent. In fully swollen state a weak hydrogel under mild stress can break apart into smaller swollen particles. These smaller particles cause faster evaporation and increase the contact area of swollen hydrogels with the dry surrounding environment. There are many factors that have an effect on evaporation of hydrogels. The evaporation rate depends on how wet the surrounding environment is. The dryer the surrounding environment is, the faster the evaporation process is. Generally, the evaporation processes occur at the liquid-air, liquid-liquid and liquid-solid interface depending on the applications. (Ottenbrite et al. 2010)

Characterization of the mechanical properties of hydrogels can be problematic due to inherent weakness of hydrogels. Measuring mechanical properties of hydrogels is important in the study of hydrogels designed to function as support structure and physical barriers. (ASTM F2900-11, Standard guide for characterization of hydrogels used in regenerative medicine 2011) There are several measurements for determining the mechanical properties of hydrogels, such as indentation testing, compression testing, tensile testing, dynamic mechanical analysis (DMA), rheology, atomic force microscopy (AFM) and magnetic resonance elastography (MRE). (Brandl et al. 2007; ASTM F2900-11, Standard guide for characterization of hydrogels used in regenerative medicine 2011)

The indentation test is a simple approach to the investigation of hydrogel mechanical properties. The indentation test is a hardness test in which the hardened intender is forced against a sample under a fixed load. The indentation test can be carried out using commercially available texture analyzers. The indentation tests can be nano-indentation or micro-indentation studies. One method to use the indentation test is that the applied load is ramped up for a given amount of time and then held at a constant

value at the defined period of time. During this measuring, the displacement of the sample with time is recorded. (ASTM F2900-11, Standard guide for characterization of hydrogels used in regenerative medicine 2011)

In **the tensile test** the sample is prepared as a dog bone shape and placed between two clamps. The sample is stretched at constant extension rates. The Young's modulus E of the hydrogel is determined from these experiments. The E is defined as the ratio of tensile stress and tensile strain. The maximal tensile stress carried by a hydrogel is defined as the tensile strength. (Brandl et al. 2007)

DMA is testing method to study and characterize mechanical properties of materials and it is typically performed to measure the viscoelastic behaviour of materials. A sinusoidal load is applied on the sample and the strain of the material is measured. In the DMA testing method various geometries and related measuring procedures exist. In the DMA measuring method the stress can be applied via torsional or axial analyzers. One common measuring system in DMA is compression, where the sample is dynamically compressed. Comparing the DMA to an oscillatory shear rheometer, the main differences are that the rheometer applies shear forces while DMA applies, for example, compression forces. (Meyvis et al. 2002; Brandl et al. 2007)

AFM is not only for imaging the topography of surfaces but also for measuring forces on a molecular level. In AFM the sample is compressed by the indenting AFM tip to investigate the mechanical properties of hydrogels. The force-indentation-curves are recorded and fitted to the Hertz model for calculation of Young's modulus. **MRE** is used to characterize the mechanical properties of hydrogels in some instance where hydrogels will be too weak to undergo rheological or mechanical testing. In MRE shear waves are caused within the sample using an electro-mechanical actuator coupled to a surface of the object. The displacement patterns corresponding to the shear waves can be measured when using a magnetic resonance imaging (MRI) system with an additional motion-sensitizing gradient. (Brandl et al. 2007)

In **the compression test**, hydrogel is placed under measuring heads and then a specific force is applied at a constant rate. The hydrogel resist the continuous load by deforming itself until the applied load becomes stronger than the resistance of the hydrogel. This point is called the breaking point and it is the point where the hydrogel reaches its maximum deformation and then fails. Deformation of the hydrogel depends on the structure of the hydrogel and it can be fast or slow. Figure 2.29 demonstrates the ideal load-deforming graft. The slope I in the load-deformation curve shows the hydrogel's resistance to the applied load. When the slope becomes sharper, the hydrogel's resistance and hydrogel's modulus become higher. The point II is a region where the hydrogel starts to break and the top of the point II expresses the maximum strength of the hydrogel. The region III illustrates the rate at which the hydrogels breaks apart, fast or slow. If the slope is sharp, the hydrogel breaks apart fast in a brittle fracture mode. The breaking or failing process occurs slowly and the hydrogel breaks in a ductile mode when the slope is mild. (Ottenbrite et al. 2010)

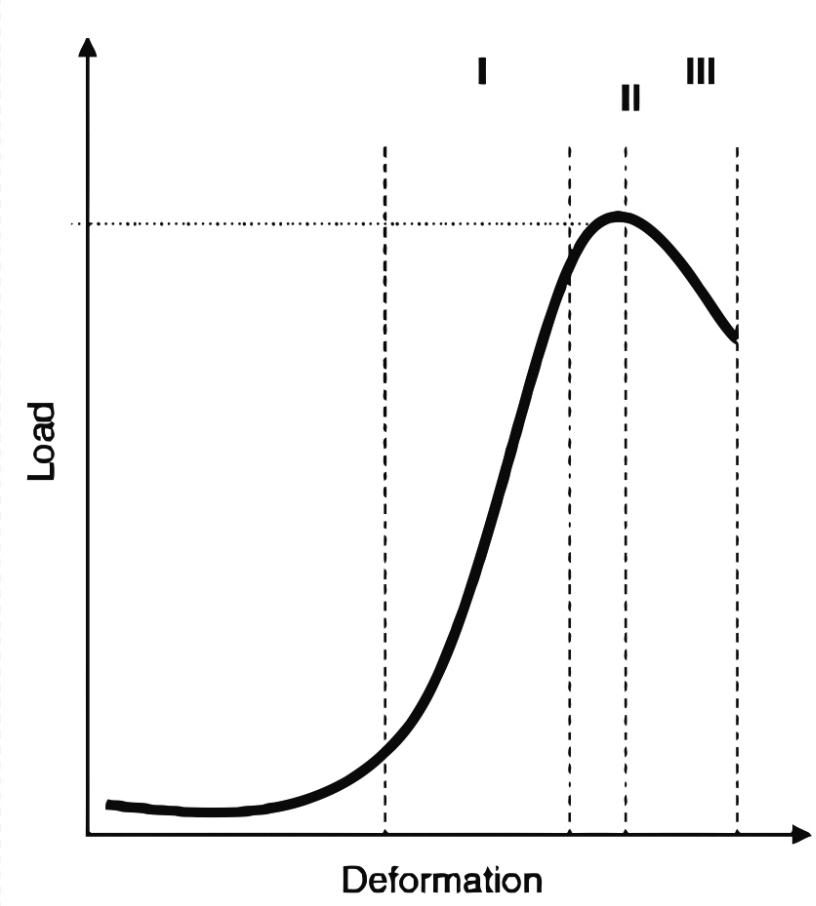

***Figure 2.29**. Load-deforming graft of hydrogels (Ottenbrite et al. 2010).*

A compression test is very similar to the tensile test except that the force is compressive and the specimen contracts along the direction of the stress. The compressive stress σ is calculated from formula

$$\sigma = \frac{F}{A_0} \qquad \textbf{(12)}$$

in which F is the instantaneous load applied perpendicular to the specimen cross section and A_0 is the original cross-sectional area before any load is applied. The unit for F is newton [N] and for A_0 square meter [m^2]. The compression stress is usually in unit megapascal [MPa], or in unit kilopascal [kPa] for less stiffer materials, and 1 MPa = 10^6 N/m^2. The compression strain ε is calculated using the formula

$$\varepsilon = \frac{l_i - l_0}{l_0} = \frac{\Delta l}{l_0} \qquad \textbf{(13)}$$

where l_i is the instantaneous length, l_0 is the original length before any load is applied and Δl is the deformation elongation. Although, the strain is unitless, sometimes strain is expressed as a percentage in which the strain value is multiplied by 100. Since, the original length is greater than the instantaneous length, the compression strain is negative. (Callister & Rethwisch 2007)

The compression stress and strain are proportional to each other through the relationship in the formula (5). The constant proportionality E [GPa] in the Hooke's law is the Young's modulus or modulus of elasticity. This kind of deformation where stress and strain are proportional is called elastic deformation. This relationship between stress and strain is linear and when the applied load is released the sample returns to its original shape. Figure 2.30 shows linear elastic deformation for loading and unloading cycles. When the load is released the line is traversed in the opposite direction compared to the loading cycle. The slope represents the modulus of elasticity E. (Callister & Rethwisch 2007)

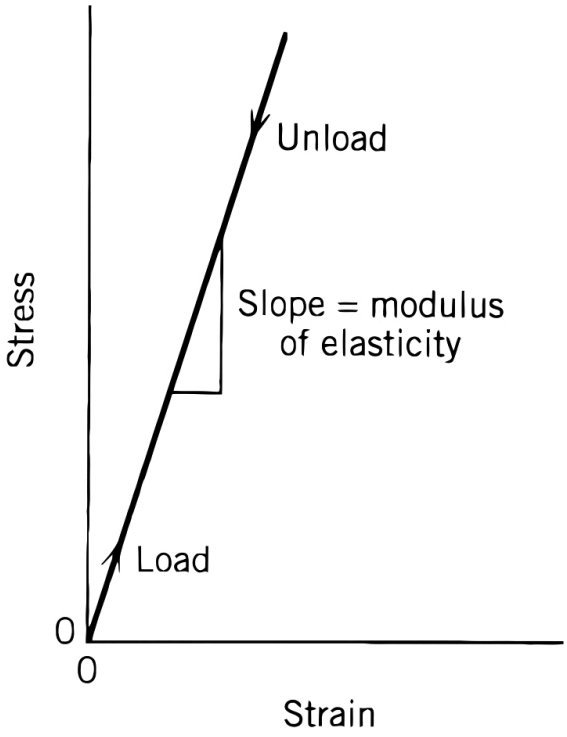

Figure 2.30. *The linear elastic deformation for loading and unloading cycles (Callister & Rethwisch 2007).*

There are materials for which the elastic portion of the stress-strain curve is not linear. Examples of these non-linear behaviour materials are grey cast iron and concrete. For determining the modulus of elasticity for these materials, the tangent or secant modulus is used. The tangent and secant moduli are demonstrated in Figure 2.31 in which the tangent modulus is taken as the slope of the stress-strain curve at a specific level of stress and the secant modulus is the slope that is drawn from origin to some

given point of the stress-strain curve. (Callister & Rethwisch 2007) When the elastic portion of the stress-strain curve is not linear, the interpretation of modulus can differ a lot depending on which point the slope is determined at.

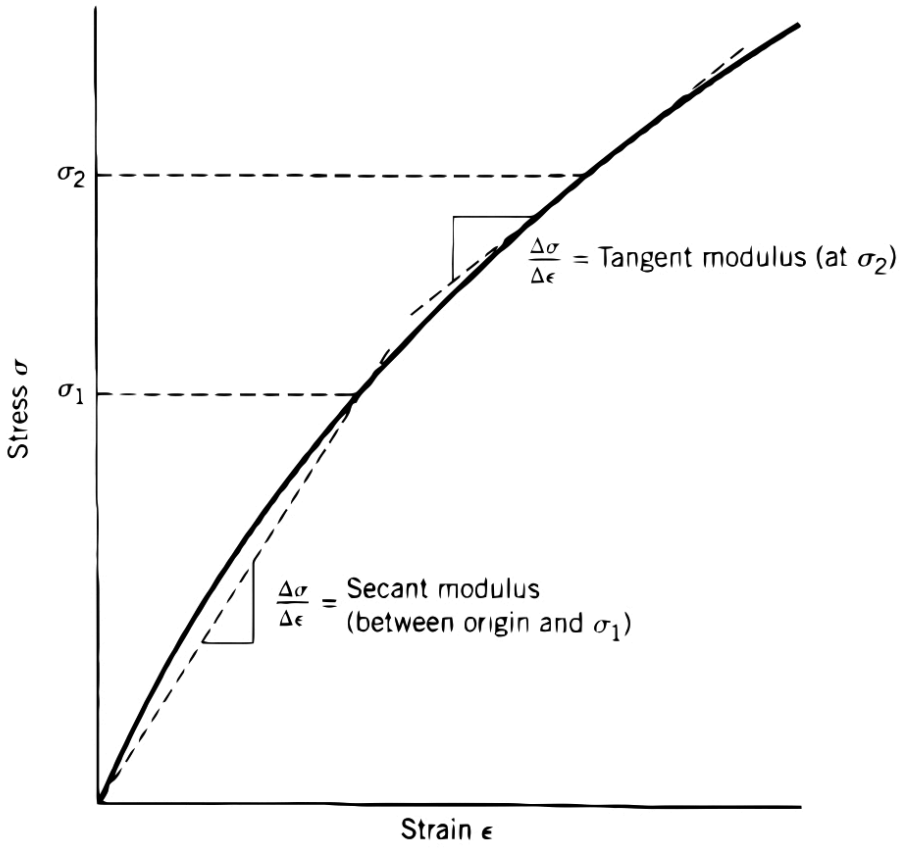

***Figure 2.31**. A demonstration of the tangent and secant moduli (Callister & Rethwisch 2007).*

2.4.3 Rheological and mechanical testing of hydrogels in previous studies

Rheological and mechanical properties of hydrogels have been measured by different methods in previous studies. Many different hydrogels have been measured with different cross-linker concentrations, with different modifications and with different combination of reactive materials.

In (Eljarrat-Binstock et al. 2007) research, the hydroxyethyl metacrylate (HEMA) hydrogels that were cross-linked with ethylene glycol dimethacrylate was compressed. They used two different types of HEMA hydrogels, wet hydrogels and dry hydrogel sponges. Dry hydrogel sponges were re-hydrated before compression test. The E varied from 0.01 to 0.09 MPa depending on the amount of water in structure. The fracture strength values were from 16 to 73 kPa and the fracture strain values were from 55.4 to 63.1 %.

In studies of (Silva et al. 2013), different forms of gellan gum hydrogels were measured by rheological and compression test. The measured E varied from 234 to 535 kPa in LAGG hydrogels whereas the E varied from 6.9 to 87 kPa in HAGG hydrogels. The LAGG and HAGG blends had the E values from 57.8 to 110.5 kPa. Fracture strength values for LAGG hydrogels were from 108 to 172 kPa, for HAGG hydrogels from 40 to 73 kPa and for LAGG and HAGG blends from 68 to 92 kPa. The fracture strain values varied from 29 to 53 % for LAGG hydrogels whereas for HAGG hydrogels fracture strain varied from 61 to 73 %. The fracture strain for LAGG and HAGG blends were from 48 to 60 %. The G' values in rheological measurements for LAGG hydrogels varied from 158 to 267 kPa and the G'' values were from 5.9 to 11.1 kPa. For HAGG hydrogels, the G' values were from 1.0 to 1.3 kPa and the G'' values were 0.02 to 0.07 kPa. For the LAGG and the HAGG blends these moduli were from 14.1 to 19.3 kPa and from 0.4 to 0.5 kPa.

According to research of (Ahearne & Kelly 2013), the fibrin, agarose and gellan gum hydrogels were measured by compression. They determined equilibrium modulus by compressing each hydrogels at a rate of 1 μm/s until reaching a 10 % strain and then holding this strain until the hydrogels had completely relaxed. In addition, the dynamic modulus was determined by applying cyclical 1 % strain at 1 Hz for 10 cycles. The equilibrium modulus for fibrin hydrogels was approximately 1.07 kPa, for agarose hydrogels 10.52 kPa and for gellan gum hydrogels 6.55 kPa. The dynamic modulus for fibrin hydrogels was 36.69 kPa, for agarose hydrogels 46.95 kPa and for gellan gum hydrogels 40.35 kPa.

In (Ghosh et al. 2005) research, the HA hydrogels with different ratio of poly-(ethylene glycol) diacrylate as a cross-linker were measured by rheological method. They used frequency sweep for determination of G' modulus. The HA hydrogels had the G' values from 0.150 to 2.0 kPa.

In research of (Stammen et al. 2001), two different formulations of PVA hydrogels were tested by compression and shear. In compression test, the samples were preloaded and cyclically preconditioned for 10 cycles between 1 and 10 N to reduce the influence of surface artifacts. In shear test, the torsional and horizontal compression were applied. The compression tangent modulus varied from 1 to 18 MPa and the shear tangent modulus varied from 100 to 400 kPa.

3 MATERIALS AND METHODS

3.1 Tested materials

Gellan gum hydrogels:

- Gellan gum (GG) + spermine (SPM) (1.1 % w/v of SPM), GG-1.1SPM
- Gellan gum + SPM (0.6 % w/v of SPM), GG-0.6SPM
- Gellan gum + SPM (0.4 % w/v of SPM), GG-0.4SPM
- Gellan gum + SPM (0.3 % w/v of SPM), GG-0.3SPM
- Gellan gum + spermidine (SPD) (3.1 % w/v of SPD), GG-3.1SPD
- Gellan gum + SPD (1.57 % w/v of SPD), GG-1.57SPD

Hyaluronic acid hydrogels:

- Hyaluronic acid (HA) + polyvinyl alcohol (PVA, P4) (1.5% w/v of PVA), HA1-P4 (1.5%)
- Hyaluronic acid + PVA (0.375% w/v of PVA), HA1-P4 (0.375%)
- Hyaluronic acid + PVA (1.5% w/v of PVA), HA3-P4 (1.5%)
- Hyaluronic acid + PVA (0.375% w/v of PVA), HA3-P4 (0.375%)
- Hyaluronic acid + PVA (1.5% w/v of PVA), HAJ1-P4 (1.5%)
- Hyaluronic acid + PVA (1.5% w/v of PVA), HAJ2-P4 (1.5%)

PuraMatrix as a reference material

3.2 Production of the solutions

A required amount of sucrose (Sucrose – BioXtra, ≥ 99.5 %, S7903, Sigma Aldrich, Saint Louis, USA) was weighed, depending on the amount of preparing solutions. Sucrose is a dissolving liquid for the GG and cross-linker solutions. Additionally, the sucrose is added to make the gel isotonic avoiding the osmotic pressure from interfering the cells. The concentration of sucrose was always 1.0 mg/10ml (10 % sucrose) regardless of the amount of prepared sucrose. The weighted sucrose was poured by distilled water and volume was adjusted after the sucrose was dissolved. After dissolving, the sucrose was sterile filtered and stored in a refrigerator.

Gellan gum (Gelzan ^{TM} CM - Gelrite ®, G1910, Sigma Aldrich, Saint Louis, USA) was weighed a required amount. The concentration of the GG was 5.0 mg/ml despite the amount of the prepared GG. The GG powder was poured by 10 % sucrose solution in desired volume and the GG solution was dissolved with magnetic stirrer

overnight. After dissolving, the GG solution was heated in a water bath to 60°C and sterile filtered. The solution was stored in a refrigerator. The GG solution can be stored up to one month.

The cross-linkers for the GG hydrogels, spermine (Spermine tetrahydrochloride, BioUltra, for molecular biology, ≥ 99.5 % (AT), 85605, Sigma Aldrich, Saint Louis, USA) and spermidine (Spermidine trihydrochloride, 85578, BioXtra, ≥ 99.5 % (AT), Sigma Aldrich, Saint Louis, USA), were weighed a required amounts. The prepared stock concentration of the SPM was 1.4 mg/ml and the prepared stock concentration of the SPD was 1.0 mg/ml. The weighed cross-linkers were poured by 10 ml of 10 % sucrose and the pH was measured. The cross-linker solutions were sterile filtered and stored in the refrigerator.

Due to the challenging production of the solutions for HA hydrogels, the HA solutions were produced in another study. For production of the HA1 and the HA3 hydrogel solutions, a higher molecular weight HA was used than for the production of the HAJ1 and the HAJ2 hydrogel solutions. The amount of the reagents was the same between the HA1 and the HAJ1 hydrogels and between the HA3 and the HAJ2 hydrogels. The molecular weight of HA for the HA1 and the HA3 hydrogels was 1.5×10^6 Da and for the HAJ1 and the HAJ2 hydrogels that was 1.0×10^5 Da. The molecular weight of the cross-linker PVA was 27×10^3 Da.

3.3 Production of the hydrogel samples

Hydrogel samples for the compression tests were produced in cut syringes of 5 ml. The diameter of the syringes was 12 mm and volume of the samples was 870 µl. The height of the samples was approximately 7 mm and the shape of the samples was cylindrical. Hydrogel samples for the rheological measurements were produced in cut syringes of 20 ml. The diameter of syringes was 20 mm and the volume of the samples was 500 µl. The height of samples was approximately 1 mm.

To prepare the GG samples for mechanical and rheological measurements, the solutions of the GG and the cross-linker were heated to 37°C and mixed by a magnetic stirrer. For all GG hydrogels, the used concentration of the GG solution was 5 mg/ml. The cross-linker solutions were diluted with 10 % sucrose solution to a needed concentration. In the GG hydrogel samples for compression tests, the volume of the GG solution was 750 µl and the volume of the cross-linker was 120 µl. For the GG hydrogel samples in the rheological tests, the volume of the GG solution was 1000 µl and the volume of the cross-linker was 160 µl. In both sample productions, the ratio of the cross-linker and the GG was 0.16. Concentrations of the GG and the cross-linkers that were used in the experiments are listed in Table 3.1.

Table 3.1. *Concentrations of the GG and the cross-linker solutions that were used in the GG hydrogel samples.*

Sample	GG	SPM	SPD
GG-1.1SPM	5.0 mg/ml	0.35 mg/ml	
GG-0.6SPM	5.0 mg/ml	0.175 mg/ml	
GG-0.4SPM	5.0 mg/ml	0.127 mg/ml	
GG-0.3SPM	5.0 mg/ml	0.10 mg/ml	
GG-3.1SPD	5.0 mg/ml		1.0 mg/ml
GG-1.57SPD	5.0 mg/ml		0.5 mg/ml

In Figure 3.1, the concentrations of the different GG hydrogels is shown; the sample number 1 is the GG-3.1SPD hydrogel, the sample number 2 is the GG-1.57SPD hydrogel, the sample number 3 is the GG-1.1SPM hydrogel, the sample number 4 is the GG-0.6SPM hydrogel, the sample number 5 is the GG-0.4SPM hydrogel and the sample number 6 is the GG-0.3SPM hydrogel. The different softness of the GG hydrogels can be seen in Figure 3.1; the GG-0.3SPM and the GG-0.4SPM on the right side cannot maintain their shape as good as the other hydrogels.

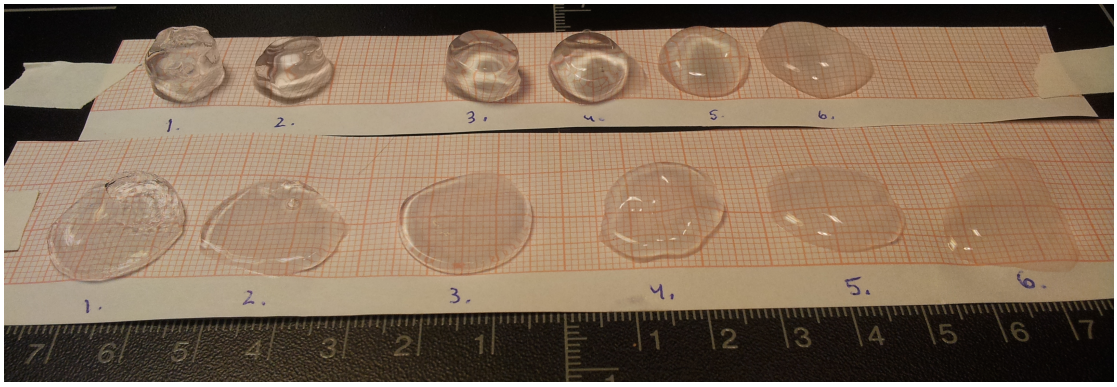

Figure 3.1. *The different GG hydrogels; the upper samples are the compression test samples and the lower samples are the rheological test samples.*

In the HA hydrogel samples in the both measurement methods, the ratio of the PVA and the HA was 1. The volumes of the HA and the PVA in compression samples were 435 µl and in the rheological samples the volumes were 250 µl. In Table 3.2, the concentrations of the HA and the PVA that were used in the experiments are listed.

Table 3.2. *Concentrations of the HA and the PVA solutions that were used in the HA hydrogel samples.*

Sample	HA1	HA3	HAJ1	HAJ2	P4
HA1-P4 (1.5%)	20 mg/ml				10 mg/ml
HA1-P4 (0.375%)	5.0 mg/ml				2.5 mg/ml
HA3-P4 (1.5%)		25 mg/ml			5.0 mg/ml
HA3-P4 (0.375%)		6.25 mg/ml			1.25 mg/ml
HAJ1-P4 (1.5%)			20 mg/ml		10 mg/ml
HAJ2-P4 (1.5%)				20 mg/ml	10 mg/ml

All of the sample syringes were covered with a plastic paraffin film to avoid the evaporation of water. The samples were measured after an approximately 18 hour gelation time.

The reference material PuraMatrix was produced by using Corning® PuraMatrix® Peptide Hydrogel and Gibco® DMEM/F-12. The production of the PuraMatrix samples was made according to the manufacture's instructions. The rheological properties of the PuraMatrix were measured by the rheometer. PuraMatrix was stirred to modify the solution to be less viscous for the production of the PuraMatrix hydrogels. Undiluted PuraMatrix solution was pipetted 500 µl to the 20 ml syringe. The cell culture medium (1 ml) was pipetted onto the PuraMatrix solution. The sample syringe was covered with a plastic paraffin film. The total number of the PuraMatrix samples was seven. The PuraMatrix samples were put to the incubator for one hour. The cell culture medium was changed after every 30 minutes. After one hour, the PuraMatrix samples were measured by the rheometer.

3.4 Oscillatory tests

The rheological properties of hydrogels were measured with the Haake RheoStress RS150, the manufacturer is Haake and the model is the RS150. The rheological measurements were done at the room temperature which varied from 21.9°C to 23.3 °C. The pressure was set at 2.5 bar and the rheological measurements were done in the air. The plate that was used in the rheological measurements was the ceramic parallel-plate measuring system (HPP20), diameter of which was 20 mm. The measuring gap was set at 0.8 mm and the trimming position was the gap + 0.025 mm. The rheological measurements were done by constant deformation (CD-AS). The measuring programs that were used were the amplitude and the frequency sweeps.

The amplitude sweep was set at the strain range from 0.01 to 5.00. The frequency used for the amplitude sweep was 1 Hz. These presets are typically used for the rheological measurements of hydrogels. The number of the measuring points in the amplitude sweep was 20. The amplitude sweep took approximately 22 minutes. The amplitude sweep was done for six hydrogel samples and two samples were measured by frequency sweep.

The frequency sweep was set at the frequency range from 0.1 Hz to 3.0 Hz. The constant strain value was determined from the LVE range of the amplitude sweep of every hydrogel. For the GG hydrogels with the SPM cross-linker, the strain was 0.1. For the HA3 and the HAJ2 hydrogels, the strain was 0.01 and for the HA1 and the HAJ1 hydrogels the strain was 0.1. The frequency sweep took approximately 7 minutes.

The measuring data was plotted out as a text file containing the values of the strain, the frequency, the time, the storage modulus, the loss modulus, the complex shear modulus, the stress and the phase shift angle. The data was imported to excel and

plotted as graphs. The LVE range values were determined manually from the data table and from the graphs.

The MCR Anton Paar rheometer was used to test the reliability of the Haake RheoStress. The manufacturer of the rheometer is Anton Paar. The amplitude sweep was used alongside with the Haake RheoStress for GG-1.1SPM hydrogels. The plate that was used was the parallel-plate measuring system whose diameter was 25 mm. The gap was set at 0.4 mm due to the wider measuring system. The strain range was set from 0.01 to 5.0 with the frequency of 1 Hz. The measuring data was plotted out in the same format as with the Haake RheoStress.

In the rheological measurements of the PuraMatrix, the Anton Paar rheometer was used alongside with the Haake RheoStress. The plate that was used was the parallel-plate measuring system in both rheometers. The diameter of the plate in the Haake RheoStress was 20 mm and in the Anton Paar it was 25 mm. The set gap in the Haake RheoStress was 0.8 mm and in the Anton Paar it was 0.6 mm due to the wider measuring system. The used frequency in both rheometers was 1 Hz. The strain range in the Haake RheoStress was set at first from 0.01 to 1,0 and then the strain range was changed to start from 0.001 to 0.1 due to the exceeded LVE range. The strain range in the Anton Paar was set also to start from 0.0001 to 0.01.

The samples were placed between the measuring system and the lower plate with the help of a spatula. The measuring system was set on the trimming position and the sample was trimmed. After the trimming, the gap was set and the measurement was started.

In rheological measurements the amplitude and frequency sweeps were measured. The total sample number of different concentrations was eight. Approximately, the amplitude sweep was measured for six samples and frequency sweep for two samples. The G', G'', G* and tan δ for both hydrogels were determined and standard deviations were calculated for the moduli values. In the results the moduli values are presented as average values for every hydrogel. The LVE moduli values are determined by using the deviation tolerance of 10 %. The modulus figures in which are collected the curves of the GG and the HA hydrogels, include the curves of the samples that represent the average values the most.

3.5 Compression test

Measuring the mechanical properties of the hydrogels, the Bose BioDynamic ElectroForce Instrument 5100 was used. The manufacturer of the instrument is Bose. Before starting the measuring, the flat nonporous platens were placed in the chamber and the chamber was attached to the frame. The surfaces of the platens were covered with plastic paraffin films and wet papers to avoid the slipping of the sample and the evaporation of water. For every new type of sample, the TuneIQ program was used. The

TuneIQ program automatically tunes and optimizes the controlling system for sample type in question.

The compression tests were done in the air and at room temperature (20.3 °C – 21.0 °C). The compression speed was kept constant; 10 mm/min. For every sample, the height was measured and the displacement was calculated. The evaluation of the displacement was determined in the earlier studies and it was 65 % of the sample height. The scan time was the displacement divided by the compression speed. The scan point, the measured data points per second, was defined in the earlier studies to be four times the scan time. The height of the sample, the displacement, the scan time and the scan points were determined for every sample.

The sample was placed between the platens and the upper platen was set to contact with the sample. The determined parameters were set to the measuring program and the sample was compressed. The measuring data was plotted out as a comma-separated values file (.csv) containing the elapsed time, the displacement and the load. The data was imported to excel and the stress and strain were calculated from the data. The stress and the strain were plotted as graphs. The E values were calculated from the stress-strain curves.

The total compression sample number of hydrogels with different concentrations was eight. The Young's moduli (E) are determined by using the whole linear part of the stress-strain curves. The E value was the slope of stress-strain curve. The fracture strength and the fracture strain values were determined from stress-strain curve at the point before the possible fracture. The values of the E, the fracture strength and the fracture strain are presented as average values for every hydrogel. The standard deviations were calculated for the E, the fracture strength and the fracture strain values.

3.6 Measuring the density of the hydrogels

The density of the hydrogels was measured weighting one compression sample by scale and calculating the volume of the sample. In calculation the diameter assumed to be the diameter of the compression sample syringe (12.0 mm). The height of the sample was determined by gauge. The density was calculated dividing the mass of the sample by the volume of the sample.

The density of every sample was measured from one sample per hydrogel. The evaporation caused changing mass result in scale and the mass results are determined after five seconds after placing the sample on the scale.

4 RESULTS AND DISCUSSION

4.1 Testing reliability of Haake RheoStress rheometer

The reliability of the Haake RheoStress rheometer was tested by defining amplitude sweep for GG-1.1SPM hydrogel. The amplitude sweep was defined by the Haake RheoStress and by the Anton Paar rheometers. The Anton Paar was reference rheometer for the Haake RheoStress due to its reliability in previous studies conducted by Material Science Department for measuring rheological properties. In amplitude sweep measuring the values of the G' and the G'' were in function of deformation. Comparison of two rheometer was determined by crosspoint values of the G' and the G''. Figure 4.1 shows the crosspoint values of the G' and the G'' that measured by the Haake RheoStress and the Anton Paar rheometer. There were measured two samples by the Anton Paar rheometer and five samples by the Haake RheoStress rheometer. The G' values measured by the Anton Paar rheometer were 18-20 Pa and the G'' values were 17.6-19 Pa. The G' values measured by the Haake RheoStress were 13.2-85.1 Pa and the G'' values were 13.3-88.8 Pa. As seen in Figure 4.1, there are two higher value of G' and G'' that measured by the Haake RheoStress. During handling those two samples, air bubbles formed between the sample and the lower plate. The air bubbles caused higher values of G' and G'' and these were removed from the end results. The end results of G' values were 13.2-18.4 Pa and G'' values were 13.3-20.1 Pa measured by the Haake RheoStress.

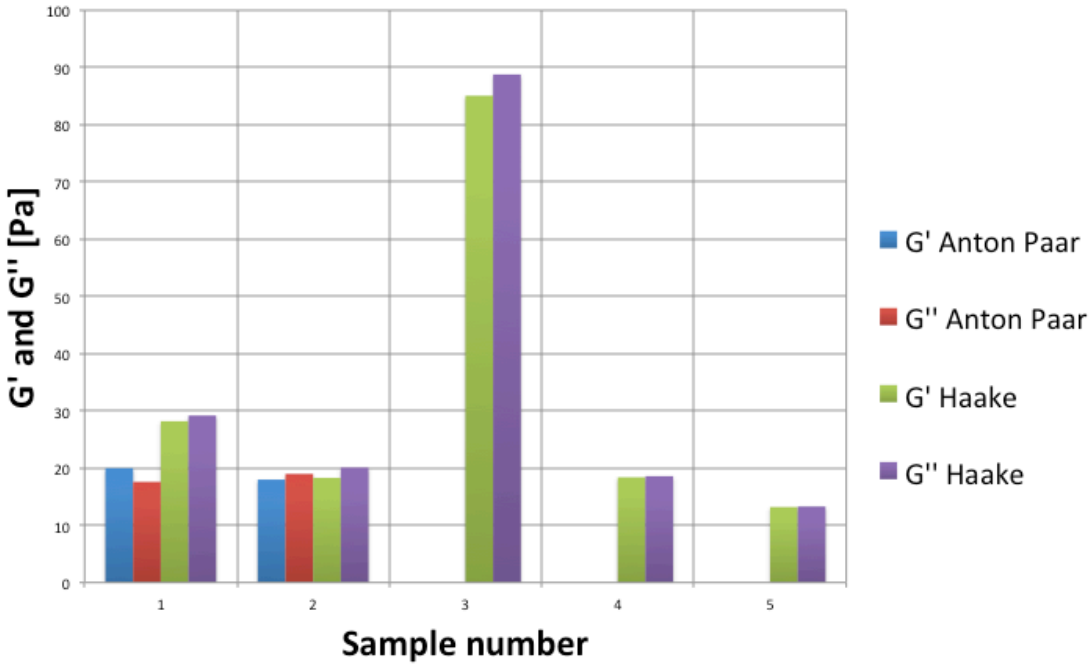

Figure 4.1. *Crosspoint values of G' and G'' measured by the Haake RheoStress and the Anton Paar rheometers. The sample numbers for the Haake RheoStress were five and for the Anton Paar two.*

The G' and the G'' crosspoint values of Haake RheoStress were lower than the results of Anton Paar. However, the deviation of results was not significant and as a conclusion the Haake RheoStress proved to be reliable rheometer. The rheological measurements of hydrogels were decided to measure by Haake RheoStress.

4.2 Rheological properties of the reference material PuraMatrix

Corning® PuraMatrix™ Peptide Hydrogel was used for the reference material in this thesis work. PuraMatrix has been used as a supportive growth matrix for human neural cells. (Ylä-Outinen et al. 2012).

In Figure 4.2, the G' and the G'' curves of 1.0 % w/v PuraMatrix are represented in a function of the strain. The G' and the G'' values were measured by the Haake RheoStress and the Anton Paar rheometers. The Anton Paar was used as a reference rheometer for the Haake RheoStress. Four PuraMatrix samples were measured by the Haake RheoStress and two PuraMatrix samples by the Anton Paar. The results of two Haake RheoStress samples were not reliable due to the anisotropy of the sample structure. As seen in Figure 4.2 the level of the G' and the G'' was very similar except the first sample that was measured by the Haake RheoStress. The insertion of the

sample could have caused error to the data. Similarity of the G' and the G'' curves indicated that the Haake RheoStress was reliable for measuring the rheological properties of the PuraMatrix.

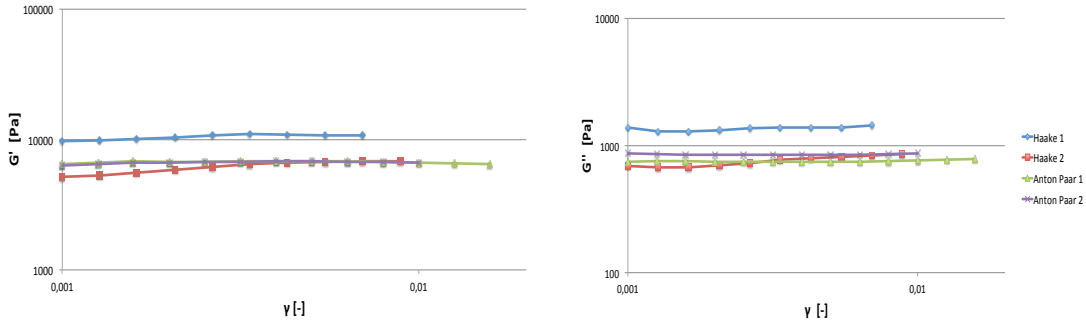

***Figure 4.2**. The G' and the G'' curves for 1.0 % w/v PuraMatrix measured by Haake RheoStress and Anton Paar rheometers.*

The average G' value for 1.0 % w/v PuraMatrix that was measured by Haake RheoStress was 8315 Pa and for 1.0% w/v PuraMatrix that was measured by Anton Paar was 6670 Pa. The corresponding G'' results were 1056 Pa and 800 Pa. These results were compared to (Shroff et al. 2010) research where the pure PuraMatrix was measured in different weight per volume percentages. The measured and results from literature are shown in Table 4.1. (Shroff et al. 2010) used PuraMatrix in weigh per volume percentages from 0.15 % w/v to 0.5 % w/v and they had approximately the G' value for 0.25 % w/v PuraMatrix 150 Pa and for 0.5 % w/v PuraMatrix 1000 Pa. The G' value of 0.5 % Puramatrix was approximately 6.7 times higher compared to 0.25 % PuraMatrix. The measured G'' value for 0.25 % w/v PuraMatrix 50 Pa and for 0.5 % w/v PuraMatrix 200 Pa. The G'' value of 0.5 % Puramatrix was 4 times higher compared to 0.25 % PuraMatrix. As a conclusion of these comparisons, the G' value was approximately 7 times higher when weight per volume percentage of PuraMatrix doubled. Also the G'' value was approximately 4 times higher when weight per volume percentage of PuraMatrix doubled. Using this assumption, the G' value for 1.0 % w/v PuraMatrix should be approximately 7000 Pa which is average of the measurements by two different rheometers. Using the same assumption for the G'' value, the 1.0 % PuraMatrix should be, approximately, 800 Pa and which is the same G'' value that was measured by Anton Paar. In further studies, it is important to measure more PuraMatrix samples with different weight per volume percentages.

***Table 4.1**. The comparison of G' and G'' values between two rheometers and literature.*

PuraMatrix sample	**G' [Pa]**	**G'' [Pa]**
Haake, 1.0 % w/v	8315	1056
Anton Paar, 1.0 % w/v	6670	800
Shroff et al. 2010, 0.25 % w/v	150	50
Shroff et al. 2010, 0.5 % w/v	1000	200

4.3 Rheological measurements

4.3.1 Rheological measurements of gellan gum hydrogels

Measuring rheological properties of GG hydrogels proved to be challenging. GG hydrogels of higher concentration had fast gelation time. The fast gelation time caused anisotropy in sample structure and the samples did not behave optimally under changing deformation or frequency. The optimal samples for rheological measurements were the GG hydrogels of lower cross-linker concentration that have cross-linker concentration of 0.3 % to 0.6 %. In GG hydrogels of higher cross-linker concentration (GG-1.1SPM, GG-3.1SPD and GG-1.57SPD) the LVE range was not obvious.

All the amplitude sweeps of GG hydrogels are determined in the frequency of 1 Hz and the values of strain were from 0.01 to 5.0. The frequency sweeps are determined in frequency values from 0.1 Hz to 3.0 Hz. The strain value of frequency sweep depends on the LVE range of every hydrogel.

Figure 4.3 illustrates the optimal result data from GG hydrogels. In Figure 4.3 the SPM concentration of the sample is 0.4%. There is obvious LVE range starting from approximately strain value 0.1 and ending to strain value 0.5. This kind of behaviour, where G' > G'' is typical for hydrogels; the elastic behaviour dominates the viscous behaviour.

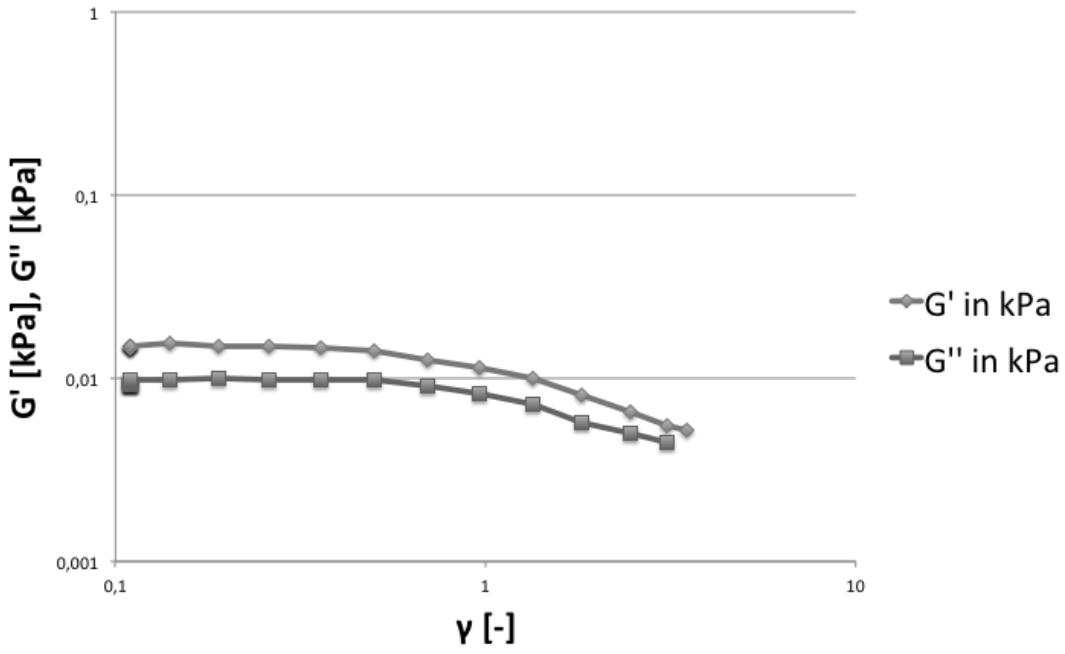

***Figure 4.3**. The amplitude sweep for GG hydrogel with 0.4 % SPM concentration, f = 1 Hz and the γ = 0.01 – 5.0.*

In measurements of GG hydrogels with SPM concentration 0.3 % and 0.4 %, air bubbles formed between the sample and the plate when inserting the sample on the lower plate. The air bubbles were removed with the help of a spatula before the measuring started, but avoiding these air bubbles in the future, the use of the cone-plate measuring system should be tested.

In GG hydrogels with SPD concentration of 3.1 % and 1.57 %, there were problems with preparation of samples. These two hydrogels have fast gelation time and that caused problems to produce these rheological samples, where the height of the sample is 1 mm and the diagram is 20 mm. Due to the fast gelation time, the mixing of the GG and the SPD had to be done straight to the cut syringe. The structure of the sample did not become homogenous because they gelated very fast. Such an unsatisfactory mixing caused anisotropic samples and the result data was not reliable. These anisotropic samples were the reasons for that there are not any results from rheological measurement for GG hydrogels with SPD cross-linker. In the future, there should pay attention to preparation of GG hydrogels with SPD cross-linker for rheological measurements.

Another problematic GG hydrogel was the hydrogel with SPM concentration of 1.1 %. Even if the gelation time was not as fast as for the GG hydrogels with SPD cross-linker, the structure of rheological samples were not homogenous. Even if the LVE range for the GG hydrogels with SPM cross-linker concentration was not obvious, the measuring of rheological parameters managed. However, the rheological measurements were done for 24 samples of 1.1 % SPM cross-linker hydrogels and in the calculation of rheological parameters there were only two successful samples. For the future measurements, the preparation of this 1.1 % SPM cross-linked GG hydrogel should be improved.

Figure 4.4 illustrates the amplitude sweep of GG hydrogels with SPM concentrations 1.1 %, 0.6 %, 0.4 % and 0.3 %. The G' value is represented in a function of the strain. As mentioned before, the LVE range for 1.1 % SPM concentration GG hydrogel was not obvious and that G' curve decrease thought the measurement. The LVE range is obvious for 0.6 % and 0.4 % gels and it continues to the γ_L, which is approximately 0.36. For the 0.3 % gel, the LVE range started from the strain value of 0.26 and continued until the γ_L of 0.67. It is important to pay attention to the point group at the beginning of the measuring data of the both hydrogels (circulated in Figure 4.4). In the future, the reason for this group should investigate; is it a slipping of the sample or is it the real data when the sample starts to resist the applied force.

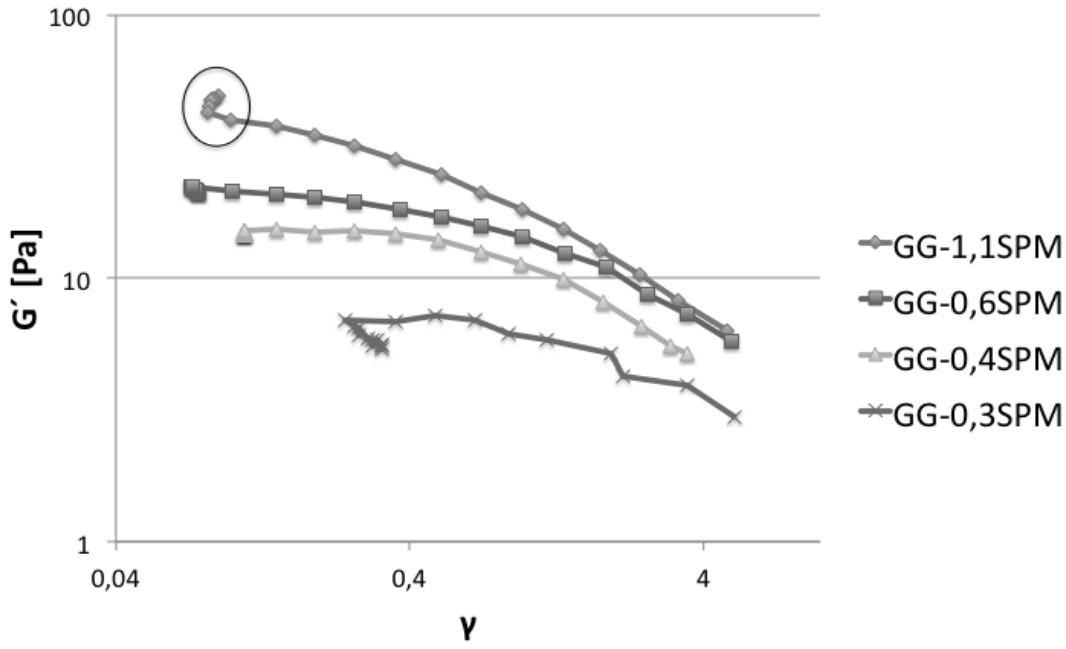

Figure 4.4. *The G' curves of GG hydrogels with concentrations 1.1%, 0.6 %, 0.4 % and 0.3 %.*

There are the average G' values for GG hydrogels in Figure 4.5. The values of G' are calculated by the formula (8). The G' value became higher when the cross-linker concentration increased. For 1.1 % gel the G' was 31.57 Pa, for 0.6 % gel 22.57 Pa, for 0.4 % gel 18.16 Pa and for 0.3 % gel 6.77 Pa. There is major difference between two softest GG hydrogels' G' values. The difference is caused by the liquid like nature of 0.3 % gel when comparing to the 0.4 % gel. The 0.4 % and the 0.6 % gels were very similar, they were obviously softer than 1.1 % gel but tougher than 0.3 %. The G' value of 1.1 % gel is calculated using the average values of two samples and that is the reason for large standard deviation.

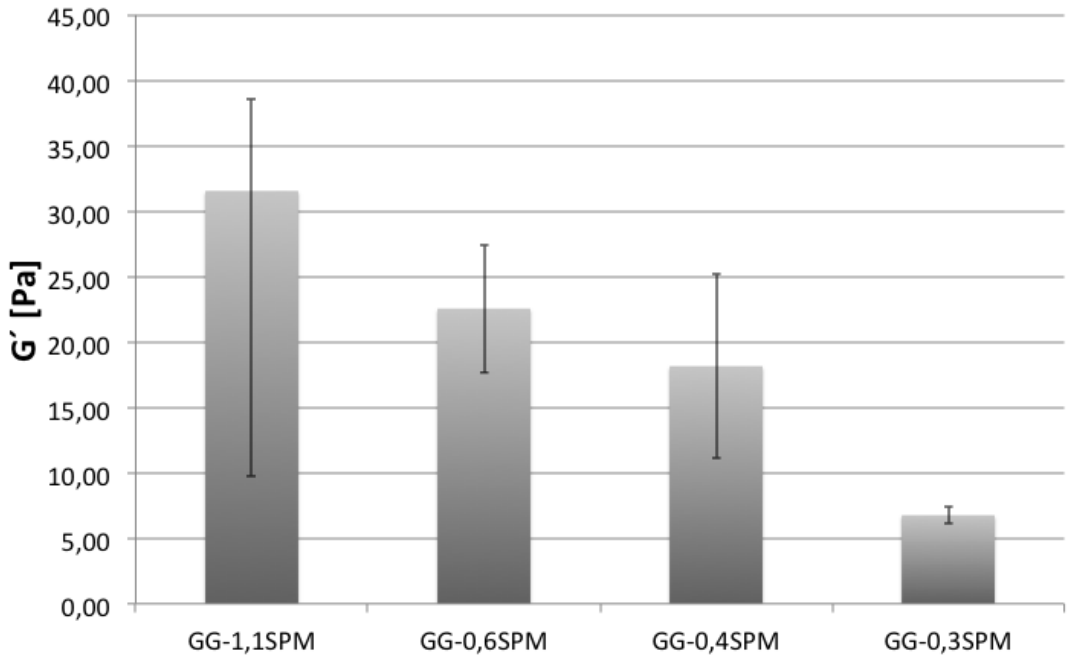

Figure 4.5. *The average G' values of GG hydrogels with concentrations 1.1%, 0.6 %, 0.4 % and 0.3 %.*

In Figure 4.6, the amplitude sweep is represented with the G'' values of GG hydrogels. The G'' value is represented in a function of the strain. Unlike the G' curves in Figure 4.4, the G'' curves were straight linear lines and the LVE range is more obvious for all four GG hydrogels. Compared to Figure 4.4, the G'' curve for 1.1 % gel did not decrease as sharply as the G' curve. The LVE range was determined from the G' and G'' values where the both G' and G'' curves showed constantly plateau values. After the γ_L, the G'' curve still showed the constant plateau value while the G' curves started to decrease. Higher strain values than the γ_L, the viscous behaviour of GG hydrogels increased and in some point, the G'' > G' and the G'' dominated the G'.

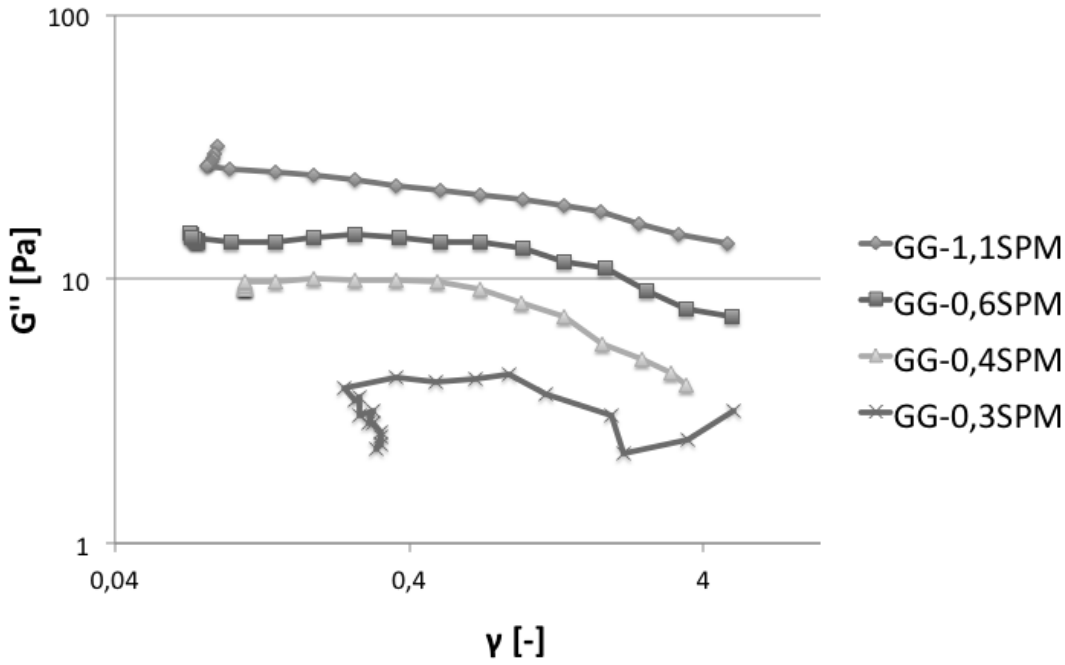

Figure 4.6. *The G'' curves of GG hydrogels with concentrations 1.1%, 0.6 %, 0.4 % and 0.3 %.*

The average G'' values of GG hydrogels are shown in Figure 4.7. The values of G'' were calculated by formula (9). The G'' value became higher when the cross-linker concentration increased. For 1.1 % gel the G'' was 22.07 Pa, for 0.6 % gel 14.99 Pa, for 0.4 % gel 13.04 Pa and for 0.3 % gel 3.85 Pa. The large difference of the G'' values between 0.4 % and 0.3 % gels is caused by the liquid like nature of 0.3 % gel. The G'' values for 0.6 % and 0.4 % are very identical because of the similar structure of the gel samples. The G'' value is highest with SPM concentration of 1.1 %. Due to the limited number of successful 1.1 % gel sample, the standard deviation is high. No obvious reasons were found for the high standard deviation of the GG hydrogel with 0.4 % of SPM.

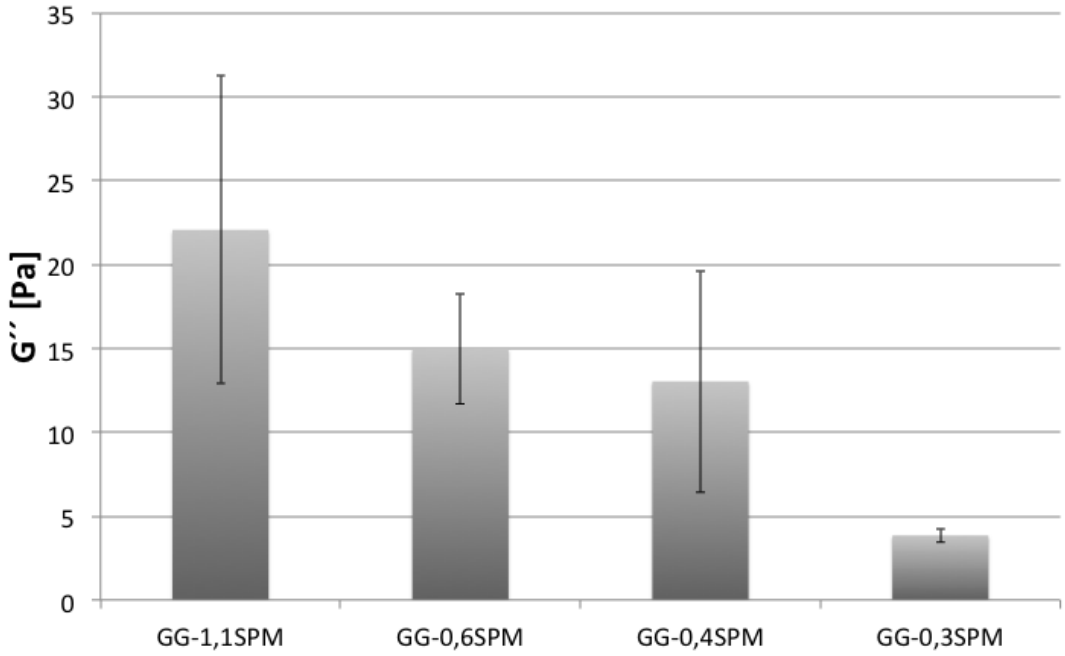

Figure 4.7*. The average G'' values of GG hydrogels with concentrations 1,1%, 0,6 %, 0,4 % and 0,3 %.*

The Figure 4.8 illustrates the amplitude sweep with the G* in a function of the strain. The G* curves behaved very similar than the G' curves in Figure 4.4. The G* curve of 1.1 % SPM concentration GG hydrogel decreased thought the measurement. The LVE ranges of 0.6 %, 0.4 % and 0.3 % gels were obvious. The G* is resultant of both components G' and G''.

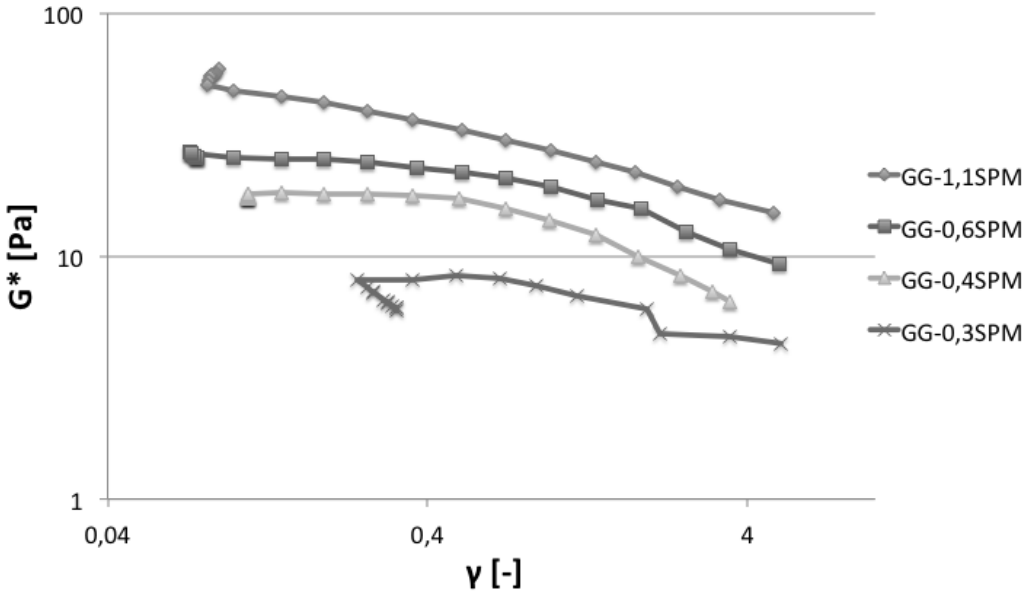

Figure 4.8. *The G* curves of GG hydrogels with concentrations 1.1%, 0.6 %, 0.4 % and 0.3 %.*

The Figure 4.9 shows the values of G* for GG hydrogels. The G* values were calculated by using the formula (11). The G* value became higher when the cross-linker concentration increased. For 1.1 % gel the G* was 38.72 Pa, for 0.6 % gel 27.11 Pa, for 0.4 % gel 22.40 Pa and for 0.3 % gel 7.79 Pa. The 1.1 % proved to be more rigid gel than the other GG hydrogels. The 1.1 % GG hydrogel resisted deformation the most.

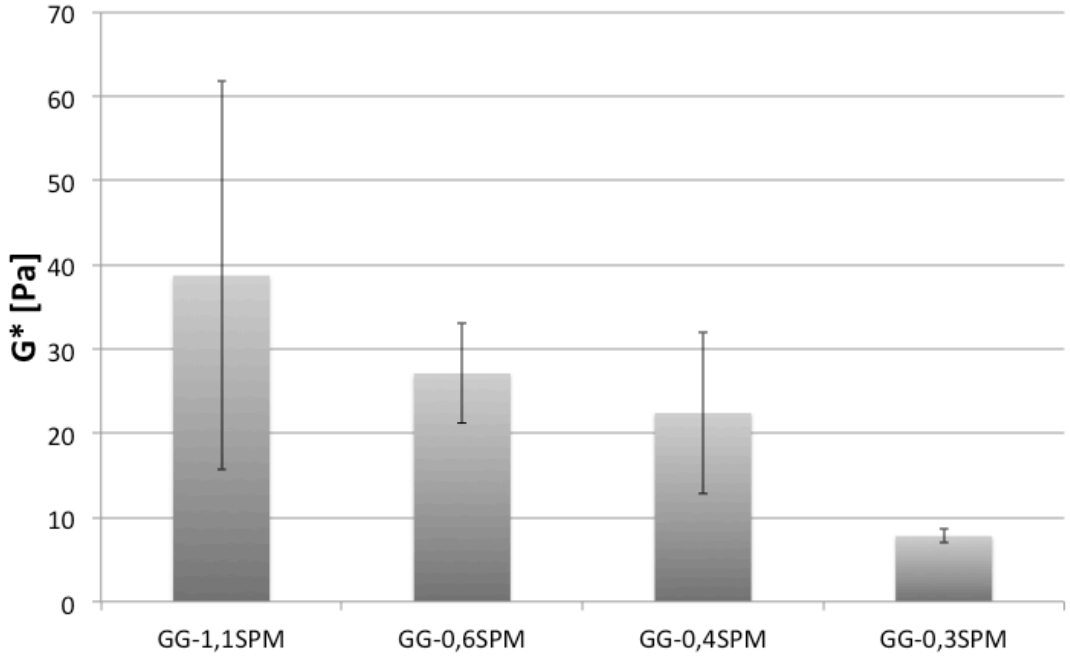

***Figure 4.9**. The average G* values of GG hydrogels with concentrations 1.1%, 0.6 %, 0.4 % and 0.3 %.*

In Figure 4.10 the frequency sweep of GG hydrogels is illustrated. The G' value is represented in a function of the strain. The G' curves of all GG hydrogels increased thought the LVE range. Therefore none of the GG hydrogels behaved like typical cross-linked material in frequency sweep. The G' values for GG hydrogels with SPM concentration of 1.1 % and 0.4 % were highest whereas the lowest G' values had the GG hydrogels with 0.6 % and 0.3 % SPM concentrations.

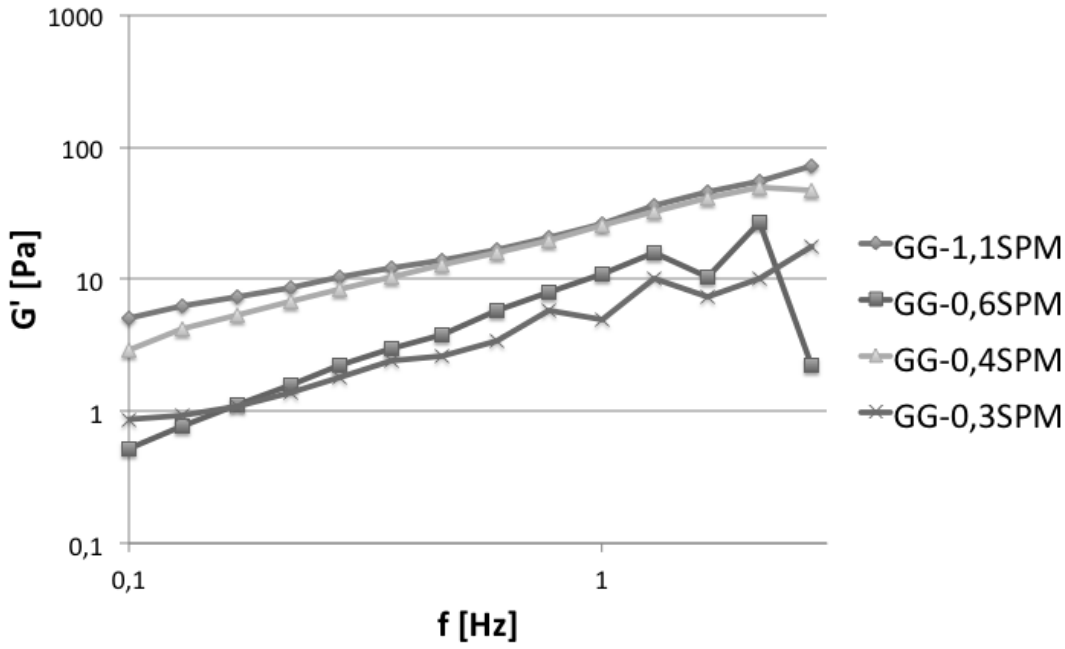

Figure 4.10. *The frequency sweep of GG hydrogels with SPM cross-linker concentrations 0.3 %, 0.4 %, 0.6 % and 1.1 %.*

4.3.2 Rheological measurements of hyaluronic acid hydrogels

The preparation method of HA hydrogel samples for rheological measurements proved to be more suitable when compared to the GG hydrogels. For GG hydrogels with high cross-linker concentration, the preparation of rheological samples was problematic due to the fast gelation time. Although, the HA is very viscous material and the addition of PVA causes very fast gelation for these hydrogels, the preparation of rheological samples managed very well. HA hydrogels proved to behave like optimal gel material under rheological testing. The LVE ranges were straight linear lines and there proved to be distinct difference in moduli values between HA hydrogels with higher and lower PVA concentrations.

All the amplitude sweeps of HA hydrogels were determined in the frequency of 1 Hz and the values of strain were from 0.001 to 5.0 or from 0.01 to 5.0 depending on the LVE range of each HA hydrogel. The frequency sweeps were determined in frequency range from 0.1 Hz to 3.0 Hz. The strain value of frequency sweep depends on the LVE range of every HA hydrogel and it varied from 0.01 to 0.1.

Figure 4.11 illustrates the amplitude sweep for HA3-P4 1.5 % hydrogel. Figure 4.11 is very representative amplitude sweep of HA hydrogels, inside the LVE range the G’ and the G’’ curves are straight and before the crossover point the G’ decreases even as the G’’ increases. In the LVE range the G’ dominates the G’’ and the hydrogel behaves elastically. The LVE range starts approximately from the strain value of 0.003 and continues to the strain value of 0.04. Comparing this Figure 4.11 to Figure 4.3

which illustrates the optimal amplitude sweep of GG hydrogels, the LVE range is more obvious and the G’ value is more than ten times higher than the G’’ value.

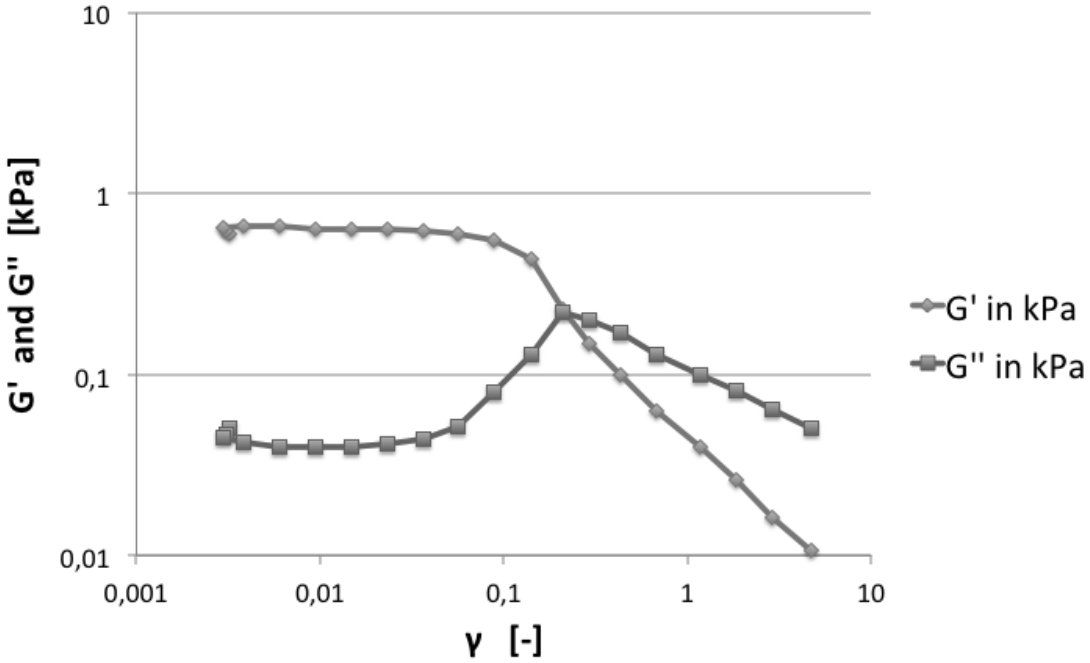

Figure 4.11. *The amplitude sweep for HA3-P4 1.5 % hydrogel.*

For HAJ1 and HAJ2 hydrogels with PVA concentrations 1.5 %, the G’’ curve fluctuates inside the LVE range. The G’ curve is straight at the same time when the G’’ curve varies. This behaviour of the G’’ needs further studies, but one reason for this kind of behaviour might due to the different modification degree of HAJ hydrogels when compare to the HA1 and HA3 hydrogels. The G’’ curves of the HAJ1 hydrogel varied more in LVE range than the G’’ curves of the HAJ2 hydrogel. This difference might due to the different degree of substituents. Figure 4.12 illustrates the amplitude sweep for HAJ1 hydrogel with 1.5 % PVA concentration. As seen in Figure 4.12, the G’ curve is straight line and the G’’ curve fluctuates in LVE range.

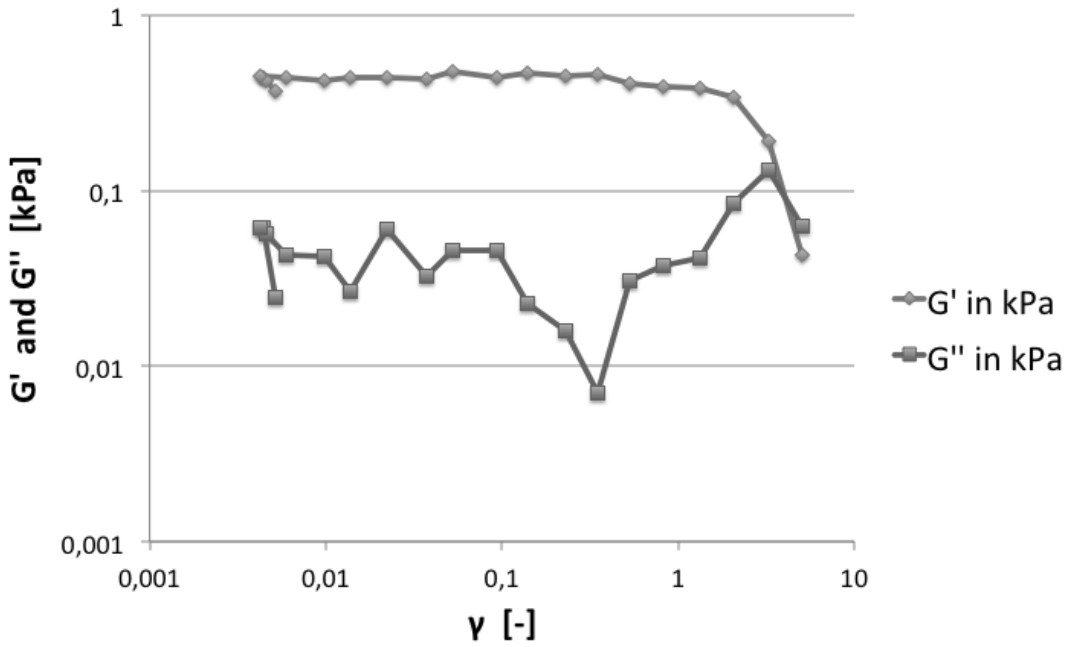

***Figure 4.12**. The amplitude sweep for HAJ1-P4 1.5% hydrogel.*

In Figure 4.13, the G' curves of different HA hydrogels are shown. The G' value is represented in a function of the strain. The HA hydrogels with PVA concentration of 1.5 % obtains higher G' values than the HA hydrogels with PVA concentration 0.375 %. The LVE range starts approximately from the strain value of 0.006 and ends to the strain value of 0.9 in HA hydrogels with 1.5 % PVA concentration. For softer HA hydrogels with 0.375 % PVA, the LVE range starts approximately from the strain value of 0.04 and ends already to the strain value of 0.1. The G' curve of the HA3 and HAJ2 behaves very similar at the beginning of the LVE range. After the strain of 0.1 the G' of HA3 hydrogel starts to decrease as the G' of HAJ2 continues straight. The behaviour of the G' for HA1 and HAJ1 is very similar. The difference between HA1 and HAJ1 comparing to the HAJ2 is the lower G' values. As seen in Figure 4.13, the LVE range for HA hydrogels with higher PVA concentration is wider than for the softer HA hydrogels excluding the HA3 hydrogel. The G' curve of HA3 hydrogel starts to decrease approximately at the same strain value as the G' curve of softer HA hydrogels. The G' value of the HA3 hydrogel is much higher than the G' value of softer HA hydrogels even the elastic behaviour in LVE range is very similar with softer HA hydrogels.

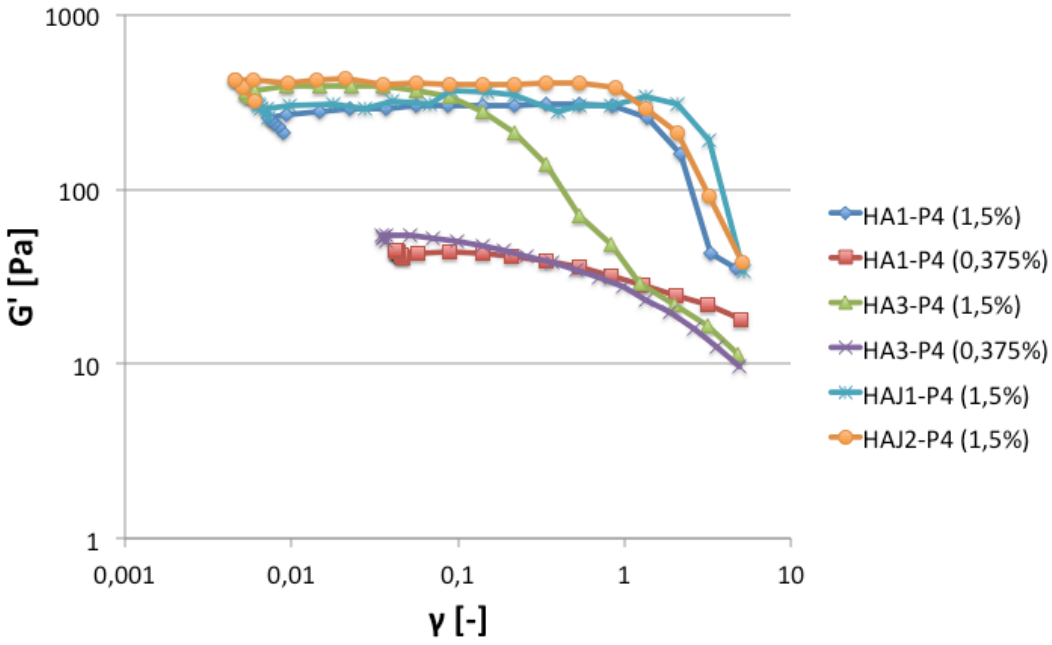

Figure 4.13. *The G' curves of different HA hydrogels with concentrations 1.1% and 0.375 %.*

Figure 4.14 shows the average G' values of HA hydrogels. The values of G' were calculated by the formula (8). The G' value became higher when the cross-linker concentration increased. The HA3 hydrogel had the highest G' value (396.88 Pa). The G' value for the HA1 with 1.5 % PVA concentration was 236.20 Pa, for the HA1 with 0.375 % of PVA 41.75 Pa, for the HA3 with 0.375 % of PVA 53.11 Pa, for the HAJ1 with 1.5 % of PVA 295.50 Pa and for the HAJ2 with 1.5 % of PVA 362.92 Pa. The standard deviation is largest for the HA3 hydrogel with 1.5 % of PVA. Although, the succeeded sample number of HA3 hydrogels with 1.5 % of PVA was 4, the standard deviation of G' values was high.

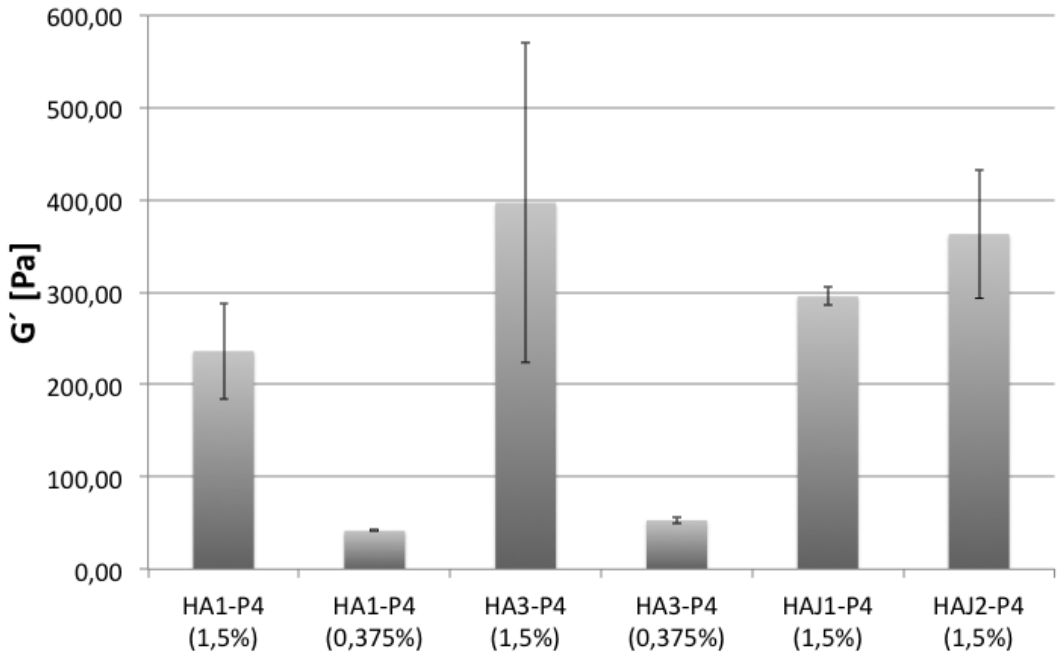

Figure 4.14. *The average G' values of different HA hydrogels with PVA concentrations 1.5% and 0.375 %.*

In Figure 4.15 the G'' curves of HA hydrogels are presented. As mentioned before, the G'' curves of HAJ1 and HAJ2 hydrogels fluctuate in LVE range. For other HA hydrogels, the G'' curve goes straight in the LVE range. Comparing the G'' curves to the G' curves (Figure 4.12), there is no obvious difference between the G'' curves of different HA gels than in the G' curves. From Figure 4.15 can be made an observation that the G'' curve of HAJ1 fluctuates more than the G'' curve of HAJ2.

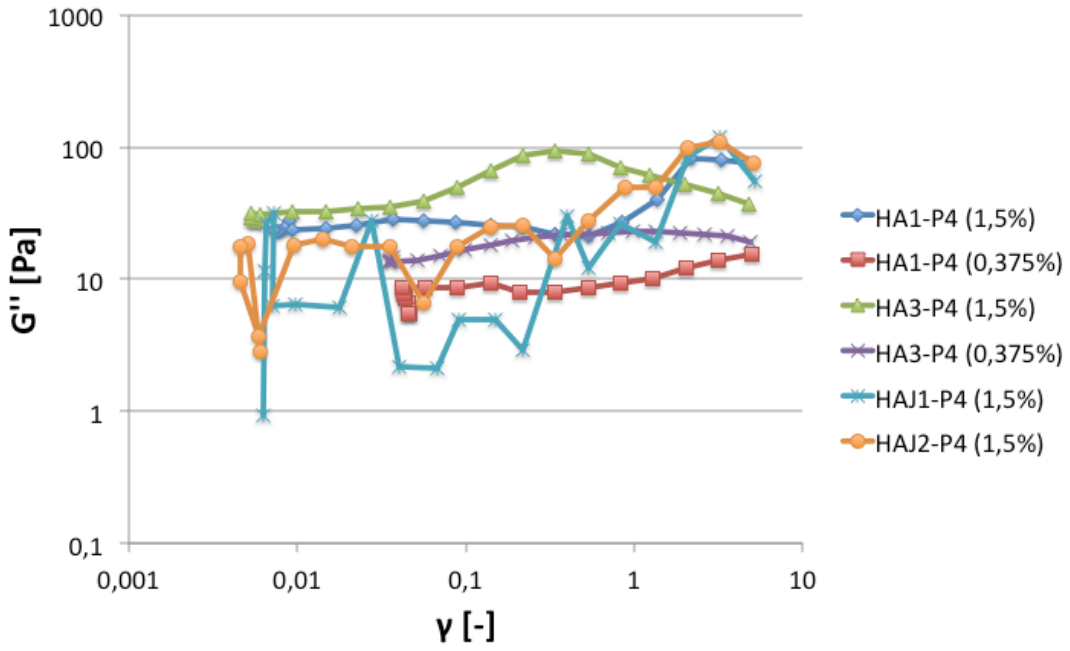

Figure 4.15. *The G'' curves of different HA hydrogels with PVA concentrations 1.5% and 0.375 %.*

The average G'' values of different HA hydrogels are shown in Figure 4.16. The values of G'' were calculated by formula (9). The G'' value became higher when the cross-linker concentration increased. As seen in Figure 4.16, the difference of G'' values between softer HA3 hydrogels and HAJ hydrogels is not high. The G'' value for the HA1 hydrogel with 1.5 % PVA concentration was 19.63 Pa, for the HA1 with 0.375 % of PVA 6.86 Pa, for the HA3 with 1.5 % of PVA 29.66 Pa, for the HA3 with 0.375 % of PVA 15.07 Pa, for the HAJ1 with 1.5 % of PVA 11.31 Pa and for the HAJ2 with 1.5 % of PVA 14.80 Pa. The HA3 hydrogel with 1.5 % of PVA had the most viscous behaviour in the LVE range whereas the HA1 hydrogel with 0.375 % of PVA had the least viscous behaviour in the LVE range. The HA3 hydrogel with 1.5 % of PVA had the highest standard deviation.

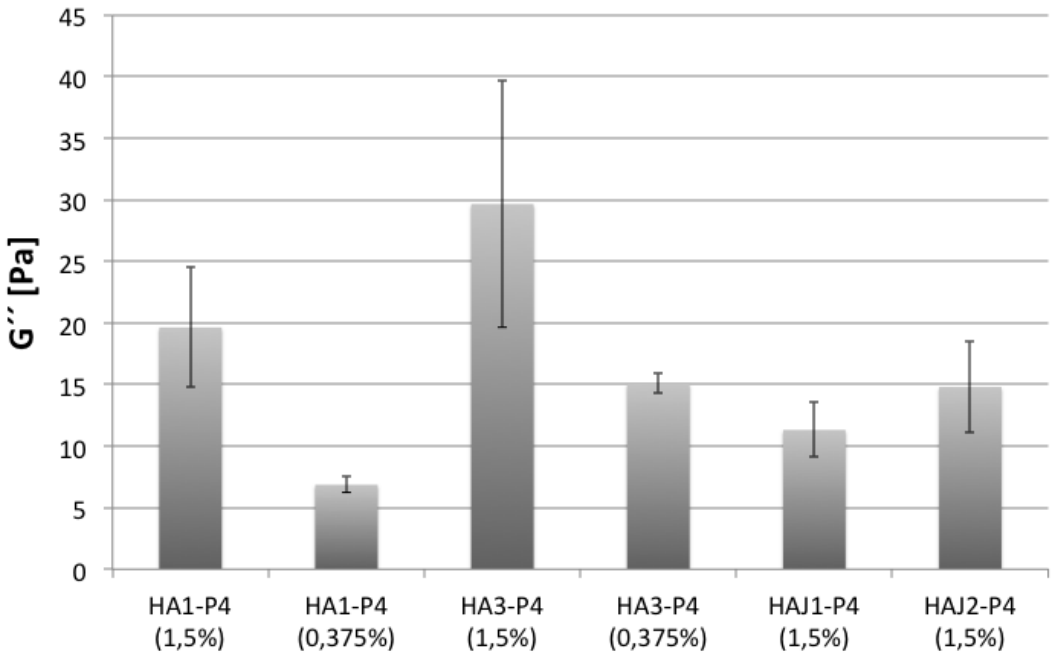

Figure 4.16. *The average G'' values of different HA hydrogels with PVA concentrations 1.5% and 0.375 %.*

The Figure 4.17 illustrates the amplitude sweep with the G* in a function of the strain. The G* curves behaved very similar than the G' curves in Figure 4.13. The G* represents the elastic (G') and viscous (G'') behaviour. In the LVE range, the G* curves were straight lines.

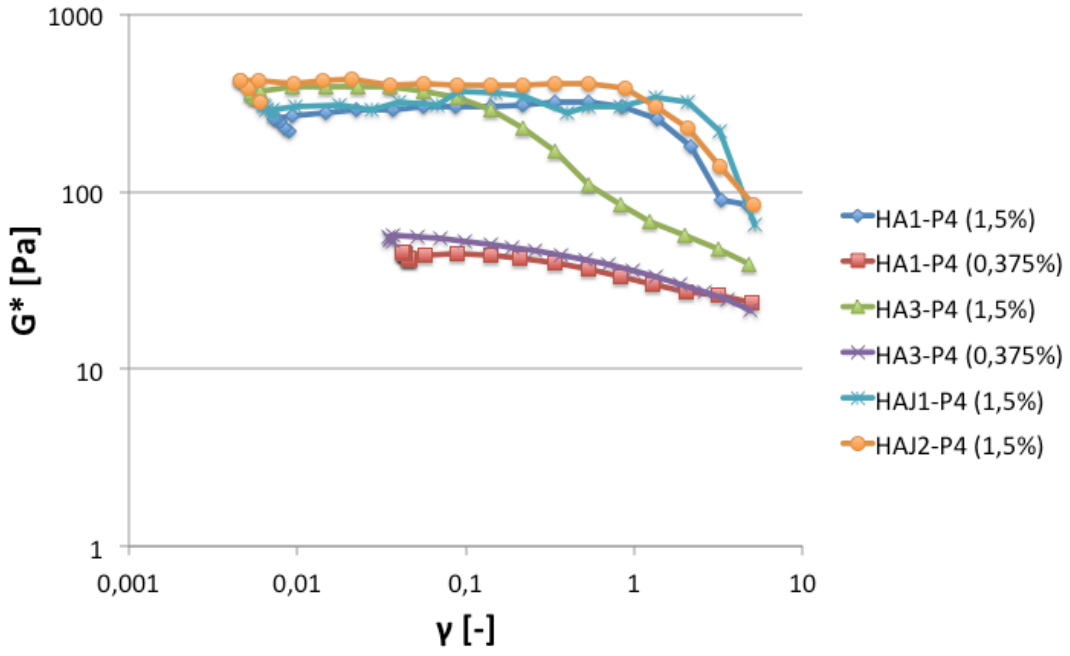

Figure 4.17. *The G* curves of different HA hydrogels with PVA concentrations 1.5% and 0.375 %.*

The average G* values of different HA hydrogels are shown in Figure 4.18. The values of G* were calculated by formula (11). The G* value obeyed the same observation than the values of G' and G''; the G* became higher when the cross-linker concentration increased. The G* value for the HA1 hydrogel with 1.5 % PVA concentration was 237.21 Pa, for the HA1 with 0.375 % of PVA 42.32 Pa, for the HA3 with 1.5 % of PVA 397.39 Pa, for the HA3 with 0.375 % of PVA 55.23 Pa, for the HAJ1 with 1.5 % of PVA 295.86 Pa and for the HAJ2 with 1.5 % of PVA 362.92 Pa. The G* values were very similar with the G' values because HA hydrogels had more elastic than viscous behaviour (G' >> G'') inside the LVE range.

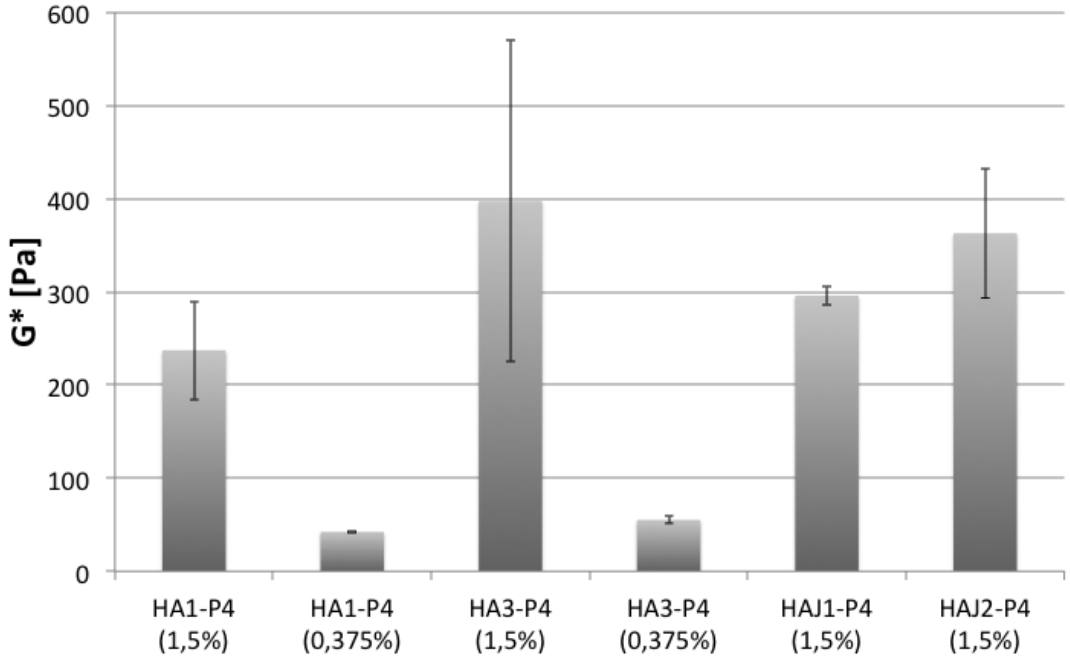

Figure 4.18. *The average G* values of different HA hydrogels with PVA concentrations 1.5% and 0.375 %.*

Figure 4.19 shows the frequency sweep for different HA hydrogels with PVA concentrations of 1.5 % and 0.375 %. The G' is presented in a function of the strain. The frequency varied from 0.1 Hz to 3.0 Hz and the strain was determined separately from the LVE range of every HA hydrogel. Typical behaviour of a gel material in a frequency sweep is straight linear G' curve and as seen in Figure 4.19, the HA hydrogels obeys that. The highest G' values in frequency sweep had HA hydrogels with 1.5 % PVA concentration. The G' curves for the HA1 hydrogels with 1.5 % of PVA and the HAJ1 with 1.5 % of PVA were identical in LVE range.

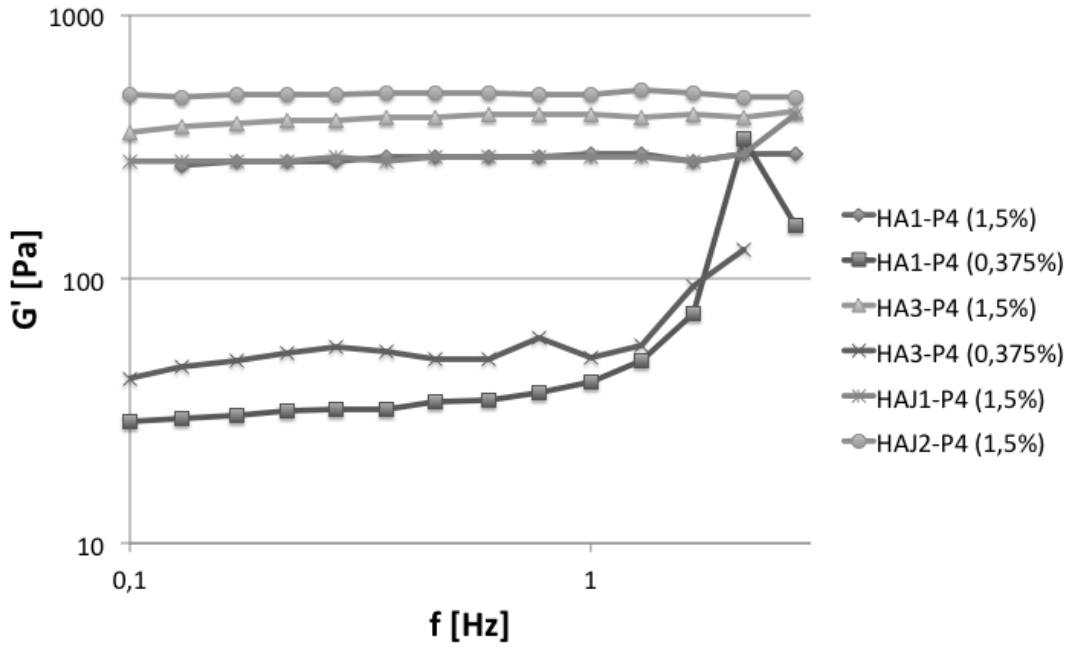

Figure 4.19. *The frequency sweep for different HA hydrogels with 1.5 % and 0.375 % PVA concentration.*

When compared the behaviour of GG and HA hydrogels in frequency sweep, it is seen that HA hydrogels represent the optimal behaviour of cross-linked material whereas the behaviour of GG hydrogels were not optimal. For HA hydrogels, the G' curves were straight lines. All the G' curves of GG hydrogels in frequency sweep increased through the LVE range.

4.4 Mechanical measurements

4.4.1 Mechanical measurements of gellan gum hydrogels

Figure 4.20 represents the stress-strain curves of GG hydrogels. The compression speed was constant and that created increasing stress. The stress was plotted in a function of the strain. The Young's modulus was calculated from the increasing linear part of the stress-strain curve. The GG hydrogels with 0.4 % and 0.3 % of SPM concentration were not possible to compress due to their softness. Figure 4.19 represents the stress-strain behaviour of the GG hydrogels with 1.1 %, 0.6 %, 3.1 % and 1.57 % of cross-linker concentrations. All GG hydrogels started to resist the constantly increasing stress already in the beginning of the test. When the applied force reached the maximum value, the hydrogel broke down.

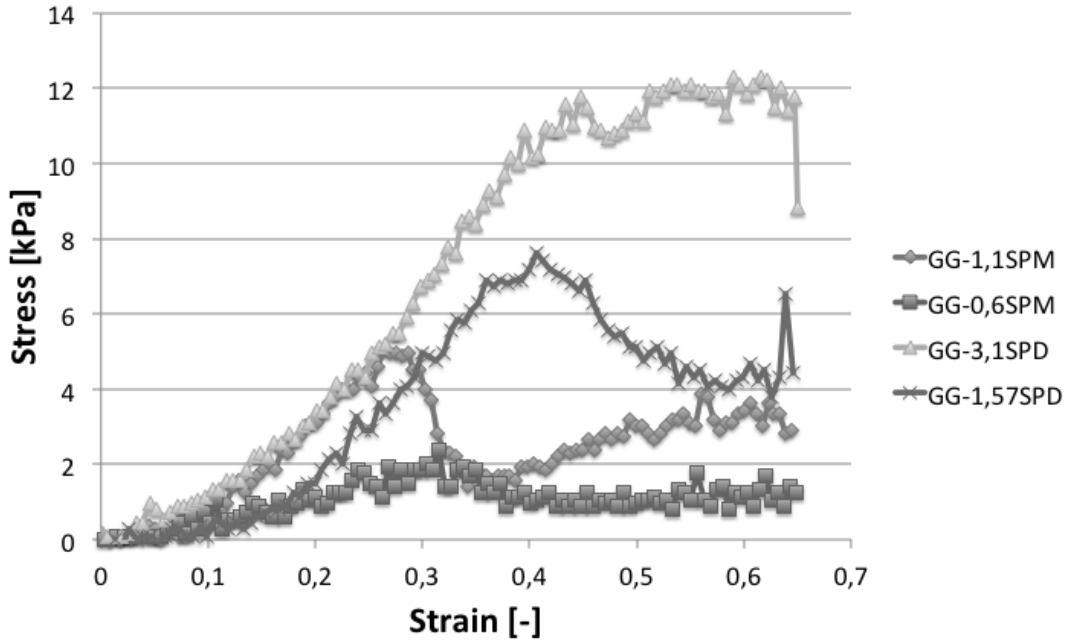

Figure 4.20. *The stress-strain curve for GG hydrogels with SPM concentrations of 1.1 %, 0.6 % and with SPD concentrations of 3.1 % and 1.57 %.*

Comparing the GG hydrogels with different cross-linker, it is seen that the GG hydrogels with SPD cross-linker reached higher fracture strength and strain values than GG hydrogels with SPM cross-linker. The softest GG hydrogel, 0.6 % of SPM, had the lowest stress-strain curve. The fracture for GG hydrogel with 1.1 % of SPM occurred approximately at the strain value of 0.28, for GG hydrogel with 0.6 % of SPM 0.30, for GG hydrogel with 3.1 % of SPD 0.5 and for GG hydrogel with 1.57 % of SPD 0.4.

In Figure 4.21, the average Young's moduli (E) are represented for GG hydrogels. The E is calculated from the formula (15). The E value for GG hydrogel with 1.1 % of SPM concentration was 21.44 kPa, for 0.6 % of SPM 6.74 kPa, for 3.1 % of SPD 21.88 kPa and for 1.57 % of SPD 18.00 kPa. Although, the fracture strain of 1.1 % SPM hydrogel occurred in a lower strain value than for 3.1 % SPD hydrogel, the fracture stress of 1.1 % SPM and 3.1 % SPD were very similar. The standard deviation was largest for 1.1 % of SPM and for 1.57 % of SPD hydrogels even when the succeeded sample number of those gels was five.

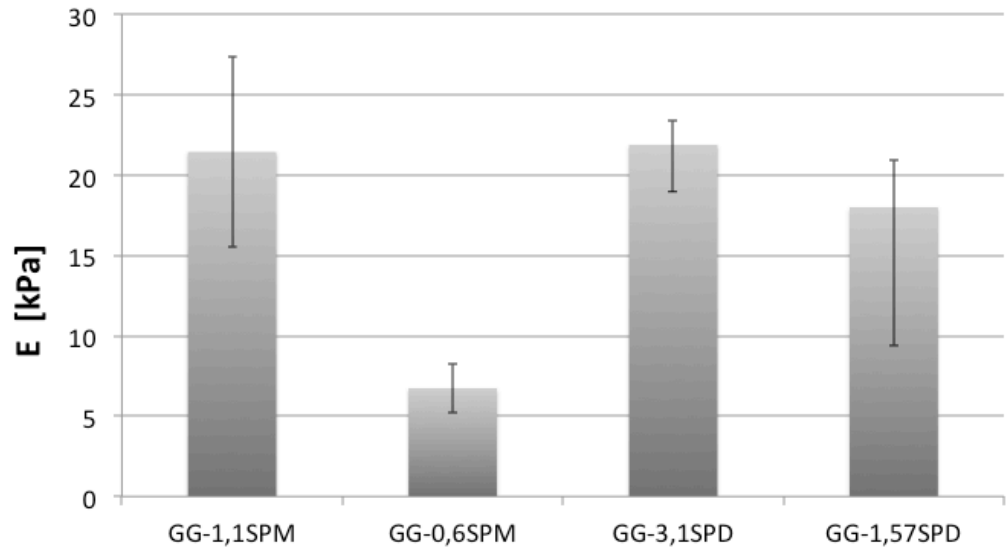

Figure 4.21. *The average Young's modulus values for GG hydrogels with 1.1 % and 0.6 % SPM concentrations and with 3.1 % and 1.57 % SPD concentrations.*

The difference of the average fracture strength values is seen in Figure 4.22. The GG hydrogels with 3.1 % of SPD had the highest fracture strength (12.38 kPa). The softest GG hydrogel had the lowest fracture strength (1.74 kPa). The fracture strength for GG hydrogel with 1.1 % of SPM was 4.22 kPa and for 1.57 % of SPD 5.89 kPa.

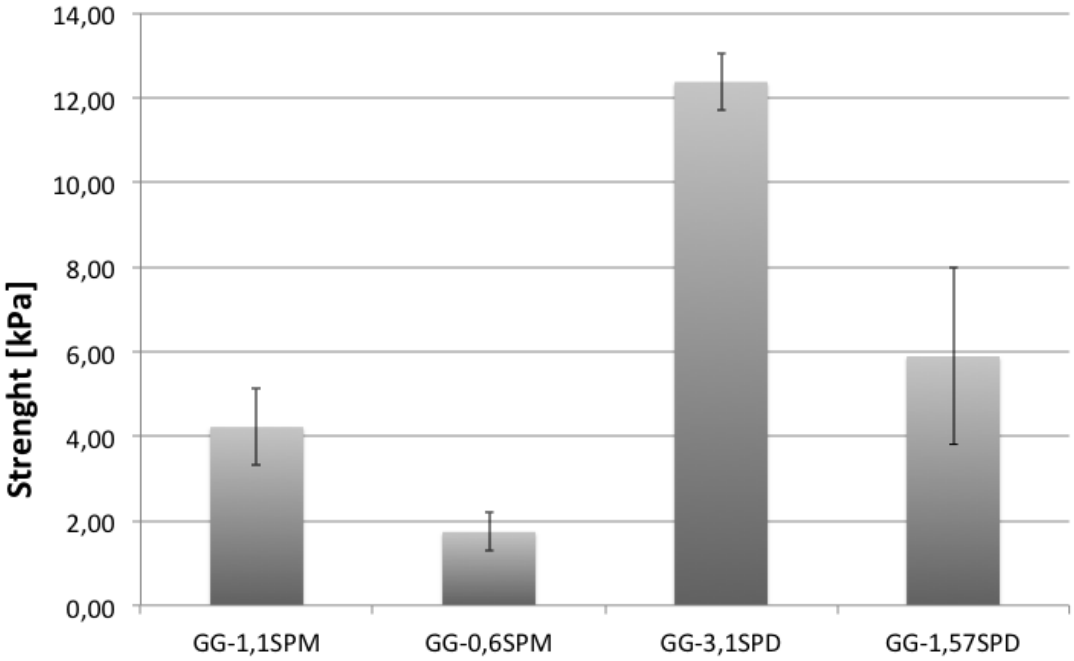

Figure 4.22. *The average fracture strength values for GG hydrogels with 1.1 % and 0.6 % SPM concentrations and with 3.1 % and 1.57 % SPD concentrations.*

In GG hydrogels the gel with 3.1 % of SPD proved to be the stiffest GG hydrogel with 1.1 % of SPM gel. The E values for both hydrogels were approximately 21 kPa. The 3.1 % of SPD gel fractured in highest stress value but the fracture strength of 1.1 % SPM gel was approximately one third from the 3.1 % SPD gel's fracture strength. Both the E value and the fracture strength of 0.6 % gel were the lowest.

4.4.2 Mechanical measurements of hyaluronic acid hydrogels

As a difference to the GG hydrogels, all of the HA hydrogels were successfully compression tested. The shape of the stress-strain curves for the HA hydrogels differs from the GG hydrogels. The GG hydrogels started to resist the applied compression force already in the beginning of the test. Whereas, when the stress increased in the compression test of HA hydrogels, polymer chains in the structure re-orientated at the beginning before the hydrogels started to resist the applied force. Figure 4.23 represents the stress-strain behaviour of the HA hydrogels. The HAJ2 and the HA3 with 1.5 % of PVA hydrogels started to resist approximately in the same strain value of 0.1. The HA1 hydrogel with 1.5 % of PVA and the HAJ1 with 1.5 % of PVA started to resist the applied force approximately in the strain values of 0.25. The softest HA hydrogels with PVA concentration of 0.375 % started to resist the applied force latest, approximately in the strain values of 0.4.

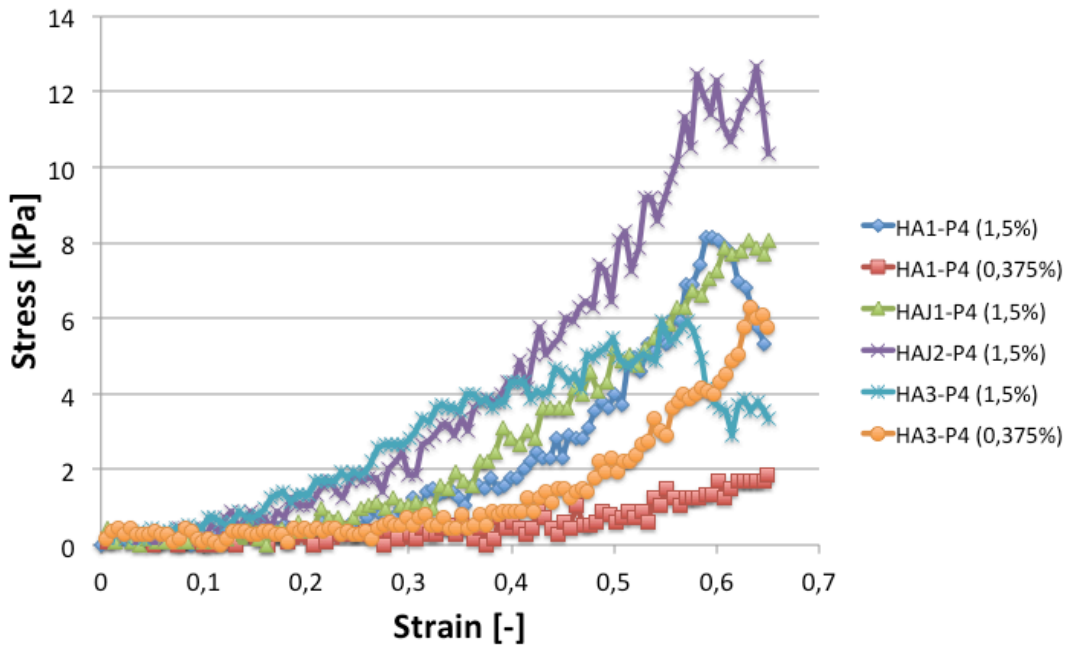

Figure 4.23. *The stress-strain curves of different HA hydrogels with PVA concentrations 1.5 % and 0.375 %.*

The average Young's modulus values are represented in Figure 4.24. The E value was calculated from formula (15). The HAJ2 hydrogel had the highest E value of HA hydrogels, 19.52 kPa. The difference of the E value between the HA3 hydrogel with 1.5 % of PVA (12.52 kPa) and the HAJ1 hydrogel (14.15 kPa), was not obvious. The HA1 hydrogel with 1.5 % of PVA and the HA3 with 0.375 % of PVA had very similar E values, 9.95 kPa and 9.65 kPa, although the PVA concentration differed remarkably. An observation can be made from the stress-strain curves that the HA3 hydrogel started to resist the applied stress in higher strain values. The HA1 hydrogel with 0.375 % of PVA had the lowest E value, 3.03 kPa.

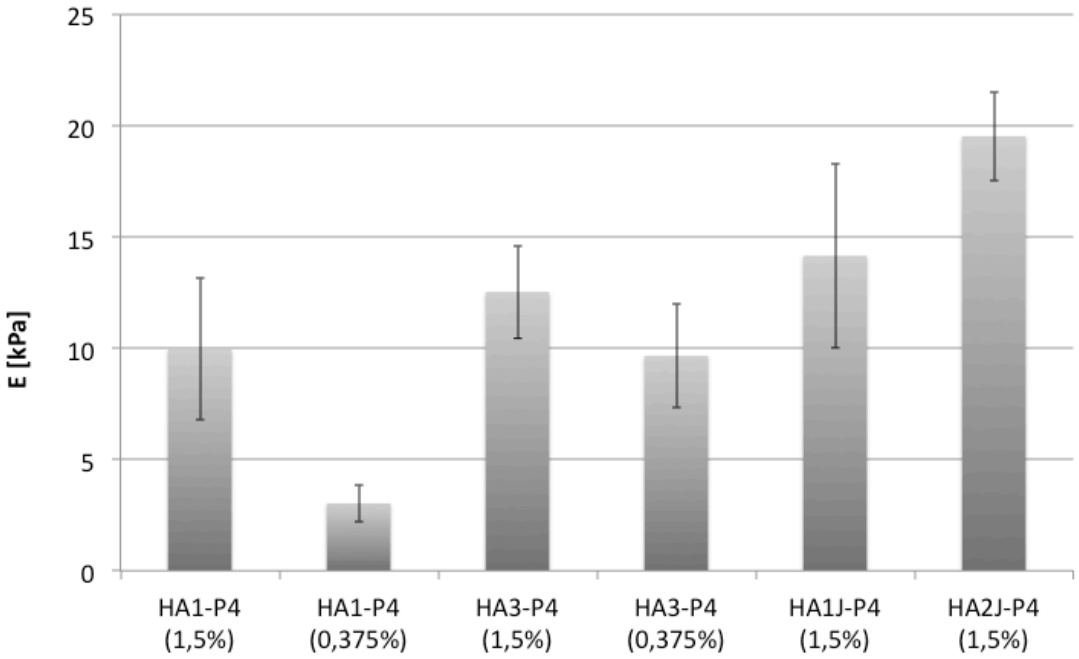

Figure 4.24. *The average Young's moduli for HA hydrogels with PVA concentrations of 1.5 % and 0.375 %.*

The Figure 4.25 shows the fracture strength of different HA hydrogels. The HA1 hydrogel with 0.375 % of PVA and the HAJ1 hydrogel did not fracture. The HAJ2 hydrogel had the highest fracture strength value, 12.02 kPa. The HA1 hydrogel with 1.5 % of PVA had the average fracture strength value of 8.84 kPa. The large standard deviation of HA1 hydrogel with 1.5 % of PVA was caused by the different fracture strength values from 4.24 kPa to 14.14 kPa. The fracture strength value for HA3 hydrogel with 1.5 % of PVA was 6.72 kPa and for HA3 with 0.375 % of PVA 5.81 kPa.

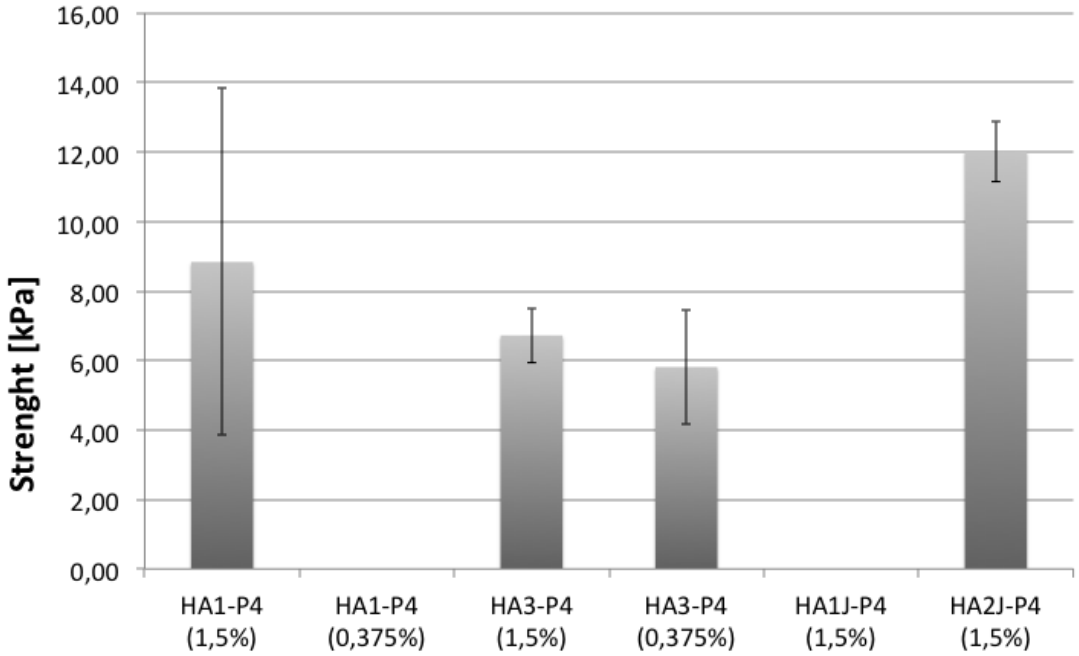

Figure 4.25. *The average fracture strength values of different HA hydrogels with PVA concentrations of 1.5 % and 0.375 %.*

4.5 Density measurements of hydrogels

The measured parameters and density calculations are shown in Table 4.2. The problem of weighting hydrogel samples was the evaporation of water, which caused changing mass result in scale. The density results of these hydrogels are not reliable and there is no difference between hydrogels where the cross-linker concentration is high or low. All these hydrogels despite of the cross-linker concentration have approximately the density of 1.0 mg/mm^3.

Table 4.2. *Measured parameters of gellan gum and hyaluronic acid hydrogels for density determination.*

Sample	Height (mm)	Diameter (mm)	Volume (mm^3)	Mass (mg)*	Density (mg/mm^3)
GG-1,1SPM	7,4	12,0	833,5	842,3	1,0
GG-0,56SPM	4,3	12,0	489,7	594,6	1,2
GG-0,4SPM	7,6	12,0	853,9	766,9	0,9
GG-0,3SPM	6,1	12,0	691,0	806,4	1,2
GG-3,1SPD	6,7	12,0	760,0	838,7	1,1
GG-1,57SPD	6,9	12,0	777,0	859,0	1,1
HA1-P4 (1,5%)	6,8	12,0	767,9	707,0	0,9
HA1-P4 (0,375%)	6,6	12,0	744,2	809,8	1,1
HA3-P4 (1,5%)	6,4	12,0	728,3	741,6	1,0
HA3-P4 (0,375%)	7,5	12,0	850,5	843,1	1,0
HAJ1-P4 (1,5%)	6,0	12,0	683,1	839,7	1,2
HAJ2-P4 (1,5%)	6,7	12,0	754,4	862,2	1,1

This method to measure the density of hydrogels was not the optimal and reliable method due to the evaporation of water. The density determination of hydrogels needs further studies.

4.6 Discussion of the rheological and mechanical data

All mechanical and rheological average results of the GG and the HA hydrogels are collected in Table 4.3. The mechanical properties of the GG hydrogels with 0.4 % and 0.3 % SPM concentrations could not be measured due to the softness of these hydrogels. The fast gelation time of the GG hydrogels with SPD cross-linker caused anisotropic structure and the rheological results were not reliable. In the upper part of the Table 4.3 are listed mechanical results from the compression test and in the lower part the rheological results. The total sample number in both measuring methods was eight, except for the GG hydrogels with 1.1 % of SPM cross-linker. The LVE range of the GG hydrogel with 1.1 % SPM cross-linker was not obvious and these hydrogels had to be re-measured. The total sample number for this 1.1 % SPM hydrogel was 24 and nevertheless, the number of successful samples was two.

The mechanical results include the Young's modulus (E), the fracture strength σ(max), the fracture strain ε(max) and the standard deviation (sd) of these results. Rheological results include the different moduli with the standard deviations and the loss factor that is calculated by the formula (10).

Table 4.3. *The collection table of mechanical and rheological results for the GG and the HA hydrogels.*

Mechanical results

Sample	E [kPa]	sd [kPa]	σ(max) [kPa]	sd [kPa]	ε(max) [%]	sd [%]	n (number of the successful samples)
GG-1,1SPM	21,44	5,93	4,22	0,90	28,3	3,92	7
GG-0,6SPM	6,74	1,55	1,74	0,45	28,4	5,20	6
GG-0,4SPM	-	-	-	-	-	-	0
GG-0,3SPM	-	-	-	-	-	-	0
GG-3,1SPD	21,88	2,92	12,38	0,67	59,43	5,84	7
GG-1,57SPD	18	8,61	5,89	2,08	41,65	8,22	7
HA1-P4 (1,5%)	9,95	5,39	8,84	4,99	58,12	4,30	7
HA1-P4 (0,375%)	3,03	0,85	0	0	0	0	7
HA3-P4 (1,5%)	12,52	2,69	6,72	0,78	53,99	3,01	8
HA3-P4 (0,375%)	9,65	2,35	5,81	1,64	58,25	5,67	7
HAJ1-P4 (1,5%)	14,15	4,14	0	0	0	0	6
HAJ2-P4 (1,5%)	19,52	2,00	12,02	0,87	64,08	0,35	6

Rheological results

Sample	G´[Pa]	sd of G' [Pa]	G´´ [Pa]	sd of G'' [Pa]	G* [Pa]	sd of G* [Pa]	tan δ	n (number of the successful samples)
GG-1,1SPM	31,57	21,84	22,07	9,17	38,72	23,02	0,70	2
GG-0,6SPM	22,57	4,89	14,99	3,29	27,11	5,90	0,66	4
GG-0,4SPM	18,16	7,06	13,04	6,62	22,40	9,56	0,72	4
GG-0,3SPM	6,77	0,66	3,85	0,41	7,79	0,78	0,57	5
GG-3,1SPD	-	-	-	-	-	-	-	0
GG-1,57SPD	-	-	-	-	-	-	-	0
HA1-P4 (1,5%)	236,20	51,89	19,63	4,86	237,21	52,93	0,08	4
HA1-P4 (0,375%)	41,75	1,14	6,86	0,62	42,32	1,22	0,16	3
HA3-P4 (1,5%)	396,88	172,83	29,66	10,01	397,39	172,29	0,07	4
HA3-P4 (0,375%)	53,11	3,88	15,07	0,79	55,23	3,75	0,28	6
HAJ1-P4 (1,5%)	295,50	9,79	11,31	2,22	295,86	9,79	0,04	5
HAJ2-P4 (1,5%)	362,92	69,53	14,80	3,69	362,92	69,53	0,04	5

Comparing the E values between GG hydrogels with SPM or SPD cross-linker, it is seen that the 1.1 % of SPM and the 3.1 % of SPD had approximately the same E values; 21.44 kPa and 21.88 kPa. However, the GG hydrogels with SPM concentration are stiffer than the GG hydrogels with SPD cross-linker although the cross-linker concentration is lower. That is also seen when comparing the 1.1 % of SPM and the 1.57 % of SPD hydrogels together; for 1.1 % SPM hydrogel the E value is higher even though the cross-linker concentration is lower. The HAJ2 hydrogels with 1.5 % of PVA had approximately the same E value (19.52 kPa) than the GG hydrogels with higher cross-linker concentrations. For both hydrogels, the E value becomes higher when cross-linker concentration increased. However, the GG hydrogels fractured in lower stress and strain values when compared to the HA hydrogels. Due to the higher fracture strength and strain values, the HA hydrogels are tougher than GG hydrogels. When the fracture strain is higher, the material withstands more deformation before it fractures and it is a more elastic material. Also, when comparing the GG hydrogels with the SPM

and the SPD together, it is seen that the SPD hydrogels are tougher than the SPM hydrogels due to the higher fracture strength and fracture strain values.

The standard deviations of the E and the fracture strength values for GG hydrogel with 1.57 % of SPD and for the HA1 hydrogel with 1.5 % of PVA are remarkable. Those standard deviations differ from the other hydrogels' corresponding values. No obvious reason was found for those high standard deviations and further measurements are needed.

Comparing the rheological results between these hydrogels, it is seen that the HA hydrogels had higher G' values than GG hydrogels. However, the G'' values were very similar between these two hydrogels. Due to the different G' values and similar G'' values, the loss factors differed greatly between these hydrogels. The loss factor of HA hydrogels was significantly lower than the loss factor of GG hydrogels. Due to the higher G' values, the HA hydrogels behaved more elastically in the LVE range than GG hydrogels. HA hydrogels are more elastic compared to the GG hydrogels and the GG hydrogels are more viscous than the HA hydrogels. For both hydrogels G' > G'' and tan $\delta < 1$, and they behave like gel materials.

When comparing the G* values of GG and HA hydrogels, it is seen that the G* values of HA hydrogels are obviously higher than for GG hydrogels. Due to the higher G* values, the HA hydrogels are more rigid than GG hydrogels. The standard deviations for GG hydrogel with 1.1 % of SPM and for HA3 with 1.5 % of SPD are higher than for other hydrogels. The reason for the high standard deviation of 1.1 % SPM hydrogel is the low successful sample number whereas there is no obvious reason for the high standard deviation of the HA3 hydrogel with 1.5 % of PVA. One possible reason is the unsuccessful sample preparation that caused anisotropy to the structure of the sample.

Rheological data between these two hydrogels differed greatly whereas the compression data was not that obviously different. Rheological measurement proved to be a more sensitive measurement for the anisotropy of the sample structure and the rheological data was not reliable if the structure of the sample was not homogenous. It seems that the rheological measurements are more sensitive and specific measuring methods than the compression test. However, it is to be noted, that the compression and the oscillatory data are not directly comparable. In the compression test, the applied force is uniaxial whereas in the oscillatory test, the applied force is torsional.

The values of the E, the G' and the G'' depend on the method they were determined by. For example, the E value can be determined by using the secant modulus or the tangent modulus. The secant modulus is the slope that is drawn between two points and the tangent modulus is taken as the slope of the stress-strain curve at some special level of stress. The values of the G' and the G'' depend on the determined LVE range. The limit of the LVE range can be determined with visual or manual analysis or automatic analysis using software analysis program.

The comparison of the G', G'' and E values to the ones reported in literature is not straightforward due to the different measuring temperature, different presets of

measurement methods and different concentrations, modifications and mixture solutions of hydrogel structures. Rheological results depend on the measuring temperature and the results that have been measured at a different temperature, are not straight comparable. Few literature results of the oscillatory and the compression test are compared to the result data of the Table 4.3. These comparable results are the GG and the HA hydrogels but the structure modifications and the structure components are different. Also the presets and the measurement conditions differ from the measuring conditions of this thesis work. The following results from literature are only examples of the mechanical and the rheological results for the GG and the HA hydrogels.

In (López-Cebral et al. 2013), the authors measured a frequency sweep at 37°C ± 0.2°C in the range 0.01-10 Hz in the LVE range with a controlled stress. The hydrogels that were measured were gellan gum hydrogels with combination of albumin, chondroitin sulfate and spermidine. They had the G' values of 110-1100 Pa and the G'' values of 9-100 Pa in 1 Hz for different composition of the hydrogel formulations. As can be seen, these results are greatly higher that the G' and the G'' values that are present in the Table 4.3 for GG hydrogels with SPD cross-linker. In (Silva et al. 2013), the amplitude sweep (up to strain value of 1.0) was conducted at 5 Hz and the frequency sweep (up to frequency value of 500 Hz) was conducted by applying a constant strain of 0.001. Both sweeps were done in the temperature of 37°C. The hydrogels that were measured were gellan gum hydrogels with a native form (HAGG), a low-acyl form (LAGG) and the blend of these two forms. The hydrogels were immersed in PBS for up to 168 days and these hydrogels with different immersions were measured. G' and G'' were measured from the LVE range. For the LAGG hydrogels the G' values were between 158-267 kPa and the G'' values were between 5.9-11.1 kPa. For the HAGG hydrogels the G' values varied between 1.0-1.3 kPa and the G'' values were between 0.02-0.07 kPa. For the LAGG and the HAGG blends these moduli were 14.1-19.3 kPa and 0.4-0.5 kPa. The moduli values of the LAGG hydrogels were greatly higher that the G' and the G'' values of the GG hydrogels in Table 4.3. There was a ten to hundred fold difference between the G' values of the HAGG hydrogels and the studied GG hydrogels. The difference between the G'' values was lower, but still two to six fold. The difference between the blend and the studied GG hydrogels was not as obvious as the results of the LAGG but higher than the results of the HAGG. (Silva et al. 2013) has also measured Young's modulus (E) by compression test at 37°C. For the LAGG hydrogels the E values were 234-535 kPa, the fracture strength values were 108-172 kPa and the fracture strain values were 29-53 %. These results were greatly higher than the compression results of the GG hydrogels in Table 4.3 excluding the fracture strain values, which were more similar for GG hydrogels with SPM cross-linker. For the HAGG the E values were 6.9-87 kPa, the fracture strength values were 40-73 kPa and the fracture strain values were 61-73 %. These results were more similar with the GG hydrogel with the SPD cross-linker in Table 4.3 excluding the fracture strength values that were approximately six times higher for the HAGG hydrogels. For the LAGG and the HAGG blends the E values were 57.8-110.5 kPa, the fracture strength values were

68-92 kPa and the fracture strain values were 48-60 %. The E and the fracture strength values were higher for blend than for the GG hydrogels in Table 4.3 although the fracture strain values were more similar with the GG hydrogels with the SPD cross-linker.

In (Ghosh et al. 2005), HA hydrogels with different ratio of poly-(ethylene glycol) diacrylate as a cross-linker were measured by frequency sweep. The frequency sweep was measured at 50 % of the ultimate stress levels of hydrogels at a temperature of 25°C, the oscillatory frequency was increased from 0.1 to 100 Hz and G' was recorded. The measured G' values at a strain value of 0.1 and at a frequency of 1 Hz were approximately 150-2000 Pa. These results were higher than the G' values of the HA hydrogels in the Table 4.3. (Burdick et al. 2005) measured the mechanical properties of metacrylated hyalyronic acid hydrogels with variations in the macromer molecular weight and the concentration by compression test. They measured the E values approximately from 2.5 kPa to 100 kPa where the lowest values were similar with the E values of HA hydrogels in the Table 4.3.

To illustrate the stiffness of the studied hydrogels, the E values are compared to some well-known materials. For example the E value for thermoplastic polymers is approximately 1000-4000 kPa, for polyethylene 200-2000 kPa, for natural gum 0.1-1 kPa, for hard rubber 100-1000 kPa, for ceramics 40000-80000 kPa, for cast iron 100000 kPa, for diamond 1200000 kPa and for bone tissue 18000-21000 kPa. (Mezger 2002) The E value of the natural gum is lower than the E values of the studied hydrogels and all other materials are greatly stiffer than studied hydrogels. The E values for articular cartilage is approximately 950 kPa and for liver tissue 640 Pa. The E value for articular cartilage is greatly higher than the E value for studied hydrogels whereas the E value for liver tissue is much lower than the E value of studied hydrogels. (Levental et al. 2007)

The reliability of the oscillatory and the compression measurements was influenced by the preparation of the hydrogel solutions and the samples, the errors of the measurement equipments and user errors. The main factor that influenced the reliability of the results is the preparations of the hydrogel solutions and the samples. The gelation time of the hydrogels with higher cross-linker concentrations was fast and that caused anisotropic hydrogel samples. The results of these anisotropic samples had wide standard deviations. To avoid errors in the rheological and the mechanical results, the preparation of hydrogels samples is in a very important role. Additionally, one error factor was the point group at the beginning of every rheological measurement, which was possibly caused by the slipping of the sample.

5 CONCLUSIONS AND FUTURE PROPOSITIONS

The cross-linker concentrations of GG and HA hydrogels influenced the stiffness of the hydrogel. When cross-linker concentration increased, the hydrogel became stiffer. The compression test measurements indicated that the HA hydrogel is a tougher and more elastic material than the GG hydrogel. The E values of both of the studied hydrogels were of the same magnitude. In the rheological measurements, the HA hydrogels proved to be more elastic than the GG hydrogels due to the higher G' values. Additionally, the loss factor of the HA hydrogels was significantly lower than the loss factor of the GG hydrogels. The GG hydrogels had relatively higher G'' values than the HA hydrogels when compared to the G' values. The GG hydrogels proved to be more viscous material than the HA hydrogels. The G* values of the HA hydrogels were higher and the HA hydrogels proved to be more rigid. According to the rheological measurement curves, the HA hydrogels behaved more ideally compared to the GG hydrogels and the LVE range was more obvious for the HA hydrogels. Therefore the HA hydrogels are more suitable to be measured by the Haake RheoStress.

For hydrogels with higher cross-linker concentrations, the compression test proved to be a more suitable method than the rheological measuring method to measure the stiffness of the hydrogels. When the cross-linker concentration increased, the preparation of the hydrogel samples became more challenging because of the fast gelation time. The fast gelation time caused anisotropy to the sample structure. Rheological measurement proved to be more sensitive and specific to the sample structure. Additionally, due to the smaller sample sizes in rheological test, the anisotropy of the sample caused errors to the rheological results. Results for the softer hydrogels with lower cross-linker concentrations show that the rheological measurement proved to be more suitable.

Taking into account the actual planned usage of these hydrogels inside the human body, further measurements are needed at the temperature of 37°C. Additionally, the measurements of real tissues are needed to compare the material properties between the tissue and the hydrogel. To improve the rheological measurement in the future, sandpaper at the plates should be tested to avoid the slipping of the sample, a cone-plate could be used to avoid the formation of air bubbles between the sample and the lower plate and a cover around the sample could inhibit the possible evaporation of the water. Sample preparation could be improved by avoiding the shear forces that are created when the sample is extracted from the syringe and one possible solution could be a "spread out cake mould" that releases the sample straight to the lower plate.

REFERENCES

ASTM F2900-11, Standard guide for characterization of hydrogels used in regenerative medicine. 2011.

DIN 53018-1:1976-03, Viscometry; measurement of the dynamic viscosity of newtonian fluids with rotational viscometers; principles. 1976.

Ahearne, M. & Kelly, D.J. 2013. A comparison of fibrin, agarose and gellan gum hydrogels as carriers of stem cells and growth factor delivery microspheres for cartilage regeneration. Biomedical Materials 8, 3, pp. 035004.

Bajaj, I.B., Survase, S.A., Saudagar, P.S. & Singhal, R.S. 2007. Gellan gum: fermentative production, downstream processing and applications. Food Technology and Biotechnology 45, 4, pp. 341.

Barbucci, R. 2009. Hydrogels: biological properties and applications. Springer. pp. 1-20.

Brandl, F., Sommer, F. & Goepferich, A. 2007. Rational design of hydrogels for tissue engineering: impact of physical factors on cell behavior. Biomaterials 28, 2, pp. 134-146.

Brandl, F., Sommer, F. & Goepferich, A. 2007. Rational design of hydrogels for tissue engineering: impact of physical factors on cell behavior. Biomaterials 28, 2, pp. 134-146.

Burdick, J.A., Chung, C., Jia, X., Randolph, M.A. & Langer, R. 2005. Controlled degradation and mechanical behavior of photopolymerized hyaluronic acid networks. Biomacromolecules 6, 1, pp. 386-391.

Burdick, J.A. & Prestwich, G.D. 2011. Hyaluronic acid hydrogels for biomedical applications. Advanced Materials 23, 12, pp. H41-H56.

Callister, W.D. & Rethwisch, D.G. 2007. Materials science and engineering: an introduction. Wiley New York. pp. 137-140.

Davis, F. & Higson, S.P. 2012. Hydrophilic polymers for biomedical applications. Materials in Biology and Medicine pp. 19.

Dealy, J.M. & Wissbrun, K.F. 1990. Melt rheology and its role in plastics processing. Springer. pp. 1-22.

Dealy, J.M. & Larson, R.G. 2006. Structure and rheology of molten polymers. Hanser, Munich pp. 109-111, 91-183.

Drury, J.L. & Mooney, D.J. 2003. Hydrogels for tissue engineering: scaffold design variables and applications. Biomaterials 24, 24, pp. 4337-4351.

Eljarrat-Binstock, E., Bentolila, A., Kumar, N., Harel, H. & Domb, A.J. 2007. Preparation, characterization, and sterilization of hydrogel sponges for iontophoretic drug-delivery use. Polymers for Advanced Technologies 18, 9, pp. 720-730.

Ferris, C.J., Gilmore, K.J. & Wallace, G.G. 2013. Modified gellan gum hydrogels for tissue engineering applications. Soft Matter 9, 14, pp. 3705-3711.

Ghosh, K., Shu, X.Z., Mou, R., Lombardi, J., Prestwich, G.D., Rafailovich, M.H. & Clark, R.A. 2005. Rheological characterization of in situ cross-linkable hyaluronan hydrogels. Biomacromolecules 6, 5, pp. 2857-2865.

Gila, M., Coelhoa, J., Ferreiraa, P. & Alvesa, P. 2012. Polymers for biomedical applications: chemical modification and biofunctionalization. Polymers for Biomedical Applications. Taylor & Francis Group, LLC. pp. 21-30.

Ha, H.C., Sirisoma, N.S., Kuppusamy, P., Zweier, J.L., Woster, P.M. & Casero, R.A.,Jr 1998. The natural polyamine spermine functions directly as a free radical scavenger. Proceedings of the National Academy of Sciences of the United States of America 95, 19, pp. 11140-11145.

Hoffman, A.S. 2002. Hydrogels for biomedical applications. Advanced Drug Delivery Reviews 54, 1, pp. 3-12.

Hutton, J., Barnes, H. & Walters, K. 1989. An introduction to rheology. pp. 1-10, 37-54, 159-170.

Kim, S.J., Park, S.J. & Kim, S.I. 2003. Swelling behavior of interpenetrating polymer network hydrogels composed of poly (vinyl alcohol) and chitosan. Reactive and Functional Polymers 55, 1, pp. 53-59.

Kishida, A. & Ikada, Y. 2001. Hydrogels for biomedical and pharmaceutical applications. Polymeric Biomaterials, Revised and Expanded pp. 133.

Levental, I., Georges, P.C. & Janmey, P.A. 2007. Soft biological materials and their impact on cell function. Soft Matter 3, 3, pp. 299-306.

López-Cebral, R., Paolicelli, P., Romero-Caamaño, V., Seijo, B., Casadei, M.A. & Sanchez, A. 2013. Spermidine-cross-linked hydrogels as novel potential platforms for pharmaceutical applications. Journal of pharmaceutical sciences 102, 8, pp. 2632-2643.

Meyvis, T.K., Stubbe, B.G., Van Steenbergen, M.J., Hennink, W.E., De Smedt, S.C. & Demeester, J. 2002. A comparison between the use of dynamic mechanical analysis and oscillatory shear rheometry for the characterisation of hydrogels. International journal of pharmaceutics 244, 1, pp. 163-168.

Mezger, T.G. 2002. The rheology handbook: For users of rotational and oscillation rheometers. Germany, pp. 13-68, 75-82, 86, 100, 112-135, 164-181.

Nair, L.S. & Laurencin, C.T. 2007. Biodegradable polymers as biomaterials. Progress in polymer science 32, 8, pp. 762-798.

Oliveira, J.T., Martins, L., Picciochi, R., Malafaya, P., Sousa, R., Neves, N., Mano, J. & Reis, R. 2010. Gellan gum: a new biomaterial for cartilage tissue engineering applications. Journal of biomedical materials research Part A 93, 3, pp. 852-863.

Ossipov, D.A. & Hilborn, J. 2006. Poly (vinyl alcohol)-based hydrogels formed by "click chemistry". Macromolecules 39, 5, pp. 1709-1718.

Ottenbrite, R.M., Park, K. & Okano, T. 2010. Biomedical applications of hydrogels handbook. Springer. pp. 203-204.

Park, H. & Park, K. 1996. Hydrogels in bioapplications. ACS Symposium Series, ACS Publications. pp. 2-10.

Park, J.H., Huh, K.M., Ye, M. & Park, K. 2012. Hydrogels. In: Lee, S. & Henthorn, D. (ed.). Materials in Biology and Medicine. CRC Press.

Patel, A. & Mequanint, K. 2011. Hydrogel biomaterials. In: Fazel, R. (ed.). Biomedical Engineering – Frontiers and Challenges. pp. 275-296.

Rana, V., Rai, P., Tiwary, A.K., Singh, R.S., Kennedy, J.F. & Knill, C.J. 2011. Modified gums: approaches and applications in drug delivery. Carbohydrate Polymers 83, 3, pp. 1031-1047.

Shroff, K., Rexeisen, E.L., Arunagirinathan, M.A. & Kokkoli, E. 2010. Fibronectin-mimetic peptide-amphiphile nanofiber gels support increased cell adhesion and promote ECM production. Soft Matter 6, 20, pp. 5064-5072.

Silva, D.A., Poole-Warren, L.A., Martens, P.J. & Panhuis, M. 2013. Mechanical characteristics of swollen gellan gum hydrogels. Journal of Applied Polymer Science 130, 5, pp. 3374-3383.

Slaughter, B.V., Khurshid, S.S., Fisher, O.Z., Khademhosseini, A. & Peppas, N.A. 2009. Hydrogels in regenerative medicine. Advanced Materials 21, 32-33, pp. 3307-3329.

Smith, A.M., Shelton, R.M., Perrie, Y. & Harris, J.J. 2007. An initial evaluation of gellan gum as a material for tissue engineering applications. Journal of Biomaterials Applications 22, 3, pp. 241-254.

Stammen, J.A., Williams, S., Ku, D.N. & Guldberg, R.E. 2001. Mechanical properties of a novel PVA hydrogel in shear and unconfined compression. Biomaterials 22, 8, pp. 799-806.

Uchegbu, I.F. & Schatzlein, A.G. 2006. Polymers in drug delivery. CRC. pp. 49-62.

Xu, X., Jha, A.K., Harrington, D.A., Farach-Carson, M.C. & Jia, X. 2012. Hyaluronic acid-based hydrogels: from a natural polysaccharide to complex networks. Soft Matter 8, 12, pp. 3280-3294.

Ylä-Outinen, L., Joki, T., Varjola, M., Skottman, H. & Narkilahti, S. 2012. Three-dimensional growth matrix for human embryonic stem cell-derived neuronal cells. Journal of tissue engineering and regenerative medicine 8, 3, pp. 186-194.

Zavan, B., Cortivo, R. & Abatangelo, G. 2009. Hydrogels and tissue engineering. Hydrogels. Springer. pp. 1-8.